

Preparation and Characterization of Stationary Phases for Hydrophilic Interaction Liquid
Chromatography and Reversed Phase Liquid Chromatography

by

Chad Douglas Iverson

A thesis submitted in partial fulfillment of the requirements for the degree of

Doctor of Philosophy

Department of Chemistry
University of Alberta

© Chad Douglas Iverson, 2016

ABSTRACT

High performance liquid chromatography (HPLC) has become an invaluable tool in modern chemical analysis. While reversed phase liquid chromatography (RPLC) is the most commonly utilized mode of HPLC, hydrophilic interaction liquid chromatography (HILIC) is gaining popularity due to its ability to retain and resolve highly polar analytes that are incompatible with RPLC. Previously, Dr. Mohammed Ibrahim developed a simple and straightforward two dimensional HILIC selectivity plot to characterize the selectivity behavior of HILIC columns. The first part of this thesis expands these plots to examine the changes in selectivity behavior that 19 HILIC columns undergo in response to changes in mobile phase pH and buffer concentration.

The second and third research chapters focus on the development of new carbon-based columns for RPLC and HILIC. The vast majority of RPLC and HILIC columns are based on silica particles. Silica is chemically unstable under extreme pH conditions. Porous graphitic carbon (PGC) is an attractive alternative to silica-based phases due to its chemical and thermal stability, and its unique selectivity. However, native PGC is strongly hydrophobic and in some instances excessively retentive. To increase the hydrophilicity of PGC and attenuate its excessive retentivity, diazonium chemistry was utilized to separately modify the surface of PGC with aniline, catechol, and amide groups. The performance of these three new phases (Aniline-PGC, Catechol-PGC, and Amide-PGC) was demonstrated by separations of phenols, nucleotides, nucleosides, carboxylic acids, alkaline pharmaceuticals, and/or performance enhancing stimulants. Notably, the Aniline-PGC and Amide-PGC phases reduced the RPLC retentivity of PGC up to 90 %.

Most HPLC methods today use acetonitrile or methanol as the organic mobile phase component. Increasing environmental consciousness (green chemistry) promotes the use of more environmentally sustainable solvents such as ethanol. In the last research chapter, I briefly discuss the feasibility and performance of ethanol as an HPLC eluent, relative to acetonitrile and methanol, in the context of a commentary on a recently published work on “cocktail chromatography”.

PREFACE

This thesis consists of six chapters including a general introduction (**Chapter 1**), four main body chapters describing four completed projects (**Chapters 2-5**), and a final chapter which summarizes the conclusions of the thesis and describes possible future directions for the work (**Chapter 6**). Versions of **Chapters 2-5** have all been either previously published or are currently under consideration for publication. In all works described below, C. A. Lucy was the supervising author. He provided high-level guidance as to the direction of each project and aided in the preparation and revision of the manuscripts

Chapter 2 has been submitted in revised form by myself, X. Gu, and C. A. Lucy as “The Hydrophilicity vs. Ion Interaction HILIC Selectivity Plot Revisited: The Effect of Mobile Phase pH and Buffer Concentration on HILIC Selectivity” for publication in the *Journal of Chromatography A*. Under my guidance and direction, undergraduate student Xinyun Gu collected the chromatographic data for 60 % of the columns investigated in this chapter. I performed the remaining characterizations, interpreted and presented the data, and prepared and revised the manuscript.

Chapter 3 has been previously published as C. D. Iverson and C. A. Lucy, Aniline-Modified Porous Graphitic Carbon for Hydrophilic Interaction and Attenuated Reverse Phase Liquid Chromatography, *Journal of Chromatography A* 1373 (2014) 17-24. Here I prepared and characterized the column, and constructed the manuscript.

Chapter 4 was previously published as C. D. Iverson, Y. Zhang, and C. A. Lucy, Diazonium Modification of Porous Graphitic Carbon with Catechol and Amide Groups for Hydrophilic Interaction and Attenuated Reversed Phase Liquid Chromatography,

Journal of Chromatography A, 1422 (2015) 186-193. All work related to the Catechol-PGC phase, including phase preparation and characterization, was performed by me. Ya Zhang synthesized the Amide-PGC phase and performed the initial characterizations of its chromatographic performance. These data have been previously reported in Chapter 3 of her 2014 University of Alberta MSc thesis entitled “Liquid Chromatography: Injection Broadening in Ion Chromatography and Retention Properties of a New Hydrophilic Interaction Liquid Chromatography Stationary Phase.” Subsequent to the work reported in her thesis, I have performed additional characterizations of the Amide-PGC phase. These are described in the manuscript and in this thesis, along with relevant previously reported data. The final published manuscript was constructed entirely by me with assistance from C. A. Lucy as described above.

A significantly condensed version of **Chapter 5** was recently published as C. D. Iverson, D. Wu, P. Jiang, B. Stanley, M. K. Pappoe, and C. A. Lucy, , Comment on “Cocktail Chromatography: Enabling the Migration of HPLC to Nonlaboratory Environments,” *ACS Sustainable Chemistry & Engineering* 3 (2015) 1898. This commentary was a collaborative effort of the entire Lucy Laboratory, but I was responsible for planning the study, coordinating the efforts of the other lab members, acquiring the HPLC and UV absorbance data, and preparing the manuscript. Following publication of the above commentary, additional data has been acquired and included in this chapter.

This thesis is dedicated to my parents, Jim and Diane Iverson, whom have proudly supported me throughout my entire academic journey.

AKNOWLEDGEMENTS

First and foremost I would like to thank my supervisor, Dr. Charles Lucy for his guidance and support. I have learned so much over the past 3.5 years working with him, and will always be a better teacher and a better scientist because of what he has taught me. Additional thanks are given to my Supervisory Committee members (Dr. Chris Le and Dr. John Vederas) as well as the other members of my Examining Committee (Dr. Mark McDermott and Dr. Caroline West) for their guidance and for taking the time to read my thesis.

The training and friendship of Dr. Farooq Wahab and Dr. Mohammed Ibrahim are also greatly appreciated. Without their kind words and inspiration I may have not been able to complete the thesis before you. I would further like to thank Ms. Xinyun (Clair) Gu. She is a brilliant young scientist that helped me immensely to turn Chapter 2 from an idea into a reality.

The technical contributions of the shops and services of the Chemistry Department and greater university community to this work are also acknowledged. These include the staff of the U of A NanoFab Surface Characterization Facility; the U of A Chemistry Department's Analytical and Instrumentation Laboratory, and Mass Spectrometry and NMR facilities; as well as the U of A Chemistry Stores and administrative staff. Additional thanks are given to Dr. Ho-Yan Sun, Dr. Dennis Hall, and Dr. Liang Li for their synthetic technical assistance and/or provision of lab space.

This work was sponsored by the Natural Sciences and Engineering Council of Canada (NSERC), Thermo Scientific, and the University of Alberta. The academic financial support from NSERC, Alberta Innovates Technology Futures (AITF), and the

University of Alberta are greatly appreciated. The collaborations and gifts in kind from Agilent, Supelco, Restek, Tosoh Biosciences, EMD Millipore, AZYP LLC, PolyLC, ES Industries, and Fortis Technologies are gratefully acknowledged. Special mention is given to Dave Bell of Supelco, Chris Pohl of Thermo Scientific, and Xiaoli Wang of Agilent for their collaborative efforts.

Special thanks go to my friends and Lucy group members for making my Doctoral program a better experience. Last but not least I wish to thank Claudia Chong Shin Sen from the bottom of my heart for standing by my side through the thick and the thin of it and for always being there to provide encouragement when I needed it.

TABLE OF CONTENTS

CHAPTER 1: Introduction to High Pressure Liquid Chromatography	1
1.1 Motivation and Thesis Overview	1
1.2 High Performance Liquid Chromatography	3
1.2.1 Important Equations and Theories in HPLC	6
1.2.1.1 Resolution	6
1.2.1.2 Retention	7
1.2.1.3 Selectivity Factor	8
1.2.1.4 Peak Efficiency (N) and Plate Height (H)	8
1.2.1.5 Band Broadening in Liquid Chromatography	9
1.2.1.6 Column Backpressure	13
1.2.1.7 Asymmetry Factor	14
1.2.2 Relevant Modes of Liquid Chromatography	16
1.2.2.1 Reversed Phase Liquid Chromatography (RPLC)	16
1.2.2.2 Hydrophilic Interaction Liquid Chromatography (HILIC)	17
1.2.2.3 Ion Exchange Chromatography	22
1.2.3 Common Column Supports in HPLC	23
1.2.3.1 Silica	23
1.2.3.1.1 Totally Porous Particles	24
1.2.3.1.2 Core Shell Particles	24

1.2.3.1.3 Silica Monoliths	25
1.2.3.2 Silica Alternatives	26
1.2.3.2.1 Porous Polymers	26
1.2.3.2.2 Porous Graphitic Carbon (PGC)	27
1.3 Summary	28
1.4 References	29
 CHAPTER 2: The Hydrophilicity vs. Ion Interaction HILIC Selectivity Plot Revisited: The Effect of Mobile Phase pH and Buffer Concentration on HILIC Selectivity	
2.1 Introduction	34
2.2 Experimental	35
2.2.1 Apparatus	35
2.2.2 Chemicals and Reagents	36
2.2.3 Tested Columns and Test Probes	36
2.2.5 Chromatographic Conditions	38
2.3 Results and Discussion	38
2.3.1 Effect of pH	49
2.3.2 Effect of Buffer Concentration	56
2.4 Conclusions	62
2.5 References	62

CHAPTER 3: Aniline-Modified Porous Graphitic Carbon for Hydrophilic Interaction and Attenuated Reverse Phase Liquid Chromatography	69
3.1 Introduction.....	69
3.2 Experimental.....	71
3.2.1 Chemicals and Reagents	71
3.2.2 Synthesis of Dimethylaniline-PGC.....	73
3.2.3 Synthesis of Aniline-PGC.....	74
3.2.4 Packing.....	77
3.2.5 Characterization of the PGC Phases	77
3.2.6 Chromatographic Separations.....	78
3.2.7 Evaluation of the Chemical Reactivity of Aniline-PGC.....	79
3.3 Results and Discussion	79
3.3.1 Synthesis of Phases	80
3.3.2 Characterization of Aniline-PGC.....	84
3.3.3 HILIC Properties of Aniline-PGC	87
3.3.4 Attenuated Reversed Phase Properties of Aniline-PGC	96
3.3.5 Low pH Separation	98
3.3.6 Evaluation of the Chemical Reactivity of Aniline-PGC.....	102
3.4 Conclusions.....	103
3.5 References.....	103

CHAPTER 4: Diazonium Modification of Porous Graphitic Carbon with Catechol and Amide Groups for Hydrophilic Interaction and Attenuated Reversed Phase Liquid

Chromatography	109
4.1 Introduction.....	109
4.2 Experimental.....	109
4.2.1 Chemicals and Reagents	109
4.2.2 Synthesis of 4-Aminocatechol.....	112
4.2.3 Synthesis of Catechol-PGC.....	116
4.2.4 Synthesis of Amide-PGC.....	116
4.2.5 Packing.....	119
4.2.6 Characterization of the PGC Phases	119
4.2.7 Chromatographic Separations.....	120
4.3 Results and Discussion	121
4.3.1 Synthesis and Characterization of Phases.....	121
4.3.1.1 Catechol-PGC	121
4.3.1.2 Amide-PGC.....	125
4.3.2 Chromatographic Retention Behavior of Catechol-PGC and Amide PGC ...	125
4.3.3 Applications of Catechol-PGC in HILIC Separations.....	132
4.3.4 RPLC Separation of Ephedrine Stimulants by Catechol-PGC	135
4.3.5 Attenuated Reversed-Phase Separations by Amide-PGC.....	136

4.4 Conclusions.....	140
4.5 References.....	140
CHAPTER 5: An Exploration of the Use of Ethanol as a HPLC Mobile Phase	145
5.1 Introduction.....	145
5.2 Experimental.....	146
5.2.1 Beverage Mobile Phases, Chemicals, Reagents, Materials, and Stationary Phase	146
5.2.2 Instrumentation and Chromatographic Conditions.....	147
5.3 Results and Discussion	148
5.3.1 Eluent Viscosity is the Key: The Backpressure Penalty of Ethanol	149
5.3.2. Solvent Quality Matters: The Choice of Vodka Brand and Ghost Peaks	151
5.3.3. Seeing the Flower Amongst the Weeds: The Importance of Solvent UV Cutoffs.....	157
5.3.4 Gradient Peak Widths with Grain Alcohol vs. HPLC Grade Ethanol	159
5.4 Conclusions.....	161
5.5 References.....	161
CHAPTER 6: Conclusions and Future Work	164
6.1 Conclusions.....	164
6.2 Future Work	166

6.2.1 Investigation of Alternate Test Probes to Measure HILIC Hydrophilic Selectivity	166
6.2.2 Investigation of Additional Factors Affecting HILIC Selectivity	167
6.2.3 Zwitterionic Porous Graphitic Carbon for HILIC	168
6.2.4 Improving the Performance of Carboxylate-PGC	171
6.3 References.....	173
BIBLIOGRAPHY.....	175
APPENDIX 1: Conversion of Mol % to Volume %.....	204
APPENDIX 2: Log P and pK _a values for test analytes utilized in this thesis.....	205

LIST OF TABLES

1.1	Representative structures of common stationary phases in HILIC	20
2.1	Characteristics of the stationary phases evaluated in this study	37
2.2	Summary of selectivity changes of HILIC columns when pH is decreased or buffer concentration is increased	41
2.3	Retention data for separations of test probes performed on 22 different HPLC (HILIC) phases at various mobile phase pH's and buffer concentrations	42
2.4	UV absorbance maxima of cytosine in different solutions	51
2.5	Summary of selectivity changes of the Acclaim HILIC-10 (column 18) as the buffer concentration is increased at different pH values	61
3.1	Surface composition from XPS survey scans of PGC, Dimethylaniline-PGC (DMA-PGC), and Aniline-PGC	82
3.2	Characteristics of tested stationary phases in Figure 3.10	94
3.3	Comparison of separation efficiencies attained by Aniline-PGC and unmodified PGC in the separation of 5 alkaline pharmaceuticals	98
3.4	Measured peak areas of 3 sugars separated by Aniline-PGC at different temperatures	102
4.1	Surface composition from XPS scans of Catechol-PGC and Amide-PGC	123
4.2	Comparison of peak efficiencies (N) and asymmetry factors ($A_s = B/A$) between Catechol-PGC and unmodified PGC for the separation of 3 phenolic compounds	134
4.3	Comparison of peak efficiencies (N) and asymmetry factors ($A_s = B/A$) between Catechol-PGC and unmodified PGC for the separation of 4 nucleosides	135
5.1	Measured peak widths of analytes separated under identical conditions using HPLC ethanol and grain alcohol as the organic modifier	159
A-2.1	Log P and pK_a values for test analytes utilized in this thesis	205

LIST OF FIGURES

1.1	Schematic of the different parts of a modern HPLC system	5
1.2	Schematic representation of Eddy diffusion (A-term)	10
1.3	The van Deemter plot	12
1.4	Measurement of the asymmetry factor ($A_s = B/A$) of a tailing peak	15
1.5	Representation of analyte-water-layer partitioning in HILIC	18
1.6	Schematic representation of some of the secondary interactions influencing HILIC retention and selectivity	19
1.7	General scheme for the preparation of a bonded silica phase	24
2.1	Hydrophilicity ($k_{\text{cytosine}}/k_{\text{uracil}}$) vs. ion interaction ($k_{\text{BTMA}}/k_{\text{uracil}}$) selectivity plots of HILIC phases acquired under different mobile phase pH's and buffer concentrations	47
2.2	Comparative hydrophilicity ($k_{\text{cytosine}}/k_{\text{uracil}}$) vs. ion interaction ($k_{\text{BTMA}}/k_{\text{uracil}}$) selectivity plots of HILIC phases as in Figure 2.1 , but utilizing the BTMA/cytosine retention ratio on the y-axis	48
2.3	Difference plots showing the effect of changing the w pH from 6.8 to (A) 5.0, (B) 3.7 and (C) 3.0 (while maintaining a 5 mM buffer concentration) on the hydrophilicity and ion interaction behavior of 19 HILIC columns	50
2.4	Hydrophilicity ($k_{\text{cytosine}}/k_{\text{uracil}}$) vs. ion interaction ($k_{\text{BTMA}}/k_{\text{uracil}}$) selectivity plot of selected HILIC phases at w pH 3.7	52
2.5	Difference plots showing the effect of increasing the buffer concentration from 5 to 25 mM at w pH (A) 6.8, (B) 5.0, and (C) 3.0 on the hydrophilicity and ion interaction behavior of 19 HILIC columns	57
3.1	Structures of analytes used to characterize the Dimethylaniline-PGC and Aniline-PGC stationary phases	72
3.2	Reaction scheme for the synthesis of Dimethylaniline-PGC	73
3.3	Scheme for the addition of aniline functionalities onto the surface of PGC by using an <i>in situ</i> generated nitrobenzene diazonium salt	76
3.4	Comparison of the HILIC separation of 3 phenolic compounds by Dimethylaniline-PGC and unmodified PGC	83
3.5	Photograph of the difference in wettability between unmodified-PGC and Aniline-PGC	85
3.6	Curve-fitted high-resolution XPS spectra of the N 1s region (A) after the grafting of nitrobenzene and (B) after the iron powder reduction of the nitro group to the aniline	86
3.7	HILIC separation of 3 nucleobases on the amine-PGC and Epic HILIC-PI columns	88
3.8	Retention behavior of (A) cytosine and (B) Thymidine on Aniline-PGC and Epic HILIC PI as a function of % ACN in the eluent, measured at two different pH values	89

3.9	Comparison of the selectivity of six aromatic carboxylic acids on eleven different column chemistries versus Aniline-PGC under HILIC mode conditions	92
3.10	HILIC selectivity plot displaying selectivity behavior of Aniline-PGC, Epic HILIC-PI, and unmodified PGC (Hypercarb) with respect to 33 commercial columns	93
3.11	Comparison of the reversed phase separation of five alkaline pharmaceuticals on (A) Aniline-PGC and (B) unmodified PGC	97
3.12	Comparison of the low pH mixed-mode separation of five organic compounds by Aniline-PGC and unmodified PGC	99
3.13	Stability of Aniline-PGC under acidic conditions	101
4.1	Structures of analytes used to characterize the Catechol-PGC and Amide-PGC phases	111
4.2	Scheme for the synthesis of 4-aminocatechol	113
4.3	Expanded ¹ H-NMR spectrum (700 MHz, CD ₃ OD) showing the aromatic region of the compound synthesized in Section 4.2.2	114
4.4	Expanded HSQC spectrum (700 MHz, CD ₃ OD) showing the aromatic regions of the compound synthesized in Section 4.2.2	115
4.5	Reaction schemes for the <i>in situ</i> diazonium modification of PGC particles with catechol and amide groups	118
4.6	Scheme for the synthesis of 4-amino-5-bromocatechol (compound 4)	124
4.7	Raw high-resolution N 1s XPS spectrum of Amide-PGC	126
4.8	Retention behavior of phenylpropanolamine and resorcinol on Catechol-PGC as a function of % ACN in the eluent	127
4.9	Retention behavior of cytosine and uracil on Amide-PGC as a function of % ACN in the eluent	128
4.10	Partitioning versus adsorption behavior on (A,B) Catechol-PGC and (C,D) Amide-PGC	131
4.11	HILIC separations of (A) phenols and (B) nucleosides, and the separation of ephedrine in (C) HILIC mode and (D) RP mode	133
4.12	Attenuated reversed phase separation of alkaline pharmaceuticals on Amide-PGC	137
4.13	Comparison of the retention behavior of C ₁ -C ₆ n-alkylbenzenes under reversed phase conditions on Amide-PGC and unmodified PGC	139
5.1	Comparison of the viscosities of aqueous mixtures of acetonitrile, methanol, and ethanol	150
5.2	UV absorbance spectra of seven brands of vodka	152
5.3	Welch et al.'s gradient RPLC separation of a 5-compound mixture using Smirnoff vodka as an eluent	153
5.4	Comparison of the gradient separation of four analytes (A) before and (B) after Brita filtration	154
5.5	Gradient separation of four analytes using (A) Absolut vodka and (B) Ketel One vodka as the organic eluent	156

5.6	UV absorption spectra of HPLC grade acetonitrile, methanol, and ethanol	158
5.7	Welch et al.'s gradient RPLC separation of a mixture of five analytes using 95 % aqueous HPLC ethanol and grain alcohol as eluents	160
6.1	Scheme for the proposed synthesis of ZIC-PGC	170
6.2	Scheme for the proposed synthesis of PAA-PGC	172

LIST OF SYMBOLS AND ABBREVIATIONS

1D-NMR	One-dimensional NMR
^1H -NMR	Proton NMR
2D-LC	Two-dimensional liquid chromatography
2D-NMR	Two-dimensional NMR
^{13}C -NMR	Carbon NMR
A term	Eddy diffusion (multipath) band broadening
ACN	Acetonitrile
API	Active pharmaceutical ingredient
A_s	Asymmetry factor
br s	Broad singlet in NMR
B-term	Longitudinal band broadening
BTMA	Benzyltrimethylammonium
C	Concentration
C_M	Equilibrium concentration of analyte in mobile phase
C_S	Equilibrium concentration of analyte in stationary phase
C-term	Mass transfer band broadening
d	Doublet in NMR
d_c	Diameter of interstitial channels
DCM	Dichloromethane
dd	Double doublet in NMR
d_f	Stationary phase film thickness
DL	Detection limit

D_M	Diffusion coefficient of analyte in mobile phase
DMF	N,N-dimethylformamide
DMSO	Dimethylsulfoxide
d_p	Particle diameter
D_S	Diffusion coefficient of analyte in stationary phase
ERLIC	Electrostatic repulsion liquid chromatography
EtOH	Ethanol
Fmoc	Fluorenylmethyloxycarbonyl
GC-MS	Gas chromatography-mass spectrometry
H	Height of a theoretical plate
HILIC	Hydrophilic interaction liquid chromatography
HPLC	High performance liquid chromatography
HRESIMS	High-resolution electrospray ionization mass spectrometry
HSQC	Heterosingular quantum coherence NMR spectroscopy
ID	Internal diameter
IEC	Ion-exchange chromatography
J	Coupling constant
K	Distribution coefficient
k	Retention factor
k_w	Analyte retention in pure water
L	Column length
LC	Liquid chromatography
LC-MS	Liquid chromatography-mass spectrometry

log P	Log of octanol water partition coefficient
MeOH	Methanol
MS	Mass spectrometry
N	Peak efficiency (number of theoretical plates)
n_M	Moles of analyte in mobile phase
n_S	Moles of analyte in stationary phase
PEEK	Polyetherether ketone
PGC	Porous graphitic carbon
PREG	Polar retention on graphite
RPLC	Reversed phase liquid chromatography
R_s	Resolution
RSD	Relative standard deviation
RSF	Relative sensitivity factors
S	Slope of line in linear solvent strength model
TGA	Thermogravimetric analysis
t_m	Dead time of mobile phase
TPPs	Totally porous particles
t_r	Retention time
U	Linear Velocity
UHMWPE	Ultrahigh molecular weight polyethylene
UHPLC	Ultra-high performance liquid chromatography
USP	United States Pharmacopeia
V_M	Volume of mobile phase

V_s	Volume of stationary phase
(V/V%)	Volume-volume percentage concentration
w, w_b	Baseline peak width
WADA	World Anti-Doping Agency
$w^s\text{pH}$	pH of aqueous/organic mixture measured based on aqueous calibration
$w^w\text{pH}$	pH of aqueous component measured based on aqueous calibration
$w^w\text{pK}_a$	Negative log of acidity constant for analyte in an aqueous solution
XPS	X-ray photoelectron spectroscopy
α	Selectivity factor
ΔP	Pressure drop across a column
λ	Packing factor (for band broadening only)
λ	Wavelength
λ_{max}	Wavelength of maximum absorption
Φ	Flow resistance
φ	Volume fraction of strong solvent in eluent
ψ	Obstruction factor of packed bed

CHAPTER 1: Introduction to High Pressure Liquid Chromatography

1.1 Motivation and Thesis Overview

When brought down to the simplest of terms, the primary role of the Analytical Chemist is to determine the identity of the components of a sample and their quantities present. To be successful in their role, the chemist needs the proper tools and techniques to complete their analyses. As sample matrices become more complex, the hyphenation of separation techniques to the detection system become essential. High performance liquid chromatography (HPLC) is an invaluable tool for the separation and analysis of complex samples such as biological fluids, pharmaceuticals, and environmental samples (e.g., identification and quantification of contaminants in river water). As will hopefully become clear throughout this thesis, the heart of any HPLC separation lies in the column. While much research and development has gone into the understanding of HPLC column behavior and improvement of column chemistries, there is still much work to be done since ‘unresolvable mixtures’ still exist under current technology.

Hydrophilic interaction liquid chromatography (HILIC, **Section 1.2.2.2**) continues to rapidly gain in popularity due to its ability to retain and resolve highly polar hydrophilic analytes which cannot be separated by traditional reversed phase liquid chromatography¹ (RPLC, **Section 1.2.2.1**). Many different HILIC column chemistries are now available (see **Section 1.2.2.2**) and they all offer different selectivities. Furthermore, the selectivities of these phases may be tuned by adjusting the composition of the mobile phase (e.g., pH and buffer concentration).^{2,3} Several research groups have undertaken in depth studies of the selectivity behavior of different HILIC phases under different mobile phase conditions.²⁻¹⁰ However, to date there has been no large-scale comprehensive study

to understand the *changes* in selectivity that occurs amongst the different classes of HILIC stationary phases when mobile phase pH or buffer concentration is altered. In **Chapter 2** I utilize a modified version of Mohammed Ibrahim's selectivity plots¹¹ to investigate the effects of changing the mobile phase pH and buffer concentration on the selectivity behavior of 19 different HILIC columns. Such information is invaluable to the chromatographer as it helps them to understand which HILIC stationary phase and which mobile phase conditions are appropriate for a particular separation, and why this is so.

Silica remains the most common choice of column packing material on account of its ease of functionalization and its ability to produce high efficiency (N, **Section 1.2.3.1**) separations. Bonded silica, however, has a limited working range with respect to pH (2-8) and temperature (≤ 60 °C).¹² Porous graphitic carbon (PGC) is an attractive alternative to silica due to its pH (1-14) and thermal (≤ 200 °C) stability.¹³ In addition, PGC is known as the ultimate reversed phase because of its strong hydrophobicity, and its increased RPLC retention of most weakly to moderately polar analytes.¹³ Unfortunately, in some instances this retention is too excessive, leading to poor peak shapes and longer retention times. In an effort to increase the hydrophilicity of PGC and to reduce its excessive retention, **Chapters 3** and **4** investigate the diazonium modification of PGC with aniline (**Chapter 3**) and catechol and amide (**Chapter 4**) groups, respectively. Each modified PGC phase was chromatographically characterized using a variety of analytes of different polarities and retention factors (*k*). The Aniline-PGC phase (**Chapter 3**) in particular demonstrated mixed-mode behavior; it acted both as a HILIC phase and as an attenuated reversed phase column.

In **Chapter 5** I switch focus from the column to the eluent. To ensure a successful analysis, the choice of HPLC eluent must be carefully considered. Most analytical methods today call for the use of acetonitrile (ACN) or methanol (MeOH) as the organic modifier. Many analysts, however, may not necessarily understand why this is so. Concurrently, the green chemistry movement is pushing towards the use of less toxic alternatives, such as ethanol, in HPLC analyses. Hence, I follow up on the recent work of Welch *et al.*¹⁴ to investigate the pros and cons of ethanol as an alternative solvent for RPLC. Additionally, throughout the chapter I outline the important considerations one must keep in mind when choosing an organic eluent for a HPLC analysis.

Chapter 6 wraps up the thesis with overall conclusions and a future outlook of work still to be done.

1.2 High Performance Liquid Chromatography

One of the best known early chemical separations was reported in the early 1900's by Mikhail Tswett when he described the separation of plant pigments.¹⁵ He named this separation process chromatography, deriving from the Greek words *chroma* (color) and *graphein* (write). In any liquid-based chromatographic separation, the analytes are dissolved into a solvent (known as the mobile phase) and carried through a column containing a tightly packed bed of particles (the stationary phase). Successful separation relies on differing degrees of interaction between the analytes and the stationary phase. Hence, analytes with higher affinity for the stationary phase will elute (leave the column) slower, while those with lower affinity for the stationary phase will elute faster. The actual interaction of the analytes with the stationary phase requires

physical movement (mass transfer) of the analytes between the mobile phase and the stationary phase. If this movement is slow, broad peaks will result. To hasten the mass transfer process and narrow the peaks, smaller diameter particles are used (see **Section 1.2.1.5** for more information on band broadening). The use of smaller particles, however, requires utilization of strong pumping systems to force the mobile phase through these beds of small packed particles. In response to this, Horvath and coworkers developed the first HPLC systems in the 1960's.^{16,17}

A block diagram of a typical HPLC system is shown in **Figure 1.1**. Here, eluent is pumped by high pressure pumps through a column containing the stationary phase. The injector injects a reproducible volume of the sample solution into the mobile phase stream passing into the column from the pumps. The analytes are separated as they pass through the column, and are detected by the detector as they elute from the column. The computer system controls all the components of the HPLC system and stores and displays the chromatographic data.

Since the first HPLC system was invented, HPLC has become one of the most powerful tools in analytical chemistry. One of the most significant developments in this time has been the introduction of sub-2 μm particles for use in ultra-fast high efficiency separations.^{18,19} Because of the high backpressure and high efficiency afforded by these particles a new class of HPLC system, dubbed ultra-high performance liquid chromatography (UHPLC), was developed which could handle the 15 000+ psi (1000+ bar) backpressures generated by use of these particles.¹⁹ Additionally, these systems are designed to significantly minimize extra-column band broadening; a factor that becomes very important in UHPLC separations.

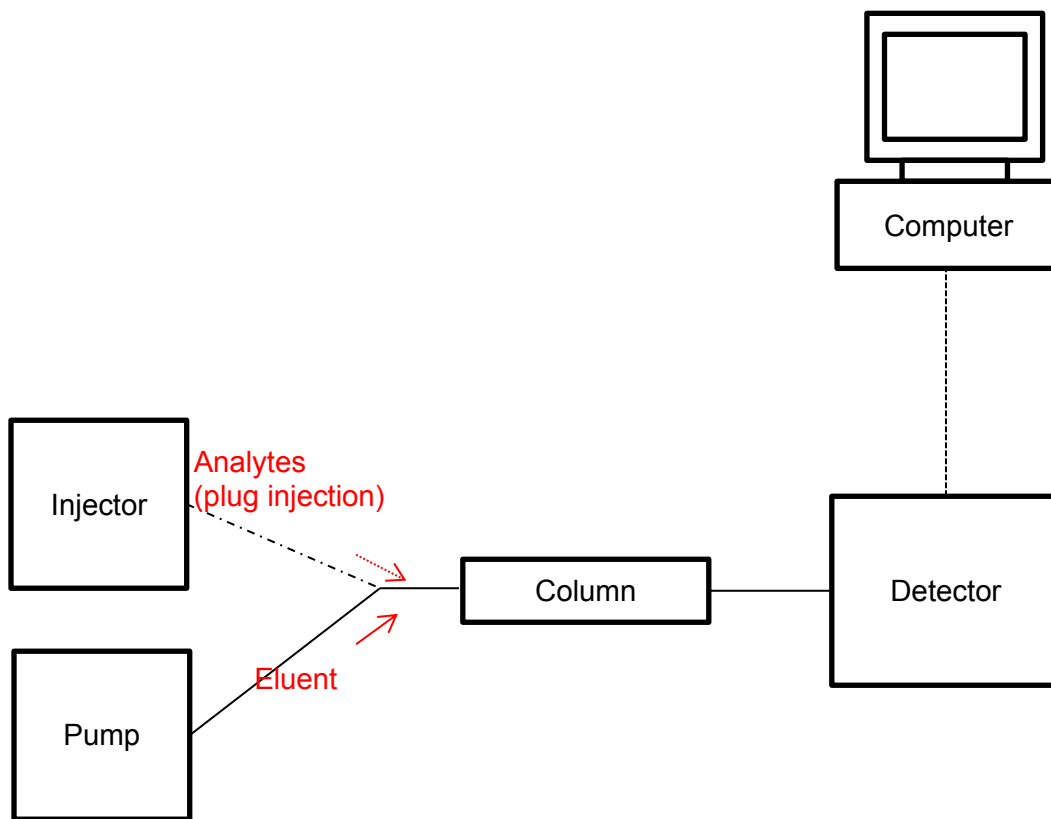


Figure 1.1. Schematic of the different parts of a modern HPLC system.

The first such UHPLC system was commercialized by the Waters Corporation in 2004.¹⁹ Waters and other companies have since developed improved UHPLC systems with even lower dead volumes and pressure capabilities up to 22 000 psi (~1500 Bar).²⁰

Based on the chemistry of the column and the eluent, four main modes of HPLC exist: reversed phase, normal phase, HILIC, and ion exchange. An overview of all of these liquid chromatographic modes, except normal phase (which is outside the scope of this thesis), will be given in **Section 1.2.2**.

*1.2.1 Important Equations and Theories in HPLC*²¹

1.2.1.1 Resolution

In any separation the primary goal is to gain adequate separation (resolution) between the peaks. Practically speaking, resolution is calculated from a chromatogram using **Equation 1.1**.

$$R_s = \frac{2(t_2 - t_1)}{w_1 + w_2} \quad (1.1)$$

where t_2 and t_1 are the uncorrected retention times of analyte 2 (later eluting) and analyte 1 (earlier eluting) and w_1 and w_2 are the baseline peak widths of the two analytes. A value of $R_s \geq 1.5$ between two peaks is considered baseline resolution, and is sufficient for quantitative analysis.

From a method development standpoint, the resolution equation may be expressed in an alternate way (**Equation 1.2**) to allow one to consider the major contributing factors to a successful separation: retention (k), selectivity (α), and peak efficiency (N). Each of these three terms will be discussed in the following subsections.

$$R_s = \left(\frac{\sqrt{N}}{4}\right) \left(\frac{k}{1+k}\right) \left(\frac{\alpha-1}{\alpha}\right) \quad (1.2)$$

1.2.1.2 Retention

Fundamentally, a chromatographic separation is based on a thermodynamic equilibrium of an analyte (A) transferring between the stationary phase (S) and the mobile phase:



The above equilibrium may be described by a distribution constant (K) which is a ratio of the concentrations of the sample in the stationary phase (C_S) and mobile phase (C_M) as given in **Equation 1.4**.

$$K = \frac{C_S}{C_M} \quad (1.4)$$

A means to quantify retention is the retention factor (k). It describes the ratio of the moles of analyte in the stationary phase (n_S) to the moles of analyte in the mobile phase (n_M) as in **Equation 1.5**.

$$k = \frac{n_S}{n_M} \quad (1.5)$$

The retention factor (**Equation 1.5**) is related to the distribution constant (**Equation 1.4**) through **Equation 1.6**.

$$k = K \frac{V_S}{V_M} \quad (1.6)$$

where V_S is the volume of the stationary phase and V_M is the volume of the mobile phase.

A more practical means of expressing k is using time (**Equation 1.7**).

$$k = \frac{t_R - t_M}{t_M} \quad (1.7)$$

where t_R is the retention time of the analyte and t_M is the time required for an unretained analyte to elute from the column (aka dead time).

1.2.1.3 Selectivity Factor

When developing a new analytical separation method or understanding the behavior of a stationary phase (as in **Chapter 2**), chromatographers are most often concerned with a column's selectivity. The selectivity factor (α , **Equation 1.8**) is another means of quantifying the spacing between two analyte peaks.

$$\alpha_{i,j} = \frac{k_j}{k_i} \quad (1.8)$$

1.2.1.4 Peak Efficiency (N) and Plate Height (H)

As an analyte band moves through the column it broadens. The sharpness of the peak is expressed as peak efficiency in terms of number of theoretical plates (N), and as plate height (H, size of theoretical plate). An ideal peak will have a higher number of theoretical plates and a shorter plate height. **Equation 1.9** describes the United States Pharmacopeia (USP) method for measurement of peak efficiency.

$$N = 16 \left(\frac{t_R}{w_b} \right)^2 \quad (1.9)$$

where t_R is the retention time of the peak of interest and w_b is the peak width measured at the baseline. This method was used to measure the efficiencies reported in **Chapters 3** and **4**. Plate heights are determined according to **Equation 1.10**.

$$H = \frac{L}{N} \quad (1.10)$$

where L is the length of the column.

1.2.1.5 Band Broadening in Liquid Chromatography

Ideally, an analyte would elute from the column as a very narrow peak. In reality, all retained analytes experiences varying degrees of broadening due to several processes. These processes are described by the van Deemter equation²² (**Equation 1.11**) which encompasses three main contributions to band spreading: eddy diffusion (A term), longitudinal diffusion (B term), and resistance to mass transfer (C term). These parameters are related to the plate height (H) and mobile phase linear velocity (u) via this equation.

$$H = A + \frac{B}{u} + Cu \quad (1.11)$$

Eddy diffusion (or multipath broadening) arises from the variation of the density of packing within a column. This variation leads to flow paths of different lengths as demonstrated in **Figure 1.2**. Analyte molecules flowing through narrower or more tortuous channels will travel slower and take longer to exit the column than those that can flow through larger or more open channels; hence band spreading will occur. This process is described mathematically according to **Equation 1.12**.

$$A = 2\lambda d_p \quad (1.12)$$

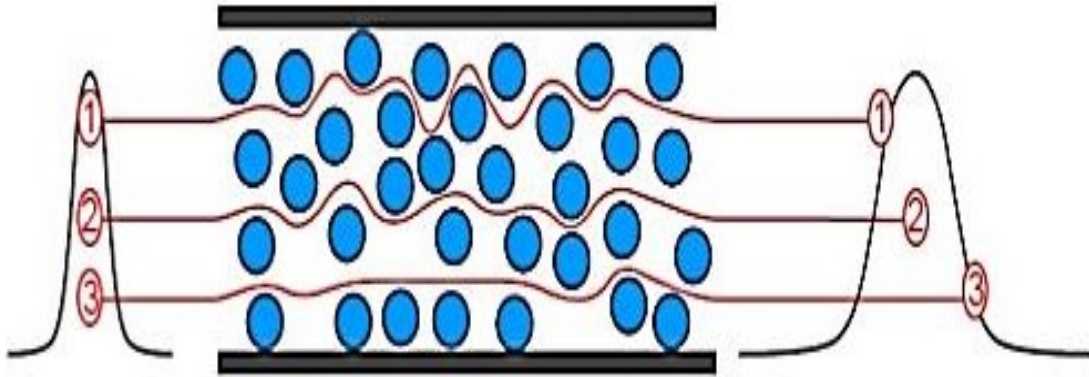


Figure 1.2. Schematic representation of Eddy diffusion (A-term). Adapted from M. Galalzidan.²³

where λ is the packing factor of a given column and d_p is the particle size. A poorly packed column will have a higher packing factor and greater A-term broadening. This phenomena is independent of flow rate (**Figure 1.3**) and of the degree of analyte retention.²⁴ Recent investigations have indicated that up to 60 % of all band broadening in UHPLC columns can be attributed to eddy diffusion.²⁵ Hence, much current work by column manufacturers is focused on reducing the distribution of particle sizes and increasing the uniformity of the packed bed.

As an analyte travels along the column, it undergoes longitudinal random motion in both the forward and backward directions. These movements are promoted by the presence of a concentration gradient within the column and further contribute to band broadening (B-term, longitudinal diffusion). **Equation 1.13** provides a simplified mathematical description of this process (Gritti *et al.*²⁴ has recently shown that several other factors further contribute to longitudinal diffusion) whereby longitudinal diffusion is related to the obstruction factor (ψ) and the diffusion coefficient of the analyte in the mobile phase (D_M).

$$B = 2\psi D_M \quad (1.13)$$

By using higher mobile phase velocities, longitudinal broadening can be minimized (**Figure 1.3**). That said, under standard HPLC conditions the B-term is minimal due to the liquid mobile phase possessing a small diffusion coefficient. However, under UHPLC conditions the C-term (discussed below) is much smaller. As such, the B term becomes comparable to the C-term so higher linear velocities must be utilized to minimize plate heights.

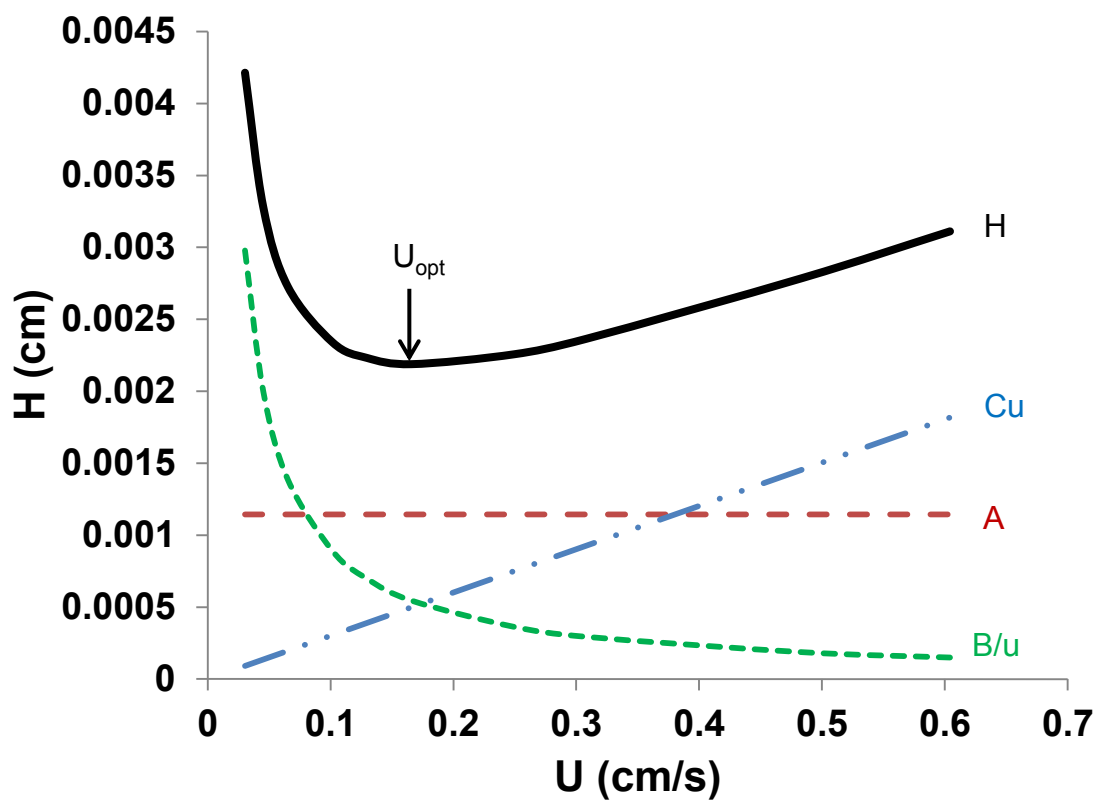


Figure 1.3. The van Deemter plot (solid curved line). Data from Katz *et al.*²⁶

The final major contribution to band broadening within the column is the resistance to mass transfer of the analyte within the stationary phase (C_S) and mobile phase (C_M). If an analyte diffuses slowly, it will be carried forward by the mobile phase before equilibrium is achieved between the stationary phase and mobile phase. Increased linear velocity worsens the problem (**Figure 1.3**). C_S and C_M are described mathematically as **Equations 1.14** and **1.15**, respectively.

$$C_S = \frac{8}{\pi^2} \frac{k}{(1+k)^2} \frac{d_f^2}{D_S} \quad (1.14)$$

$$C_M = \frac{(1+6k+11k^2)d_c^2}{96(1+k)^2 D_M} \quad (1.15)$$

where d_f is the film thickness of the stationary phase, d_c is the diameter of the spaces between the particles which are occupied by mobile phase, and D_S and D_M are the analyte diffusion coefficients in the stationary and mobile phases. Like the B-term, **Equations 1.14** and **1.15** provide simplified representations of the mass transfer processes.²⁴ As discussed in **Section 1.2.3.1.2**, more uniform particles are beneficial in improving efficiency as they reduce the size of the interstitial channels (d_c).

1.2.1.6 Column Backpressure

Based on the previous discussion of band broadening the question may arise as to why particles are not made infinitely small to greatly improve efficiency? One reason is that as the particle size decreases, it becomes more difficult to maintain uniformity in particle diameter, thereby increasing the A-term broadening and diminishing the potential returns. The ultimate limitation, however, to particle size is the ability of the HPLC or UHPLC instrumentation to handle the resulting significant increase in column

backpressure accompanying the reduction in particle size. A typical HPLC system can pump at pressures up to 6000 psi (400 bar), while modern UHPLC systems can handle pressures above 20 000 psi (1300 bar). Darcy's law (**Equation 1.16**) describes the relationship between column backpressure (ΔP) observed across a column of length L and linear velocity (u), viscosity (η), flow resistance (Φ), and particle diameter (d_p).

$$\Delta P = \frac{u\eta\phi L}{d_p^2} \quad (1.16)$$

Thus, reducing the particle diameter by half will increase the column backpressure by 4-fold. As will be discussed in **Chapter 5**, Darcy's law also has implications on the choice of mobile phase used due to differing viscosities amongst organic solvents.

1.2.1.7 Asymmetry Factor

Although symmetrical Gaussian peaks are predicted by **Section 1.2.1.4** and preferred, such idealized behavior is often not observed. Column overload and strong interactions between the analyte and the stationary phase (amongst other factors) can lead to asymmetrical peaks. The degree of asymmetry is determined by the asymmetry factor (A_s). The asymmetry factor is determined by drawing a vertical line through the peak maximum and calculating the ratio of the later eluting (B) to the earlier eluting (A) portion of the peak width at 10 % of the maximum peak height. This procedure is illustrated in **Figure 1.4**. A value of $A_s = 1$ indicates a perfectly symmetrical peak; $A_s < 1$ indicates fronting; $A_s > 1$ (more common in HPLC) indicates tailing.

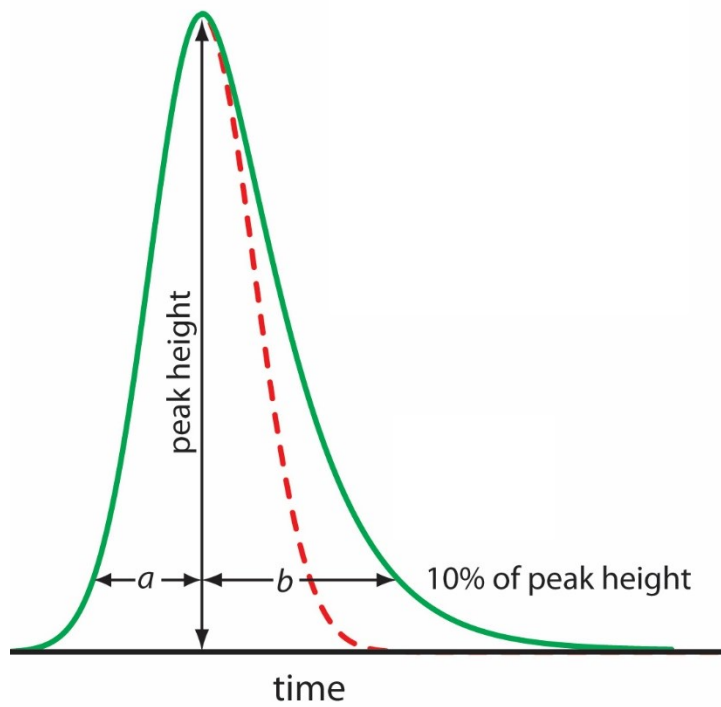


Figure 1.4. Measurement of the asymmetry factor ($A_s = B/A$) of a tailing peak. The red dotted line indicates the boundary of a normal Gaussian peak. Adapted from the University of California Davis Chem Wiki.²⁷

1.2.2 Relevant Modes of Liquid Chromatography

1.2.2.1 Reversed Phase Liquid Chromatography (RPLC)

Today, RPLC is the workhorse of liquid chromatography. This separation mode utilizes a non-polar stationary phase in conjunction with a polar eluent to separate mixtures of weakly to moderately polar analytes. The stationary phase is most typically C₈ or C₁₈ alkyl bonded silica, albeit the use of alternative materials such as porous graphitic carbon and porous polymers is also prevalent (see **Section 1.2.3** for a description of common HPLC packing materials). The mobile phase typically consists of a mixture of water (buffered if the sample contains ionisable compounds) and a polar organic solvent such as methanol or acetonitrile.

Separation in RPLC arises from the differential partitioning of analytes between the stationary phase and the mobile phase. Retention of the analyte depends on the polarity of the analyte and the strength of the mobile phase. A higher polarity analyte will more strongly interact with the polar mobile phase via polar interactions (such as hydrogen bonding and dipolar interactions) and hence will elute sooner. A lower polarity analyte, conversely, will not interact as strongly with the mobile phase and will be more retained by the stationary phase. Thus, by adding more organic solvent to the eluent mixture, the polarity of the organic phase decreases, and all analytes elute faster. The relationship between retention of analyte and the overall strength of the eluent mixture is described by the linear solvent strength model²⁸ (**Equation 1.17**).

$$\log k = \log k_w - S\phi \quad (1.17)$$

where ϕ is the volume fraction of the strong solvent (organic component for RPLC); k_w is the retention of the analyte in the absence of the strong solvent (i.e., pure water); and S is

the slope of the line. Thus, for a partitioning mechanism (such as RPLC) a plot of $\log k$ vs. ϕ should yield a straight line. However, this model is an approximation which generally displays linear behavior over limited solvent ranges between 10-90 % organic eluent, but not at the extremes.

1.2.2.2 Hydrophilic Interaction Liquid Chromatography (HILIC)

Although RPLC can be used to resolve a large proportion of organic analytes, highly polar analytes such as metabolites (e.g., sugars, nucleobases, and amino acids) and pharmaceutical compounds are difficult to resolve by RPLC due to their low retention by the nonpolar stationary phase. In 1990, Andrew Alpert first coined the term ‘hydrophilic interaction liquid chromatography’ (HILIC) for the separation of peptides and carbohydrates.²⁹ Today, HILIC is an increasingly popular mode of liquid chromatography for the separation of these highly polar hydrophilic analytes.³⁰ Also popularly (but incorrectly) known as “aqueous normal phase” liquid chromatography, HILIC utilizes a polar stationary phase in conjunction with a polar RPLC-type eluent (typically 70-95 % acetonitrile in buffered water). Unlike in RPLC, however, water is the stronger solvent in HILIC mode. Additionally, the retention order is reversed relative to RPLC; that is, the higher polarity analytes favor stronger interactions with the polar stationary phase and hydrophilic layer (see following discussion), hence eluting after the less hydrophilic analytes.

Since Alpert’s original paper,²⁹ much work has been done to understand the separation mechanism of HILIC. It is currently accepted that retention in HILIC arises

from a combination of partitioning into a water-rich layer that forms on the surface of the stationary phase³¹ (**Figure 1.5**), and other interactions such as adsorption.³²

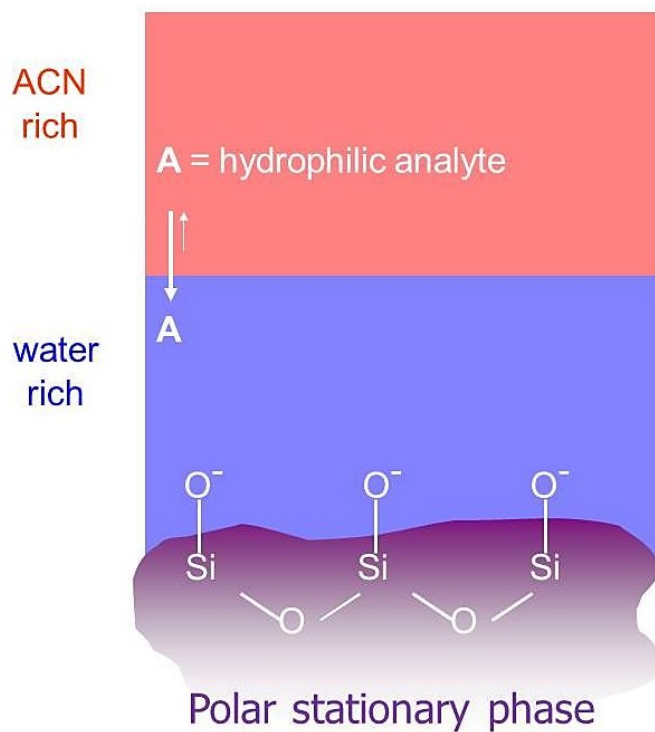


Figure 1.5. Representation of analyte-water-layer partitioning in HILIC. Adapted from C.A. Lucy.³³

Secondary interactions between the analytes and the stationary phase such as ion exchange, hydrogen bonding, and dipole interactions (**Figure 1.6**) further contribute to the retention and selectivity behavior of different HILIC phases.² Further discussion of the basis of HILIC selectivity is given in **Chapter 2**.

Table 1.1 illustrates the structures of some of the common HILIC stationary phases available today. These phases may be based on either a silica or polymeric backbone (see **Section 1.2.3** for information on column supports), and as shown in **Table 1.1**, classified based on their functionalities as neutral, cationic, anionic, or zwitterionic.

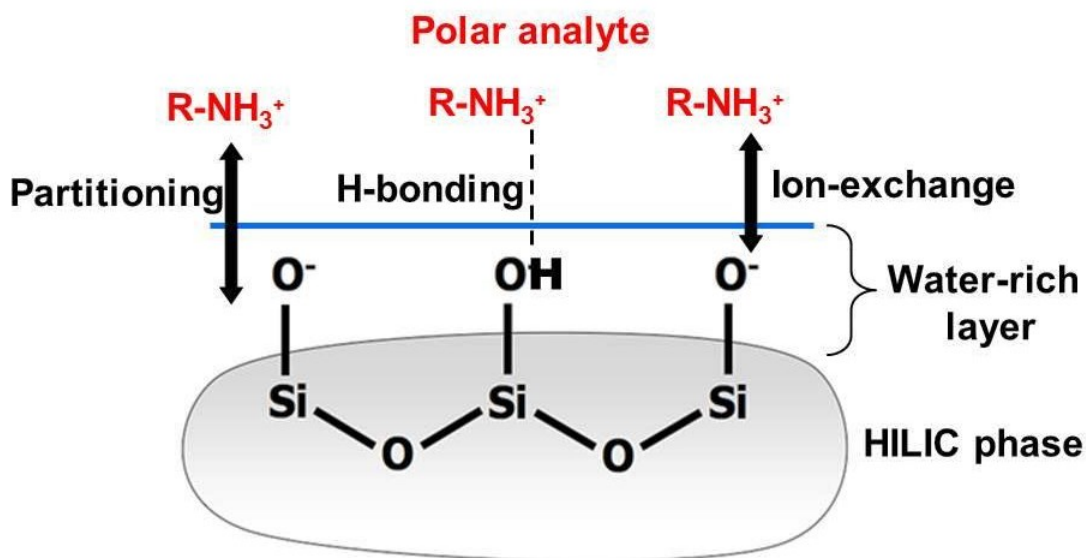


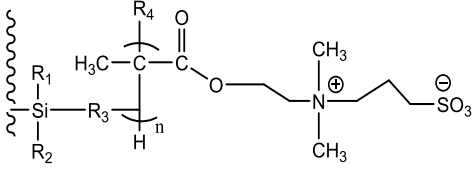
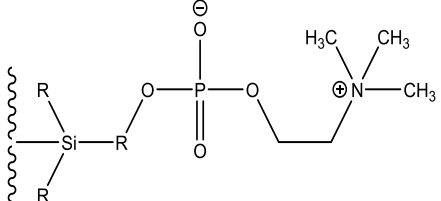
Figure 1.6. Schematic representation of some of the secondary interactions influencing HILIC retention and selectivity. Reproduced with permission from Dr. M. E. Ibrahim.³⁴

Table 1.1. Representative structures of common stationary phases in HILIC.

Charge	Functionality	Representative structure
Neutral	Amide	
	Diol	
	Cross-linked diol	
	Cyclodextrin ^a	
	Cyanopropyl	
Cationic	Aminopropyl	
	Triazole	
Anionic	Underivatized silica	

^aCyclodextrin structure adapted from Sigma-Aldrich.³⁵

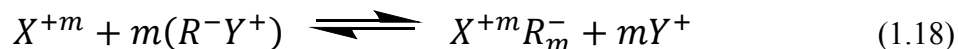
Table 1.1 continued.

Zwitterionic	Sulfoalkylbetaine	
	Phosphorylcholine	

1.2.2.3 Ion Exchange Chromatography^{21,36}

While the first reports of ion exchange chromatography (IEC) date back to 1850, modern analytical ion chromatography arises from the work of Small *et al.* in 1975.³⁷ Today, IEC is commonly used for the separation of inorganic anions and cations, as well as peptides proteins, polymers, and charged small organic molecules. This thesis will focus on the organic small molecule applications of IEC. The majority of ion exchangers are polymer based, and mainly impart retention due to their charged bonded functional groups, albeit other interactions (e.g., hydrophobic) may contribute to retention and selectivity.³⁸ Eluents in IEC mainly consist of an aqueous salt solution plus perhaps a small percentage of organic solvent (such as acetonitrile) to facilitate dissolution of the analyte. Retention of strong ion exchanging analytes is decreased by using a higher salt concentration.

Based on the charge on the analyte, IEC is subdivided into two types: cation exchange chromatography and anion exchange chromatography. Cation exchange chromatography uses a negatively charged stationary phase for the separation of cations while anion exchange chromatography uses a positively charged stationary phase for the separation of anions. Focusing on cation exchange chromatography, the process of ion exchange between analyte cations and the negatively stationary phase is described by **Equation 1.18**.



where X, R, and Y, are the analyte, negatively charged stationary (resin) phase, and eluent ion, respectively; m is the absolute charge ($|z|$) on the analyte.

The retention of a cationic analyte is then given by **Equation 1.19**.

$$\log k = \text{constant} - m \log C \quad (1.19)$$

where k is the retention factor, m is the absolute charge ($|z|$) on the analyte, and C is the molar concentration of the counter-ion. Hence a plot of $\log k$ vs. $\log C$ should produce a straight line with a slope of m for a pure ion exchange model.³⁹⁻⁴¹

1.2.3 Common Column Supports in HPLC

1.2.3.1 Silica

Silica is the most commonly used HPLC column packing material for several reasons. Firstly, silica's high mechanical strength allows for the formation of packed beds that remain stable under high operating pressures. Secondly, compared to other packing materials (see **Section 1.2.3.2**), silica provides significantly higher peak efficiency (N) due to its uniform particle size and open pore structure. Thirdly, silica is easy to chemically modify. Although unmodified silica is often a popular choice for some HILIC separations (see **Section 1.2.2.2**), most silica phases contain alkyl bonded groups. Addition of these alkyl groups is readily achieved through reaction of the surface silanols (Si-OH , present at a surface concentration of $\sim 8 \mu\text{mol/m}^3$)⁴² with a chlorosilane possessing the desired alkyl moiety (R_1) of interest (**Figure 1.7**). As noted previously in this chapter, the R_1 groups are typically hydrophobic (C_8 or C_{18}) for RPLC, while HILIC phases normally contain a polar hydrophilic group (see **Table 1.1** for representative examples). The R_2 groups are often methyl, ethyl, or *t*-butyl groups and act to block unwanted interactions (especially in RPLC phases) from unreacted silanol sites on the silica surface.

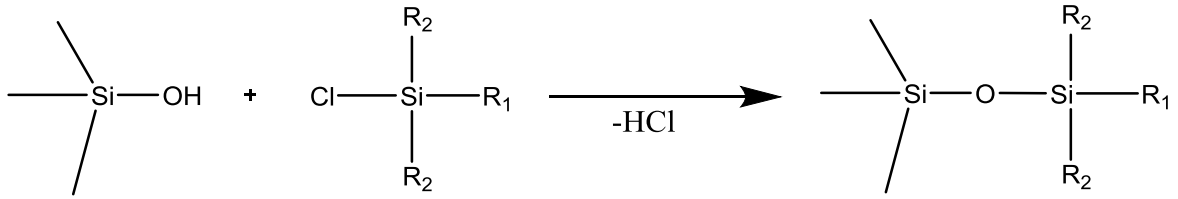


Figure 1.7. General scheme for the preparation of a bonded silica phase.

Irrespective of the bonding chemistry, silica packing materials commonly exist in several forms.

1.2.3.1.1 Totally Porous Particles

Totally porous particles (TPPs) have traditionally been the most commonly used form of silica packing material in modern HPLC columns. The particles are spherical in nature and contain numerous pores of controllable sizes passing through the particle. The bonded groups are found throughout all surfaces of the particle, but especially within the pores. Hence, the resulting high surface area for chromatographic interaction gives these particles the capacity to handle injection of a larger mass of sample. TPPs are currently commercially available in several diameters ranging from $>10 \mu\text{m}$ down to $<1 \mu\text{m}$.

1.2.3.1.2 Core Shell Particles

As mentioned in **Section 1.2.1.5**, smaller diameter particles provide very high efficiency separations which allow for shortened run times. However, the potential gain in efficiency is significantly offset by the significant increase in column backpressure ($\Delta P \propto 1/d_p^2$; see **Section 1.2.1.6**). To accommodate the $>10\,000$ psi backpressures associated with these small diameter particles, special UHPLC instrumentation is required.

In response to the need for high efficiencies without the use of more expensive UHPLC equipment, core shell particles have recently gained significant popularity.⁴³ Such particles consist of a solid core surrounded by a thin porous layer (aka superficially porous particles). The advantage of core shell particles are that they are able to attain comparable or better efficiencies as sub-2 μm TPPs while maintaining a diameter of 3.5-5 μm and the associated lower backpressure of such particle sizes. (Note: TPP's in smaller particle diameters are now commercially available). The reasons for the improved efficiencies attained by core-shell particles are twofold: 1) the smaller thickness of the shell reduces mass transfer distance, thereby reducing C-term broadening (see **Section 1.2.1.5**); and 2) more importantly, the uniform shape of core-shell particles reduces the packing factor (λ), significantly reducing A-term broadening (**Equation 1.12**).

Although these improvements in efficiency are paramount, one must be aware that the lower surface area of core-shell particles equates to lower sample capacity. This consideration is of particular importance to pharmaceutical analysts who must be able to resolve, identify, and quantify trace impurities within a sample containing a high concentration of the active pharmaceutical ingredient (API).

1.2.3.1.3 Silica Monoliths

Although currently less popular than core-shell particles, silica monoliths are another high efficiency low backpressure alternative to TPPs.^{44,45} Silica monoliths are prepared as rods from a single piece of porous silica. Surface modification is then carried out after the rod is encapsulated within the column. Inside the monolith two types of pores exist: large macropores ($\sim 2 \mu\text{m}$ diameter) and small mesopores ($\sim 10 \text{ nm}$ diameter).

The mesopores give the monolith a very high surface area ($\sim 300 \text{ m}^2/\text{g}$) while the lower backpressure in monolithic columns arises from the mobile phase mainly flowing through the relatively wide low-resistance macropores.

Nevertheless, monolithic phases do suffer from several limitations.²¹ These include a limited availability of different stationary phase chemistries; a restricted range of column dimensions; and a tendency for all compounds, including both ionisable and neutral, to show peak tailing.

1.2.3.2 Silica Alternatives

Although silica is the material of choice for many HPLC separations, the chemical properties of bonded silica restrict its applicability in some instances. Specifically, bonded silica phases are only useable in the pH range of 2 to 8. Below pH 2 the bonding material is hydrolyzed, while above pH 8 silica dissolves.⁴⁶⁻⁴⁸ Since both chemical processes are accelerated at high temperature, most column manufacturers recommend operating temperatures of no higher than $60 \text{ }^\circ\text{C}$.⁴⁸ For separations under conditions where silica is not useful (e.g., high pH separations of strong bases or very high speed high temperature separations), several alternative materials have been developed. Examples of such alternatives include porous polymeric phases and porous graphitic carbon, which are discussed below.

1.2.3.2.1 Porous Polymers

Porous polymeric phases are one of the most commonly used silica alternatives. The majority of polymeric phases are based on a cross-linked polystyrene backbone.⁴⁹ This backbone can be derivatized with a variety of functionalities for different modes of

HPLC, including C₁₈ for RPLC, polar groups for HILIC, and ionic groups for ion exchange chromatography.^{21,49} Compared to silica-based phases, however, the number of different commercially available bonded polymeric phases is small.

The main advantage of these polymeric phases is their tolerance of pH across the entire spectrum (1-14).⁴⁹ Continuing from the example in the previous section, the separation of a mixture of strong organic bases could be performed at a mobile phase pH above 10. Deprotonation of the bases increases RPLC retentivity and improves peak shape through the elimination of the analytes' positive charges.

Polymeric phases, however, do suffer from some limitations. Compared to a porous silica particle of similar size, a porous polymeric particle exhibits lower peak efficiency (N).²¹ Additionally, a more significant drawback is that many polymeric phases swell or shrink with changing concentrations of the organic mobile phase component. This is especially problematic for gradient separations, and may cause significant losses of peak efficiency and large fluctuations in column backpressure. Some polymeric phases which are designed to minimize swelling are now commercially available.³¹

1.2.3.2.2 Porous Graphitic Carbon (PGC)

In the 1980's, Knox and co-workers introduced porous graphitic carbon (PGC) as a chemically robust alternative to silica.⁵⁰ PGC consists of continuous layers of hexagonal graphite. Due to the structure of this material, unique selectivity is achieved through a different separation mechanism.^{13,51} Like porous polymeric phases, PGC is stable across pH 1-14. Unlike the porous polymeric phases, however, PGC is

mechanically stable, will not swell or shrink in response to organic solvents, and can withstand high temperatures (≤ 200 °C).¹³ Because of its chemical nature and hydrophobicity, PGC is primarily utilized in RPLC separations. Nevertheless, PGC will weakly retain polar analytes via dipolar interactions. The retention of polar analytes by PGC is known as the polar retention on graphite (PREG) effect.^{13,51} **Chapters 3 and 4** further discuss the properties of PGC and explore the use of diazonium chemistry to generate aniline, catechol, and amide modified PGC phases with unique hydrophilic selectivities.

1.3 Summary

HPLC has become an invaluable tool in modern Analytical Chemistry. The majority of HPLC separations are performed under either reversed-phase or HILIC modes. In **Chapter 2**, a comprehensive investigation is carried out to determine the changes in selectivity behavior of different classes of HILIC stationary phases in response to changes in mobile phase pH or buffer concentration. It was generally observed in these studies that the selectivity behavior of silica based phases is dominated by silanol activity, and that increased buffer concentration mutes ionic interactions between the analyte and stationary phase. **Chapters 3 and 4** describe the preparation and characterization of aniline (**Chapter 3**) and catechol and amide- (**Chapter 4**) modified PGC phases, respectively. All phases demonstrated mixed HILIC and RPLC behaviour for a variety of analytes and increased hydrophilicity overall compared to unmodified PGC. Lastly, **Chapter 5** looks at the pros and cons of the use of ethanol as an alternative

RPLC eluent, and in doing so, discusses the important factors to consider when choosing a mobile phase for a separation.

1.4 References

- (1) Hemström, P.; Jonsson, T.; Appelblad, P.; Jiang, W. *Chromatogr. Today* **2011**, 4–8.
- (2) Dinh, N. P.; Jonsson, T.; Irgum, K. *J. Chromatogr. A* **2011**, *1218*, 5880–5591.
- (3) Guo, Y.; Gaiki, S. *J. Chromatogr. A* **2011**, *1218*, 5920–5938.
- (4) Guo, Y. In *Hydrophilic Interaction Liquid Chromatography (HILIC) and Advanced Applications*; Wang, P. G.; He, W., Eds.; CRC Press: Boca Raton, FL, 2011; pp. 401–426.
- (5) McCalley, D. V. *J. Chromatogr. A* **2015**, *1411*, 41–49.
- (6) Kumar, A.; Heaton, J. C.; McCalley, D. V. *J. Chromatogr. A* **2013**, *1276*, 33–46.
- (7) Kawachi, Y.; Ikegami, T.; Takubo, H.; Ikegami, Y.; Miyamoto, M.; Tanaka, N. *J. Chromatogr. A* **2011**, *1218*, 5903–5919.
- (8) Wang, J.; Guo, Z.; Shen, A.; Yu, L.; Xiao, Y.; Xue, X.; Zhang, X.; Liang, X. *J. Chromatogr. A* **2015**, *1398*, 29–46.
- (9) Periat, A.; Debrus, B.; Rudaz, S.; Guillarme, D. *J. Chromatogr. A* **2013**, *1282*, 72–83.
- (10) Schuster, G.; Lindner, W. *J. Chromatogr. A* **2013**, *1301*, 98–110.

- (11) Ibrahim, M. E. A.; Liu, Y.; Lucy, C. A. *J. Chromatogr. A* **2012**, *1260*, 126–131.
- (12) Pereira, L. *LC-GC North Am.* **2011**, *29*, 262–269.
- (13) West, C.; Elfakir, C.; Lafosse, M. *J. Chromatogr. A* **2010**, *1217*, 3201–3216.
- (14) Welch, C. J.; Nowak, T.; Joyce, L. A.; Regalado, E. L. *ACS Sustain. Chem. Eng.* **2015**, *3*, 1000–1009.
- (15) Tswett, M. *Ber. Dtsch. Bot. Ges.* **1906**, *24*, 384–393.
- (16) Unger, K. K.; Lamotte, S.; Machtejevas, E. *Liquid Chromatography*; Elsevier, 2013.
- (17) Horvath, C. G.; Preiss, B. A.; Lipsky, S. R. *Anal. Chem.* **1967**, *39*, 1422–1428.
- (18) Unger, K. K.; Ditz, R.; Machtejevas, E.; Skudas, R. *Angew. Chemie Int. Ed.* **2010**, *49*, 2300–2312.
- (19) Mazzeo, J. R.; D. Neue, U.; Kele, M.; Plumb, R. S. *Anal. Chem.* **2005**, *77*, 460 A – 467 A.
- (20) Fekete, S.; Veuthey, J.-L.; Guillarme, D. *J. Chromatogr. A* **2015**, *1408*, 1–14.
- (21) Snyder, L. R.; Kirkland, J. J.; Dolan, J. W. *Introduction to Modern Liquid Chromatography*; 3rd ed.; John Wiley & Sons: Hoboken, NJ, 2011.
- (22) van Deemter, J. J.; Zuiderweg, F. J.; Klinkenberg, A. *Chem. Eng. Sci.* **1956**, *5*, 271–289.

- (23) Galalzidian, M. Principles of Chromatography
<http://www.slideshare.net/mahmoudgalalzidan/principles-in-chromatography>
(accessed Sep 8, 2015).
- (24) Gritti, F.; Guiochon, G. *J. Chromatogr. A* **2013**, *1302*, 1–13.
- (25) Gritti, F.; Guiochon, G. *Anal. Chem.* **2013**, *85*, 3017–3035.
- (26) Katz, E.; Ogan, K. L.; Scott, R. P. W. *J. Chromatogr. A* **1983**, *270*, 51–75.
- (27) UC Davis. 12B: General Theory of Column Chromatography
http://chemwiki.ucdavis.edu/Analytical_Chemistry/Analytical_Chemistry_2.0/12_Chromatographic_and_Electrophoretic_Methods/12B%3A_General_Theory_of_Column_Chromatography (accessed Sep 8, 2015).
- (28) Snyder, L. R.; Poppe, H. *J. Chromatogr. A* **1980**, *184*, 363–413.
- (29) Alpert, A. J. *J. Chromatogr. A* **1990**, *499*, 177–196.
- (30) Guo, Y. *Analyst* **2015**, *140*, 6452–6466.
- (31) Hemström, P.; Irgum, K. *J. Sep. Sci.* **2006**, *29*, 1784–1821.
- (32) Gritti, F.; Hölzel, A.; Tallarek, U.; Guiochon, G. *J. Chromatogr. A* **2015**, *1376*, 112–125.
- (33) Lucy, C. A. Exploration and Understanding of Hydrophilic Interaction Liquid Chromatography (HILIC). Presented at Simon Fraser University, 2015.
- (34) Ibrahim, M. E. A. Development and Characterization of New Stationary Phases for

Hydrophilic Interaction Liquid Chromatography. Ph.D Thesis, University of Alberta, 2014.

- (35) Caligur, V. Cyclodextrins <http://www.sigmaaldrich.com/technical-documents/articles/biofiles/cyclodextrins.html> (accessed Nov 14, 2015).
- (36) Acikara, O. B. In *Column Chromatogr.*; InTech, 2013; pp. 31–58.
- (37) Small, H.; Stevens, T. S.; Bauman, W. C. *Anal. Chem.* **1975**, *47*, 1801–1809.
- (38) Liang, C.; Lucy, C. A. *J. Chromatogr. A* **2010**, *1217*, 8154–8160.
- (39) Madden, J. E.; Haddad, P. R. *J. Chromatogr. A* **1998**, *829*, 65–80.
- (40) Madden, J. E.; Haddad, P. R. *J. Chromatogr. A* **1999**, *850*, 29–41.
- (41) Madden, J. E.; Avdalovic, N.; Jackson, P. E.; Haddad, P. R. *J. Chromatogr. A* **1999**, *837*, 65–74.
- (42) Nawrocki, J. *J. Chromatogr. A* **1997**, *779*, 29–71.
- (43) Bell, D. S.; Majors, R. E. *LCGC North Am.* **2015**, *33*, 386–395.
- (44) Liu, K.; Aggarwal, P.; Lawson, J. S.; Tolley, H. D.; Lee, M. L. *J. Sep. Sci.* **2013**, *36*, 2767–2781.
- (45) Majors, R. E. *LCGC North Am.* **2014**, *32*, 8,10.
- (46) Kirkland, J. J. *J. Chromatogr. Sci.* **1996**, *34*, 309–313.
- (47) Kirkland, J. J.; van Straten, M. A.; Claessens, H. A. *J. Chromatogr. A* **1995**, *691*,

3–19.

- (48) Borges, E. M.; Collins, C. H. *J. Chromatogr. A* **2012**, *1227*, 174–180.
- (49) Pohl, C. *LCGC North Am.* **2013**, 16–22.
- (50) Knox, J. H.; Kaur, B.; Millward, G. R. *J. Chromatogr. A* **1986**, *352*, 3–25.
- (51) Pereira, L. *J. Liq. Chromatogr. Relat. Technol.* **2008**, *31*, 1687–1731.

CHAPTER 2: The Hydrophilicity vs. Ion Interaction HILIC Selectivity Plot

Revisited: The Effect of Mobile Phase pH and Buffer Concentration on HILIC Selectivityⁱ

2.1 Introduction

As noted in **Chapter 1**, the popularity of hydrophilic interaction liquid chromatography (HILIC) has steadily increased since Alpert¹ coined the term in 1990. This popularity is due to HILIC's ability to retain and resolve highly polar analytes that are difficult to separate by reversed phase chromatography, and to HILIC's compatibility with mass spectrometry.²⁻⁶ HILIC has been the subject of many reviews^{2,4,5,7-11} and several recent large-scale comprehensive studies.¹²⁻¹⁵ Additionally, this mode of liquid chromatography has found utility in the analysis of small molecules such as metabolites,^{2,16,17} pharmaceuticals,¹⁸⁻²³ and food chemicals,²⁴⁻³¹ as well as larger biomolecules such as glycans³²⁻³⁴ and peptides/proteins.³⁵⁻³⁸ Today, many types of HILIC phases are commercially available, including bare silica, amine, amide, diol, and zwitterionic phases^{8,39} (see **Table 1.1**).

Retention in HILIC is due to partitioning into a surface water layer that forms in the presence of an ACN-rich mobile phase as well as adsorptive interactions.^{7,40-42} Secondary interactions such as dipole-dipole, hydrophilic interactions, hydrophobic interactions, and electrostatic interactions are responsible for the different selectivity classes of HILIC phases.^{12,15,43}

ⁱ A version of this chapter has been submitted in revised form to the *Journal of Chromatography A* for consideration for publication. See the Preface for further details.

In 2011, Dinh et al.¹⁵ characterized these interactions on 22 HILIC stationary phases using principal components analysis (PCA). Their approach successfully classified the behavior of the different phases, but was necessarily complex. Inspired by the two-dimensional RPLC selectivity plot developed by Neue and co-workers,^{44,45} Ibrahim et al.⁴⁶ developed several two-dimensional plots to characterize the selectivity of HILIC phases based on the relative retention of a subset of the test probes studied by Dinh et al.¹⁵ The objective of these two-dimensional plots was to frame the selectivity in a format that was visually easier to comprehend.

One drawback of the selectivity plots of Dinh et al.¹⁵ and Ibrahim et al.⁴⁶ are that they reflect HILIC selectivity under a single set of mobile phase conditions. Altering mobile phase conditions such as pH and buffer concentration can fine-tune HILIC selectivity by affecting the water layer thickness, silanol activity and/or the ionization state of polar bonded groups.^{8-11,47-49}

In this chapter I investigate the effect of pH and buffer concentration on the selectivity behavior of many classes of HILIC phases. Specifically, the hydrophilicity vs. ion interaction selectivity plot of Ibrahim et al.⁴⁶ is reconstructed under three different pH values and two different buffer concentrations. I then focus on the changes in selectivity caused by the new mobile phase conditions.

2.2 Experimental

2.2.1 Apparatus

All experiments were performed on a Varian ProStar HPLC system (Varian, Palo Alto, CA, USA) consisting of a Varian 210 ProStar Pump and a Varian ProStar 410

Autosampler fit with a 40 μL loop. This system was connected to a Knauer Smartline 2500 UV detector (Knauer-ASI, Franklin, MA, USA) with a 2 μL flow cell connected via fibre optic cables. The detector time constant was 0.1 s.

2.2.2 Chemicals and Reagents

All solutions were prepared with nanopure water (Barnstead, Dubuque, IA, USA). Cytosine, uracil, Optima-grade ACN, and HPLC-grade ammonium formate were from Sigma Aldrich (St. Louis, MO, USA). HPLC-grade ammonium acetate was from Fisher Scientific (Fair Lawn, NJ, USA). HCl was from Caledon Laboratory Chemicals (Caledon, ON, Canada) Benzyltrimethylammonium chloride (BTMA) was from Acros Organics (Fair Lawn, NJ, USA).

2.2.3 Tested Columns and Test Probes

Table 2.1 lists the 22 columns evaluated in this study and their characteristics. Retention factors (k) for cytosine, uracil and BTMA were calculated as the average of three injections. Toluene was used as the unretained dead time marker (t_m) for all HILIC phases. The standard deviations of the retention ratio measurements shown in **Figure 2.1** are smaller than the size of the marker symbol (RSD's typically < 1%).

Table 2.1. Characteristics of the stationary phases evaluated in this study.

Col. #	Brand Name	Manufacturer	Support	Functionality	Particle size (μm)	Pore size (\AA)	Surface area (m^2/g)	Column length (mm)	Column diameter (mm)
1	Zorbax HILIC Plus	Agilent	Silica	Underivatized	3.5	95	160	100	4.6
2	Chromolith Si	Merck	Silica monolith	Underivatized	N/A	130	300	100	4.6
3	Ascentis Express HILIC	Supelco	Fused core silica	Underivatized	2.7	90	150	100	4.6
4	Xbridge HILIC	Waters	Silica (BEH)	Underivatized	3.5	130	185	150	2.1
5	Cosmosil HILIC	Nacalai	Silica	Triazole	5	120	300	150	4.6
6	Ultra Amino	Restek	Silica	Aminopropyl	3	100	300	50	3.0
7	TSKgel NH ₂ -100	Tosoh Bioscience	Silica	Aminoalkyl	3	100	450	150	4.6
8	ZIC-HILIC	Merck	Silica	Polymeric sulfoalkylbetaine zwitterionic	3.5	100	180	150	4.6
9	ZIC-pHILIC	Merck	Porous polymer	Polymeric sulfoalkylbetaine zwitterionic	5	—	—	150	4.6
10	ZIC-HILIC	Merck	Silica	Polymeric sulfoalkylbetaine zwitterionic	5	200	135	150	4.6
11	ZIC-cHILIC	Merck	Silica	Polymeric phosphorylcholine zwitterionic	3	100	180	150	4.6
12	TSKgel Amide-80	Tosoh Bioscience	Silica	Amide (polymeric carbamoyl)	5	80	450	100	4.6
13	AdvanceBio Glycan Map	Agilent	Poroshell silica	Proprietary amide	2.7	120	130	100	4.6
14	Fortis HILIC Diol	Fortis Technologies	Silica	Alkyl diol	3	100	380	100	4.6
15	Ascentis Express OH5	Supelco	Fused core silica	Penta hydroxy	2.7	90	150	100	4.6
16	FRULIC-N	AZYP LLC	Silica	High loaded propylcarbamate cyclofructan 6	5	100	440	150	4.6
17 ^a	Ultra IBD	Restek	Silica	Proprietary polar alkyl embedded	5	100	300	100	4.6
18	Acclaim HILIC-10	Thermo Scientific	Silica	Proprietary neutral polar functionality	3	120	300	150	4.6
19 ^a	Ascentis Express F5	Supelco	Fused core silica	Pentafluorophenyl propyl	2.7	90	150	100	4.6
20 ^a	Ultra PFP	Restek	Silica	Pentafluorophenyl propyl	5	100	300	100	4.6
21	Poly-HYDROXY-ETHYL A	PolyLC	Silica	Poly(2-hydroxyethyl aspartamide)	5	200	188	150	4.6
22	Poly-SULFO-ETHYL A	PolyLC	Silica	Poly(2-sulfoethyl aspartamide)	5	200	188	150	4.6

^aColumn was studied but excluded from plots as it exhibited reversed phase behavior under the conditions studied.

2.2.4 UV Spectroscopy of Cytosine

UV spectra of 0.25 mM cytosine were recorded on a Genesys 10S UV-visible spectrophotometer (Thermo Scientific) using a 1.00 cm path length quartz cuvette. Measurements were referenced against unbuffered 80 % ACN_(aq). Buffers did not alter the cytosine λ_{max} .

2.2.5 Chromatographic Conditions

The premixed mobile phases consisted of a mixture of ACN and water (80:20 v/v) containing ammonium acetate (w^w pH 6.8 or 5.0) or ammonium formate (w^w pH 3.7 or 3.0). Analytes (20 μ L partial loop fill injection) were separated under ambient temperature (23 ± 3 °C) at 0.5 mL/min and detected at 254 nm. The buffer strength (5 or 25 mM) is that present after ACN addition. The % ACN quoted in this work represents the volume of the ACN relative to the total volume of the solvents including buffer and ACN. The pH for each aqueous component was measured prior to adding ACN (w^w pH). Early studies suggested that the w^w pH value is more representative of the surface aqueous layer in HILIC.^{43,49} More recently, direct pH measurement of the buffered aqueous/organic mobile phase (after calibrating in aqueous buffers; w^s pH) has been advocated.^{12,50,51} While neither measure is truly an ideal descriptor of the mobile phase acidity, both the w^s pH and w^w pH are quoted in this chapter.

2.3 Results and Discussion

This work focuses on the effect of pH and buffer concentration on the selectivity of various HILIC phases, using the hydrophilicity vs. ion interaction HILIC selectivity plot.⁴⁶ To probe selectivity, the retention ratio of probe analytes is used.^{15,46,52} By using

probe pairs, column properties that affect absolute retention (e.g., column size, pore size, surface area, etc.) are factored out by the measurement of relative retention.¹⁵ To measure the hydrophilicity, the relative retention of cytosine and uracil are used. These compounds are both hydrophilic (log P = -1.97 and -1.05, respectively at pH 7),⁵³ and are structurally similar (effectively negating other interactions). Thus, both compounds show strong HILIC retention, and their retention ratio ($k_{\text{cytosine}}/k_{\text{uracil}}$) has been ascribed as a convenient measure of the hydrophilicity of the HILIC phase,¹⁵ within the pH limitations discussed below.

Likewise, the retention ratio of $k_{\text{BTMA}}/k_{\text{uracil}}$ provides a measure of the electrostatic interactions of a phase.^{54,55} Benzyltrimethylammonium (BTMA) is a quaternary amine which maintains its positive charge under all pH conditions and will thus undergo cation exchange interactions. Uracil, on the other hand, remains uncharged under all pH conditions. Therefore uracil will not undergo cation exchange interactions but will experience other HILIC interactions similar to BTMA. Further, although $k_{\text{BTMA}}/k_{\text{uracil}}$ primarily reflects the cation exchange interactions of a phase, the strong HILIC retention of BTMA on all HILIC phases allows the probe pair to also reflect the cationic nature of phases via electrostatic repulsion.⁵⁶ Hence, a high $k_{\text{BTMA}}/k_{\text{uracil}}$ indicates stronger cation exchange behavior, while a low $k_{\text{BTMA}}/k_{\text{uracil}}$ indicates cationic surface functionalities that would be important either for anion exchange retention or electrostatic repulsion liquid chromatography (ERLIC).⁵⁶

Table 2.2 summarizes the selectivity behavior of the columns investigated in this work. Three columns (Ultra IBD phase (column no. 17), Ascentis Express F5 (19), and Ultra PFP (20)) were studied but are excluded from the table and plots. These columns

(17, 19, 20) displayed reversed phase behavior, as evidenced by weaker retention of cytosine and uracil, and stronger retention of toluene. **Table 2.3** summarizes the retention for all columns under the mobile phase conditions studied. Such behavior for the fluorinated phases (19, 20) is consistent with the finding of less than a full monolayer water layer.⁴¹ Similar hydration studies of the IBD phase have not been reported, albeit the manufacturer does advertise the IBD phase for use in HILIC separations.

Table 2.2. Summary of selectivity changes of HILIC columns when pH is decreased or buffer concentration is increased.

Col. #	Brand Name	Effect of decreased pH		Effect of increased [buffer]	
		Ion Interaction	Hydrophilicity	Ion Interaction	Hydrophilicity
	<i>silica</i>				
1	Zorbax HILIC Plus	--- CE	0	-- CE	-
2	Chromolith SI	--- CE	++	--- CE	-
3	Ascentis Express HILIC	-- CE	++	-- CE	--
4	Xbridge HILIC	-- CE	0	-- CE	0 to --
	<i>amine</i>				
5	Cosmosil HILIC	-- AE	0	complex	0 to -
6	Ultra Amino	++ AE	0	complex	0 to -
7	TSKgel NH ₂ .100	- AE	0	complex	0 to +
	<i>zwitterionic</i>				
8	ZIC-HILIC	-- CE	++ ^c	-- CE	complex ^c
9	ZIC-pHILIC	-- CE	++ ^c	-- CE	complex ^c
10	ZIC-HILIC	-- CE	++ ^c	-- CE	complex ^c
11	ZIC-cHILIC	-- CE	+++ ^c	-- CE	complex ^c
	<i>amide</i>				
12	TSKgel Amide-80	-- CE	0	- CE	0
13	AdvanceBio Glycan Map	-- CE	0	- CE	0 to -
	<i>hydroxylated</i>				
14	Fortis HILIC Diol	--- CE	--	complex	0 to +
15	Ascentis Express OH5	-- CE	0	0	0
16	FRULIC-N	-- CE	-	complex	0 to +
	<i>specialty</i>				
18	Acclaim HILIC-10	complex	complex	complex	complex
21	PolyHYDROXYETHYL A	- CE	+	-CE	0 to +
22	PolySULFOETHYL A	0	++++ ^c	--- CE	---- ^c

^aLegend: ++++/---- very strong increase/decrease, +++/--- strong increase/decrease, ++/-- moderate increase/decrease, +/- weak increase/decrease, 0 no effect, CE cation exchange, AE anion exchange.

^bColumns 17, 19, and 20 exhibited reversed phase retention and are therefore excluded from this table.

^cSelectivity behavior at low pH may be biased by cytosine protonation.

Table 2.3. Retention data for separations of test probes performed on 22 different HPLC (HILIC) phases at various mobile phase pH's and buffer concentrations. Conditions: columns, see column numbers in **Table 2.1**; flow rate, 0.5 mL/min; eluents, 5 and 25 mM ammonium acetate (w pH 6.8 and 5.0) or ammonium formate (w pH 3.7 and 3.0) in 80 % ACN; test analytes 0.25-1.5 mM cytosine, uracil, and BTMA prepared in 80 % ACN containing 5 mM of the appropriate buffer; UV detection at 254 nm with a 20 μ L partial loop fill injection.

Col. #	pH 6.8, 5 mM buffer				pH 6.8, 25 mM buffer			
	t_m (min)	k_{cytosine}	k_{uracil}	k_{BTMA}	t_m (min)	k_{cytosine}	k_{uracil}	k_{BTMA}
1	1.98	1.32	0.45	6.38	1.83	2.10	0.77	2.69
2	2.81	0.59	0.20	6.20	2.69	0.82	0.31	2.01
3	1.84	1.11	0.38	4.86	1.68	1.24	0.55	1.70
4	1.82	0.68	0.24	1.51	1.72	0.41	0.95	1.10
5	3.08	1.37	0.63	0.17	2.91	1.78	0.81	0.48
6	0.41	2.17	0.91	0.25	0.38	2.73	1.12	0.62
7	3.18	2.35	0.94	0.18	2.42	4.01	1.50	0.71
8	2.64	2.15	0.88	2.58	2.35	2.68	1.14	1.24
9	2.51	2.05	0.93	0.94	2.72	2.58	1.09	0.65
10	3.12	1.26	0.54	1.59	3.01	1.54	0.65	0.89
11	2.66	2.29	1.00	1.21	2.43	3.02	1.29	1.29
12	1.89	2.60	1.10	2.43	1.77	3.17	1.36	1.83
13	1.78	1.42	0.70	1.38	1.60	1.61	0.87	1.03
14	2.05	1.81	0.66	2.89	1.97	2.31	0.84	2.72
15	1.68	1.52	0.61	0.56	1.68	1.98	0.70	0.63
16	2.47	3.76	1.35	3.38	2.37	5.17	1.69	2.84
17 ^{a,b}	2.21	0.24	0.01	1.50	—	—	—	—
18	3.32	1.92	0.51	1.04	3.42	2.01	0.66	0.79
19 ^a	1.61	0.17	0.08	7.52	—	—	—	—
20 ^a	1.90	0.02	0.02	0.34	—	—	—	—
21	2.73	2.43	0.95	0.77	2.57	3.27	1.21	0.63
22	2.50	3.97	1.35	7.19	2.35	5.40	1.74	2.42

^aFull studies of selectivity behavior was not performed due to column displaying apparent reversed phase retention.

^bDead time measured using water dip.

Table 2.3 continued.

Col. #	pH 5.0, 5 mM buffer				pH 5.0, 25 mM buffer			
	t_m (min)	k_{cytosine}	k_{uracil}	k_{BTMA}	t_m (min)	k_{cytosine}	k_{uracil}	k_{BTMA}
1	2.04	1.27	0.43	4.67	1.91	1.47	0.56	2.30
2	2.78	0.60	0.20	4.53	2.73	0.74	0.26	1.44
3	1.86	1.12	0.37	3.72	1.72	1.17	0.50	1.54
4	1.79	0.70	0.28	1.27	1.19	1.86	0.98	2.27
5	3.07	1.38	0.63	0.13	2.67	1.76	0.90	0.47
6	0.41	2.23	0.89	0.25	0.38	2.65	1.03	0.54
7	2.95	2.64	0.99	0.56	2.86	3.14	1.13	0.64
8	2.65	2.25	0.89	2.05	2.42	2.47	1.04	1.06
9	2.51	2.17	0.98	0.92	2.44	2.31	1.05	0.44
10	3.14	1.33	0.53	1.45	3.04	1.53	0.63	0.81
11	2.66	2.31	1.01	1.20	2.31	2.42	1.21	0.75
12	1.88	2.37	1.08	2.07	1.80	3.03	1.30	1.46
13	1.77	1.45	0.72	1.29	1.75	1.79	0.82	0.95
14	2.06	1.69	0.66	2.92	2.01	2.09	0.77	2.04
15	1.68	1.60	0.61	0.49	1.66	1.99	0.70	0.46
16	2.47	3.77	1.35	2.60	2.40	4.82	1.60	2.09
17 ^{a,b}	—	—	—	—	—	—	—	—
18	3.40	2.02	0.51	0.53	3.42	2.07	0.58	0.58
19 ^a	—	—	—	—	—	—	—	—
20 ^a	—	—	—	—	—	—	—	—
21	2.72	2.48	0.95	0.69	2.56	3.04	1.15	0.54
22	2.41	4.49	1.47	5.47	2.27	4.99	1.70	1.70

^aFull studies of selectivity behavior was not performed due to column displaying apparent reversed phase retention.

^bDead time measured using water dip.

Table 2.3 continued.

Col. #	pH 3.7, 5 mM buffer ^c				pH 3.0, 5 mM buffer			
	<i>t_m</i> (min)	<i>k_{cytosine}</i>	<i>k_{uracil}</i>	<i>k_{BTMA}</i>	<i>t_m</i> (min)	<i>k_{cytosine}</i>	<i>k_{uracil}</i>	<i>k_{BTMA}</i>
1	—	—	—	—	2.04	1.12	0.37	1.19
2	—	—	—	—	2.83	0.59	0.17	0.95
3	1.91	1.04	0.32	1.66	1.90	1.06	0.31	1.35
4	—	—	—	—	1.85	0.65	0.24	0.58
5	—	—	—	—	3.07	1.29	0.63	0.39
6	0.43	2.21	0.84	0.02	0.41	2.07	0.87	0.05
7	—	—	—	—	2.97	2.56	0.97	0.32
8	3.19	1.40	0.51	0.79	2.71	2.89	0.83	0.97
9	—	—	—	—	2.51	2.89	0.96	0.52
10	—	—	—	—	3.16	1.62	0.50	0.61
11	2.74	2.58	0.95	0.66	2.69	3.89	0.97	0.62
12	1.89	2.56	1.08	1.37	1.88	2.61	1.07	0.91
13	—	—	—	—	1.96	1.48	0.65	0.44
14	2.06	1.63	0.65	0.81	2.05	1.37	0.64	0.47
15	—	—	—	—	1.67	1.52	0.60	0.24
16	—	—	—	—	2.50	3.40	1.30	0.96
17 ^{a,b}	—	—	—	—	—	—	—	—
18	—	—	—	—	3.58	1.65	0.49	0.21
19 ^a	—	—	—	—	—	—	—	—
20 ^a	—	—	—	—	—	—	—	—
21	—	—	—	—	2.74	2.60	0.89	0.41
22	2.37	9.82	1.38	4.54	2.58	17.62	1.25	4.49

^aFull studies of selectivity behavior was not performed due to column displaying apparent reversed phase retention.

^bDead time measured using water dip.

^cData under this mobile phase condition only acquired on representative columns to verify validity of cytosine at low pH.

Table 2.3 continued.

Col. #	pH 3.0, 25 mM buffer			
	t_m (min)	k_{cytosine}	k_{uracil}	k_{BTMA}
1	2.73	1.09	0.57	1.09
2	2.81	0.57	0.18	0.66
3	1.84	0.83	0.34	0.80
4	1.81	0.70	0.27	0.61
5	2.93	1.34	0.70	0.27
6	0.38	2.12	0.98	0.40
7	2.85	2.61	1.03	0.44
8	2.61	3.07	0.78	0.94
9	2.43	2.91	1.03	0.34
10	3.07	1.81	0.58	0.50
11	2.56	3.89	1.14	0.55
12	1.80	3.05	1.21	0.82
13	1.76	1.83	0.78	0.41
14	1.95	1.80	0.78	0.88
15	1.66	1.87	0.67	0.32
16	2.39	4.75	1.59	2.05
17 ^{a,b}	2.21	0.20	0.01	0.35
18	3.33	1.59	0.35	0.55
19 ^a	1.61	0.26	0.08	1.30
20 ^a	—	—	—	—
21	2.65	3.42	1.07	0.45
22	2.48	9.54	1.41	1.26

^aFull studies of selectivity behavior was not performed due to column displaying apparent reversed phase retention.

^bDead time measured using water dip.

Figure 2.1A shows the ion interaction ($k_{\text{BTMA}}/k_{\text{uracil}}$) vs. hydrophilicity ($k_{\text{cytosine}}/k_{\text{uracil}}$) under Ibrahim et al.'s⁴⁶ original conditions (5 mM buffer at w^{w} pH 6.8 (w^{s} pH 7.7)) in 80 % ACN. As observed previously,⁴⁶ the columns cluster within groups (i.e., bare silica, amine, amide, hydroxylated, zwitterionic, and specialty phases). The high pH (w^{w} pH 6.8) ensures deprotonation of silanols and the dilute 5 mM buffer ensures strong electrostatic interactions **Figures 2.1B-F** show selectivity plots for 5 and 25 mM total buffer concentrations at w^{w} pH 6.8, 5.0, and 3.0 (w^{s} pH 7.7, 7.2, and 4.8). $k_{\text{BTMA}}/k_{\text{uracil}}$ ⁵⁵ was utilized in this work rather than $k_{\text{BTMA}}/k_{\text{cytosine}}$ ^{15,46} to minimize the potential bias due to the possible protonation of cytosine at low pH (see **Section 2.3.1**). Selectivity plots using $k_{\text{BTMA}}/k_{\text{uracil}}$ vs. $k_{\text{cytosine}}/k_{\text{uracil}}$ (**Figure 2.1**) are similar to those using $k_{\text{BTMA}}/k_{\text{cytosine}}$ vs. $k_{\text{cytosine}}/k_{\text{uracil}}$ (**Figure 2.2**) at w^{w} pH 6.8 and 5.0, but show some differences at w^{w} pH 3.0.

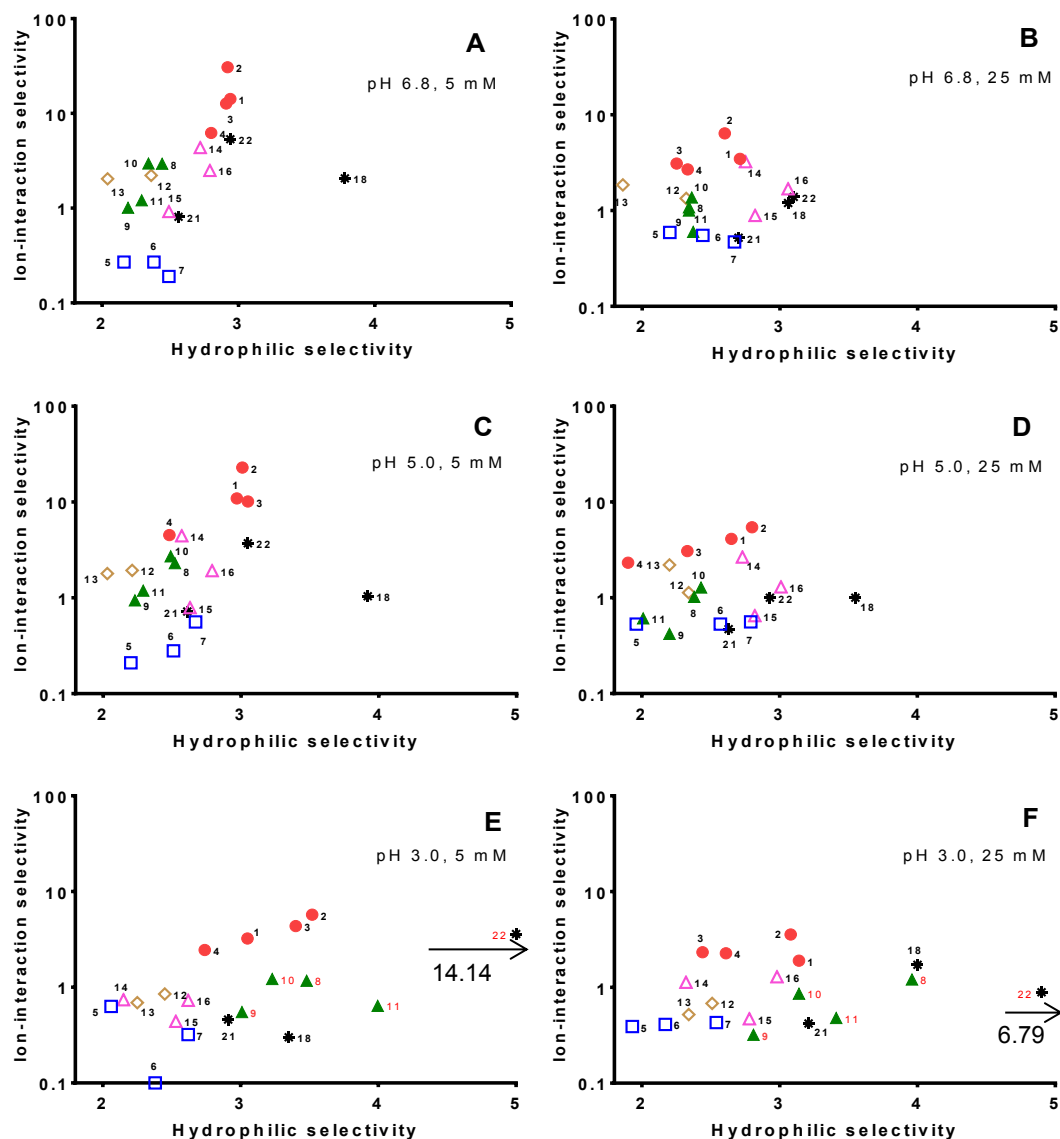


Figure 2.1. Hydrophilicity ($k_{\text{cytosine}}/k_{\text{uracil}}$) vs. ion interaction ($k_{\text{BTMA}}/k_{\text{uracil}}$) selectivity plots of HILIC phases acquired under different mobile phase pH's and buffer concentrations. Symbols: bare silica (\bullet); amine (\square); zwitterionic (\blacktriangle); amide (\diamond); hydroxylated (\triangle); and specialty phases ($*$). See **Table 2.1** for column numbers. Red colored numbers beside markers indicate data points demonstrated to be biased by cytosine protonation. Eluents: (A) 5 mM ammonium acetate, w^w pH 6.8, in 80 % ACN, (B) 25 mM ammonium acetate, w^w pH 6.8, in 80 % ACN, (C) 5 mM ammonium acetate, w^w pH 5.0, in 80 % ACN, (D) 25 mM ammonium acetate, w^w pH 5.0, in 80 % ACN, (E) 5 mM ammonium formate, w^w pH, in 80 % ACN, and (F) 25 mM ammonium formate, w^w pH 3.0, in 80 % ACN Cytosine/uracil ratios for column 22 were offset in **Figures 2.1E** and **2.1F** to bring them on-scale. The true values were 14.14 and 6.79, respectively. See **Table 2.3** for raw retention data of all columns.

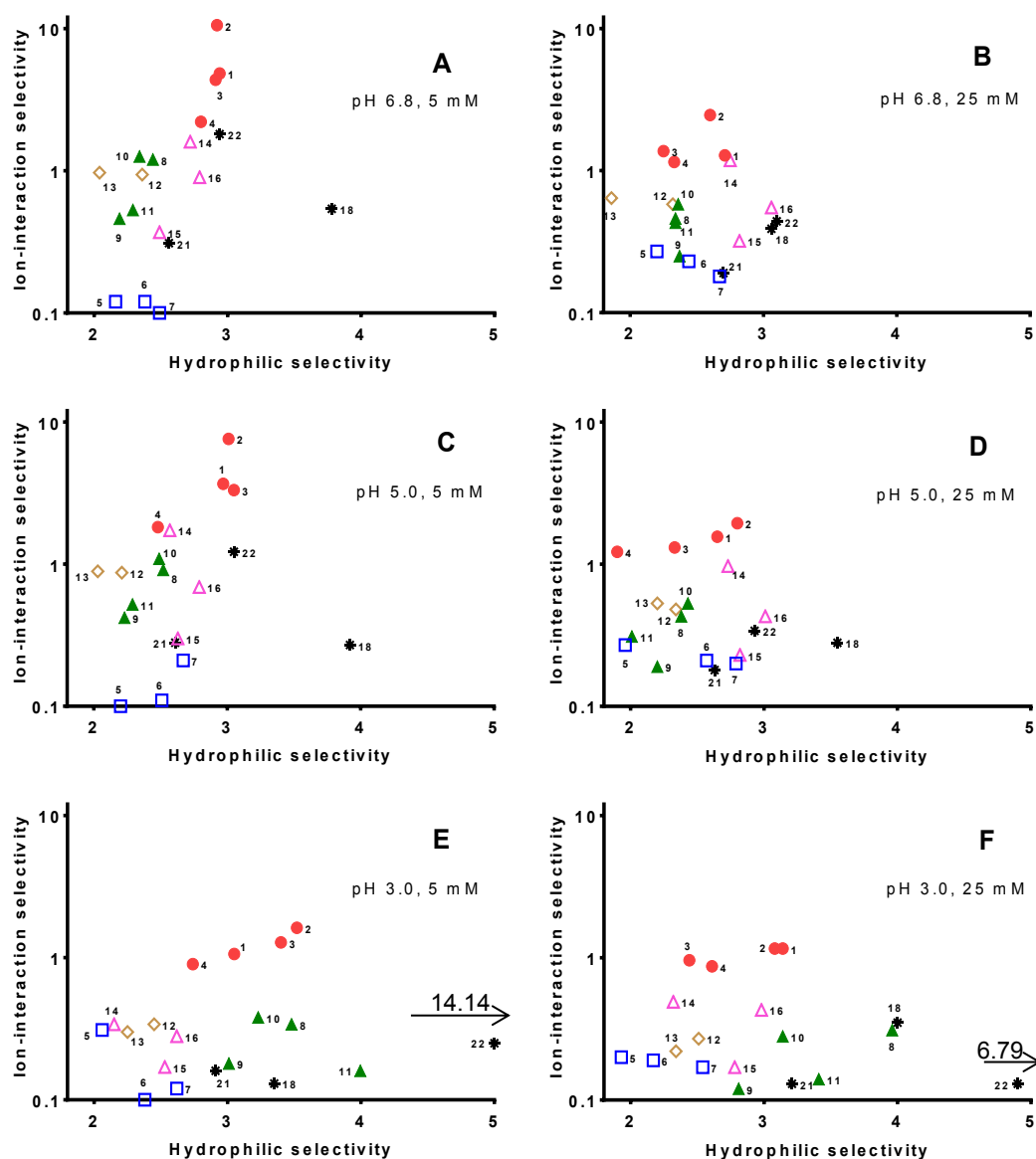


Figure 2.2. Comparative hydrophilicity ($k_{\text{cytosine}}/k_{\text{uracil}}$) vs. ion interaction ($k_{\text{BTMA}}/k_{\text{uracil}}$) selectivity plots of HILIC phases as in **Figure 2.1**, but utilizing the BTMA/cytosine retention ratio on the y-axis. Symbols: bare silica (●); amine (□); zwitterionic (▲); amide (◇); hydroxylated (△); and specialty phases (*). See **Table 2.1** for column numbers. Red colored numbers beside markers indicate data points demonstrated to be biased by cytosine protonation. Eluents: (A) 5 mM ammonium acetate, w^w pH 6.8, in 80 % ACN, (B) 25 mM ammonium acetate, w^w pH 6.8, in 80 % ACN, (C) 5 mM ammonium acetate, w^w pH 5.0, in 80 % ACN, (D) 25 mM ammonium acetate, w^w pH 5.0, in 80 % ACN, (E) 5 mM ammonium formate, w^w pH, in 80 % ACN, and (F) 25 mM ammonium formate, w^w pH 3.0, in 80 % ACN. Cytosine/uracil ratios for column 22 were offset in **Figures 2.1E** and **2.1F** to bring them on-scale. The true values were 14.14 and 6.79, respectively. See **Table 2.3** for raw retention data of all columns.

2.3.1 Effect of pH

To better illustrate the effect of eluent conditions on HILIC selectivity, **Figure 2.3** presents the *change* in the relative probe retention *between* two eluent conditions. For instance, **Figure 2.3A** compares column selectivity using $w^w\text{pH } 5.0$ ($w^s\text{pH } 7.2$)/5.0 mM eluent relative to a $w^w\text{pH } 6.8$ ($w^s\text{pH } 7.7$)/5.0 mM eluent, which was the focus of previous studies.^{15,46} The dotted horizontal and vertical lines indicate no change in hydrophilicity or ion interaction selectivity, respectively. The majority of the columns in **Figure 2.3A** cluster around the (0, 0) point in the plot, indicating that the change in eluent $w^w\text{pH}$ from 6.8 to 5.0 has minimal effect on HILIC selectivity, consistent with the literature.^{11,12} The minimal change in HILIC selectivity observed upon decreasing $w^w\text{pH}$ from 6.8 to 5.0 is to be expected since the actual difference in $w^s\text{pH}$ is small (7.7 vs. 7.2). Similar to other weak acids,⁵⁷ addition of ACN causes up to a 1-2 pH unit increase in the pK_a of the silanols relative to a purely aqueous system.⁵⁸ Hence, no significant change in silanol protonation would yet be expected.

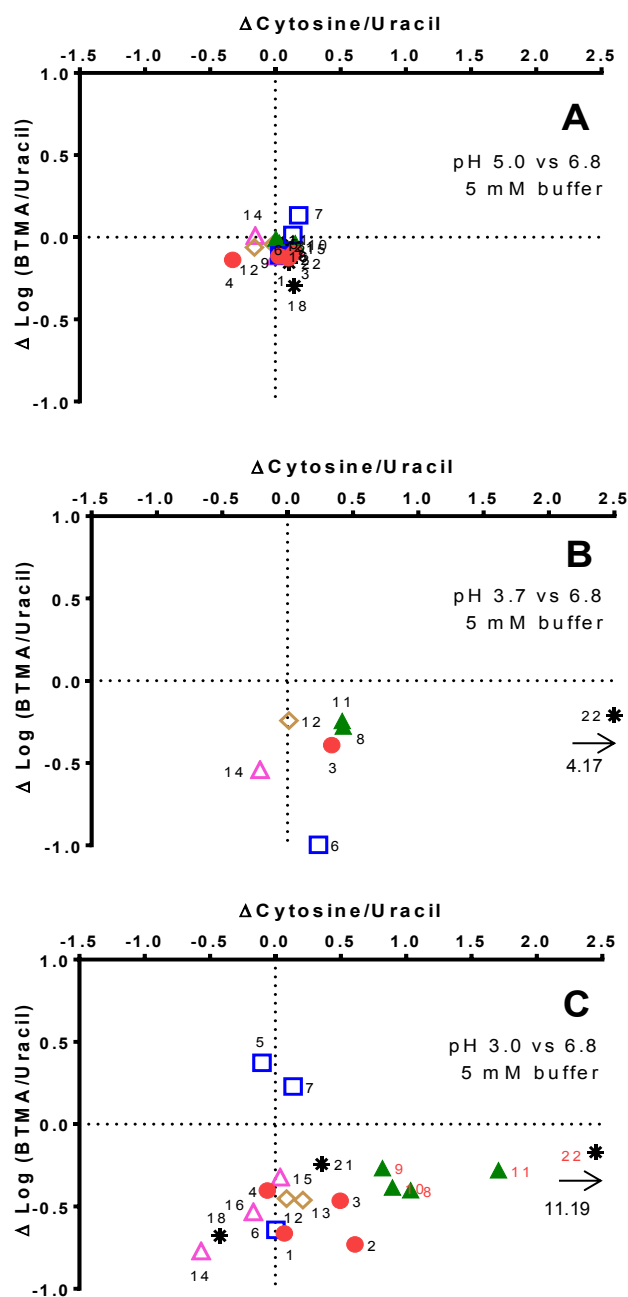


Figure 2.3. Difference plots showing the effect of changing the w^w pH from 6.8 to (A) 5.0, (B) 3.7 and (C) 3.0 (while maintaining a 5 mM buffer concentration) on the hydrophilicity and ion interaction behavior of 19 HILIC columns. Symbols: bare silica (●), amine (□), zwitterionic (▲), amide (◇), hydroxylated (△), and specialty phases (*). See **Table 2.1** for column numbers. Red colored numbers beside markers indicate data points demonstrated to be biased by cytosine protonation. All difference values were calculated relative to the data points obtained at pH 6.8 using a 5 mM buffer concentration. Note that in **Figure 2.3C** the actual $\Delta k_{\text{cytosine}}/k_{\text{uracil}}$ for col. 22 was 11.19.

Cytosine has a ${}^w\text{pK}_a$ of 4.6.⁴⁹ The pK_a of weak bases such as cytosine may be 1 or more pH units lower in 80 % ACN than in water.⁵⁷ Based on the method of Lopnow and co-workers⁵⁹ (see **Section 2.2.4**), UV absorbance spectra of cytosine were recorded in various eluents. Protonated cytosine absorbs at 276 nm (due to increased conjugation⁵⁹) vs. 267 nm for the uncharged. Based on the λ_{max} values in **Table 2.4**, the ${}^w\text{pK}_a$ of cytosine in 80 % ACN is estimated to be 2.6-3.0; hence at ${}^w\text{pH}$ 3.0 cytosine is partially charged. Therefore, caution must be taken in the interpretation of the hydrophilicity behavior ($k_{\text{cytosine}}/k_{\text{uracil}}$) at ${}^w\text{pH}$ 3.0, but the ion interaction based on $k_{\text{BTMA}}/k_{\text{uracil}}$ is uncompromised. Additional studies of selected columns were performed at ${}^w\text{pH}$ 3.7 (**Figures 2.3B and 2.4**) to guide interpretation of the hydrophilicity behavior.

Table 2.4. UV absorbance maxima of cytosine in different solutions. The cytosine concentration was maintained at approximately 0.25 mM at all conditions.

Solution Conditions	Cytosine λ_{max}
5 mM ammonium acetate (${}^w\text{pH}$ 6.8) in water	267
5 mM ammonium acetate (${}^w\text{pH}$ 6.8) in 80 % ACN	267
50 mM HCl (${}^w\text{pH}$ ~ 1) in water	276
50 mM HCl (${}^w\text{pH}$ ~ 1) in 80 % ACN	276
5 mM ammonium formate (${}^w\text{pH}$ 4.0) in 80 % ACN	267
5 mM ammonium formate (${}^w\text{pH}$ 3.7) in 80 % ACN	267
5 mM ammonium formate (${}^w\text{pH}$ 3.5) in 80 % ACN	268
5 mM ammonium formate (${}^w\text{pH}$ 3.0) in 80 % ACN	271

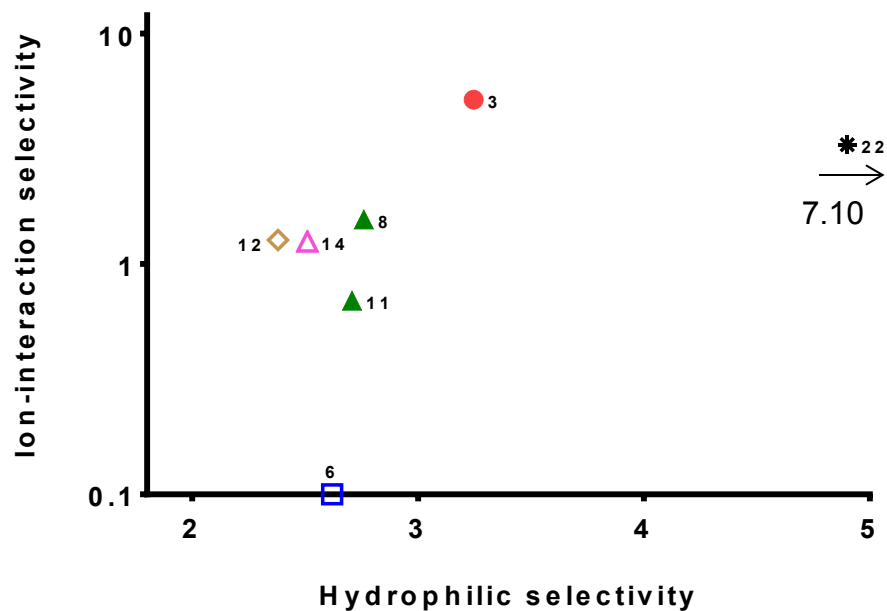


Figure 2.4. Hydrophilicity ($k_{\text{cytosine}}/k_{\text{uracil}}$) vs. ion interaction ($k_{\text{BTMA}}/k_{\text{uracil}}$) selectivity plot of selected HILIC phases at ^wpH 3.7. Symbols: bare silica (\bullet); amine (\square); zwitterionic (\blacktriangle); amide (\diamond); hydroxylated (\triangle); and specialty phases (*). See **Table 2.1** for column numbers. Eluent: 5 mM ammonium formate, ^wpH 3.7, in 80 % ACN. Note the cytosine/uracil ratio for column 22 was offset bring it on-scale. The true value was 7.10. See **Table 2.3** for raw retention data of all columns.

At $w^w\text{pH}$ 3.0 ($w^s\text{pH}$ 4.8, **Figure 2.3C**), a larger number of selectivity differences are evident. The ion-interaction selectivity of the bare silica phases (red circles, columns 1-4) is dominated by pH-dependent silanol activity.^{11,15,43} At $w^w\text{pH}$ 3.0 most silanols are protonated (silanol $w^w\text{pK}_a = 4-7$).^{11,49} Therefore, all bare silica phases (1-4) displayed a moderate decrease in cation exchange activity at $w^w\text{pH}$ 3.0 relative to $w^w\text{pH}$ 6.8 ($y < 0$ in **Figure 2.3C**) due to a reduction in cation exchange between the silanols and cationic BTMA.

The amine columns (blue squares, 5-7) are protonated under all pH values used in this study ($w^w\text{pH}$ 6.8–3.0). Thus, BTMA experiences electrostatic repulsion.^{11,15} At $w^w\text{pH}$ 5.0 and 6.8 this repulsion behavior is similar ($\Delta k_{\text{BTMA}}/k_{\text{uracil}} \sim 0$ in **Figure 2.3A**). At $w^w\text{pH}$ 3.0 the underlying exposed silanols are protonated (uncharged) and so repulsion of BTMA by amine phases should be enhanced (i.e., $\Delta k_{\text{BTMA}}/k_{\text{uracil}} < 0$ in **Figure 2.3C**). The Ultra Amine (6) showed increased anion exchange (lower $k_{\text{BTMA}}/k_{\text{uracil}}$) at $w^w\text{pH}$ 3.0 in **Figure 2.3C** (also compare **Figure 2.1E** vs. **2.1A**), but both the Cosmosil (5) and TSK-gel NH2-100 (7) displayed an increase in $k_{\text{BTMA}}/k_{\text{uracil}}$ in **Figure 2.3C**. These unusual findings may be due to the low retention of BTMA on columns 5 and 7 (**Table 2.3**). Based on investigations by Guo *et al.*⁶⁰ the nature of the buffer (acetate vs. formate) is not believed to affect retention of cationic species on amino columns. The hydrophilicity of the amine phases (5-7) did not change when the $w^w\text{pH}$ was lowered to 3.0.

All zwitterionic phases (green triangles, 8-11) experienced a similar weak to moderate reduction in $k_{\text{BTMA}}/k_{\text{uracil}}$ upon lowering $w^w\text{pH}$ to 3.0 (**Figure 2.3C**). The reduction in cation exchange behavior of the ZIC-HILIC (8 and 10) and ZIC-cHILIC (11) phases at $w^w\text{pH}$ 3.0 may be ascribed to the protonation of exposed silanols,^{48,49,61} causing

reduced retention of BTMA. Similarly, studies of a zwitterionic polymethacrylate monolith (similar polymer backbone to pHILIC⁶²) showed less anionic character at w pH 3.5 vs. 9.5.⁶³

The $k_{\text{cytosine}}/k_{\text{uracil}}$ (hydrophilicity) of the zwitterionic phases (green triangles, 8-11) increased dramatically upon reducing the w pH from 6.8 to 3.0 (**Figure 2.3C**, and **Figure 2.1E** vs. **2.1A**). Based on selectivity measurements at w pH 3.7/5 mM (w pH 5.5; **Figures 2.3B** and **2.4**) vs. w pH 5.0/5 mM (**Figures 2.1C** and **2.3B**) it is apparent that the observed hydrophilicity behaviors in **Figure 2.3C** for columns 8-11 are biased by cytosine protonation.

At w pH 3.0 the amide phases (brown diamonds; 12, 13) displayed a comparable loss of cation exchange activity to the BEH silica (columns 12 and 13 vs. 4; **Figure 2.3C**). This reduction in cation exchange may be ascribed to protonation of underlying silanols.^{49,54} The $k_{\text{cytosine}}/k_{\text{uracil}}$ of these phases (12, 13) was minimally affected by reducing the w pH to 3.0.

The selectivity behavior of the hydroxylated phases (pink open triangles, 14-16) and the PolyHYDROXYETHYL A (black asterisk, 21) in **Figure 2.3C** were more column dependent than other classes, as observed previously.⁵⁴ A >4-fold decrease in ionic interaction behavior was observed for the Fortis Diol (column 14), while others displayed little (15, 21) to moderate (column 16; FRULIC-N, a commercialized analog of a column reported by Armstrong and co-workers⁶⁴) reduction in cation exchange activity. In general, the Ascentis Express OH5 (15) and the PolyHYDROXYETHYL A (21) displayed relatively little shift in selectivity over all mobile phase conditions examined.

The stability in ionic selectivity observed in the Ascentis Express OH5 (15) is consistent with the manufacturer's claims.

The Fortis HILIC Diol (14) showed the greatest (50 %) decrease in $k_{\text{cytosine}}/k_{\text{uracil}}$ in **Figure 2.3C** when the $w^w\text{pH}$ was decreased to 3.0, arising from decreased cytosine retention (**Table 2.3**). Similar change in hydrophilicity behavior was observed at $w^w\text{pH}$ 3.7 (**Figure 2.3B**), indicating cytosine protonation was not responsible for the change. Given the multiple secondary interactions contributing to the HILIC retention of diol phases,¹⁵ it is difficult to attribute the change in hydrophilicity behavior of column 14 to a single interaction. The other hydroxylated phases (15, 16, and 21) displayed minimal change in hydrophilicity.

The Acclaim HILIC 10 (black asterisk, 18) is a silica-based HILIC phase containing a proprietary covalently bonded hydrophilic layer. It exhibited a moderate reduction in both cation exchange activity and hydrophilicity when the $w^w\text{pH}$ was decreased from 6.8 to 3.0 (**Figure 2.3C**). Due to the proprietary nature of the Acclaim HILIC-10 (18), I am unable to confidently rationalize the behavior of this column. No previous studies of the effect of mobile phase conditions on the selectivity of this column have been performed.

The PolySULFOETHYL A (black asterisk, 22) behaves as a pseudo-zwitterionic phase (due to unbonded cationic taurine groups) with some strong cation exchange character (due to the anionic sulfonate groups).^{15,54} This column (22) remained near zero on the ionic interaction axis in **Fig. 2.3C**. Conversely, column 22 displayed almost a 5-fold increase in $k_{\text{cytosine}}/k_{\text{uracil}}$ at $w^w\text{pH}$ 3.0 vs 6.8 (14.1 vs. 2.9, respectively; see **Figures 2.1A** and **2.1E**) due to a >4-fold increase in k_{cytosine} (17.6 vs. 4.0). The strong increase in

cytosine retention may be substantially attributed to ionic interactions with the sulfonate head group⁵⁴ at w^w pH 3.0. Nevertheless at w^w pH 3.7 (**Figure 2.3B** and see also **Figure 2.4** vs **2.1A**) this phase still displayed a greater than 2-fold increase in $k_{\text{cytosine}}/k_{\text{uracil}}$ vs. w^w pH 6.8. Broad tailing peak shapes were observed for this phase under all of our mobile phase conditions (data not shown), as had been reported previously.^{15,54}

Table 2.2 summarizes the pH-dependent selectivity behaviors of the various HILIC phases detailed above. The magnitude of the changes in ion interaction and hydrophilicity are scaled from 0 (no change) to ++++/----- (very large increase or decrease). For example, **Table 2.2** outlines how the silica phases (1-4), as discussed in the preceding section, display a moderate to strong decrease in cation exchange activity (-- to --- CE in **Table 2.2**) and either no change (0) or a moderate increase (++) in hydrophilicity in response to decreasing the w^w pH from 6.8 to 3.0. Those phases (such as the Acclaim HILIC 10; column 18) which display complex changes in response to changes in mobile phase conditions are listed as “complex.”

2.3.2 Effect of Buffer Concentration

Figure 2.5 illustrates the effect of increasing the buffer concentration from 5 to 25 mM, while keeping the pH constant at w^w pH 6.8 (**Figure 2.5A**), 5.0 (**Figure 2.5B**), and 3.0 (**Figure 2.5C**). As noted in the literature,^{40,48,49} more concentrated buffer mutes ionic interactions for most phases due to increased ionic shielding.

At w^w pH 6.8 (**Figure 2.5A**) and 5.0 (**Figure 2.5B**), all silica phases (red circles, 1-4) experienced a 50-100% decrease in $k_{\text{BTMA}}/k_{\text{uracil}}$ arising from decreased ionic interactions between BTMA and the deprotonated silanols. Additionally, one can

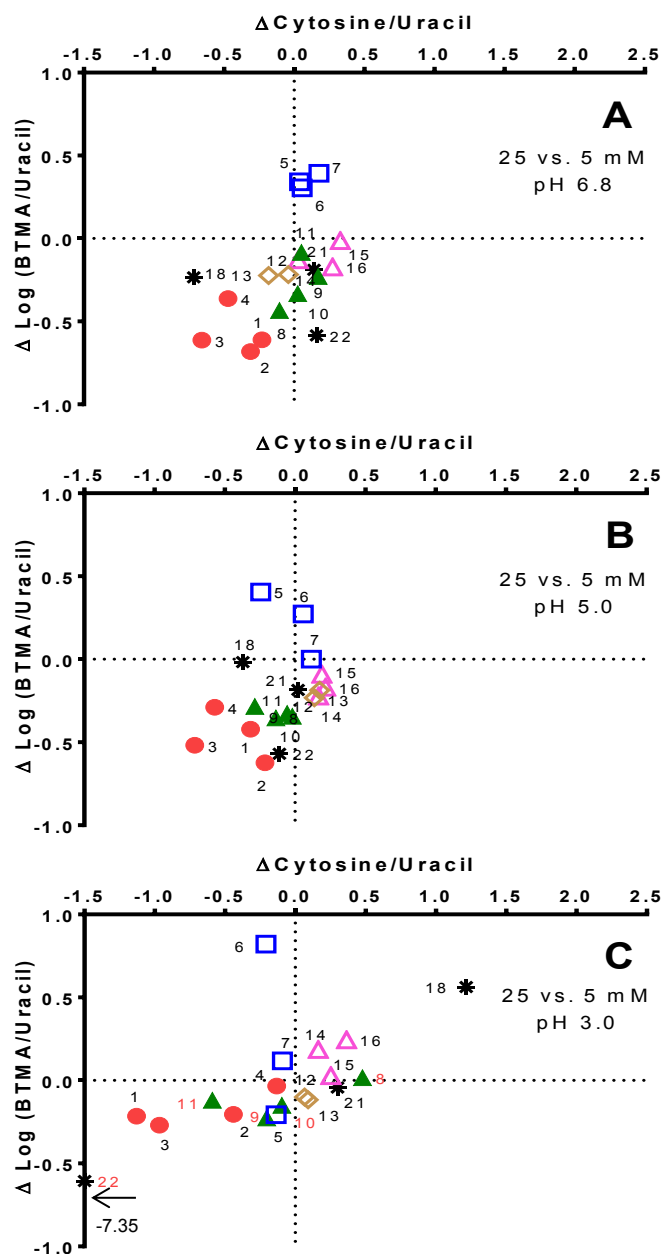


Figure 2.5. Difference plots showing the effect of increasing the buffer concentration from 5 to 25 mM at w^w pH (A) 6.8, (B) 5.0, and (C) 3.0 on the hydrophilicity and ion interaction behavior of 19 HILIC columns. Symbols: bare silica (\bullet), amine (\square), zwitterionic (\blacktriangle), amide (\diamond), hydroxylated (\triangle), and specialty phases ($*$). See **Table 2.1** for column numbers. Red colored numbers beside markers indicate data points demonstrated to be biased by cytosine protonation. All difference values were calculated relative to the data points obtained at the same pH using a 5 mM buffer concentration. Note that in **Figure 2.5C** the actual $\Delta k_{\text{cytosine}}/k_{\text{uracil}}$ for column 22 was -7.35.

distinguish the silanol activity of the phases based on the change in $k_{\text{BTMA}}/k_{\text{uracil}}$ upon increasing buffer concentration. At $^{\text{w}}\text{pH}$ 6.8/5 mM the silica phases (1-4) in **Figure 2.1A** group together.^{15,46} Upon increasing the buffer concentration, however, the silica phases respond differently (**Figure 2.5A**). The Chromolith Si (2) exhibits strong silanol activity due to its use of a silica which contains a wide array of highly acidic and less acidic silanols;⁵⁴ hence the strong cation exchange character in **Figure 2.1A**. Resultantly, Chromolith Si experiences the greatest shielding effects and loss of cation exchange activity upon increasing buffer concentration in **Figure 2.5A** ($k_{\text{BTMA}}/k_{\text{uracil}}$ 30.7 vs. 6.4 in 5 vs. 25 mM buffer at $^{\text{w}}\text{pH}$ 6.8). At the other extreme, the blocked and less active silanols of the BEH silica (4)⁴⁹ display a much smaller decrease in cation exchange activity (**Figure 2.5A**). The Type B silica phases (Zorbax HILIC Plus (1) and Ascentis Express HILIC (3)) displayed a median decrease in cation exchange activity.

At $^{\text{w}}\text{pH}$ 3.0, the cation exchange behavior of the silica columns (1-4) is weak (**Figure 2.1E**) due to protonation of the silanols (see **Section 2.3.1**). Hence, as shown in **Figure 2.5C**, increasing the buffer concentration from 5 to 25 mM caused little change in the cation exchange behavior of the silicas (red circles, 1-4).

For the amine columns (blue squares, 5-7), the ion interaction behavior was more complex. At $^{\text{w}}\text{pH}$ 6.8 (**Figure 2.5A**) ionic shielding of the cationic amino groups due to increased buffer concentration reduced electrostatic repulsion of BTMA, leading to a 100-150% increase in $k_{\text{BTMA}}/k_{\text{uracil}}$, consistent with the literature.¹⁵ Similar changes in ion interaction behavior were observed at $^{\text{w}}\text{pH}$ 5.0 (**Figure 2.5B**), albeit the TSKgel NH₂-100 (7) was unaffected by increasing the buffer concentration at this pH. At $^{\text{w}}\text{pH}$ 3.0/25 mM (**Figure 2.5C**), each amine phase (5-7) displayed different behaviors.

All zwitterionic phases (green triangles, 8-11) experienced some loss of cation exchange activity in **Figure 2.5A**. The reduction in ion interaction can mainly be ascribed to shielding of multi-point ionic interactions by the buffer salt, as noted by Chirita et al.⁶¹ and Dinh et al.¹⁵ Furthermore, although the surface functionalities significantly shield the underlying backbone of the ZIC-HILIC phases (8, 10),^{7,61} interactions with the silica backbone are still apparent. Namely, more significant reductions in cation exchange interactions (resulting from a 50-110 % reduction in BTMA retention) were observed for the ZIC-HILIC phases (8, 10) as compared to the ZIC-pHILIC (9). Interestingly, the ZIC-cHILIC (11) remained nearly unaffected (0, 0 in **Figure 2.5A**) when the buffer concentration was increased at w^w pH 6.8.

At w^w pH 5.0 (**Figure 2.5B**), the differences in ion interaction between the zwitterionic phases (green triangles) collapse such that the columns 8-11 all display similar loss of cation exchange activity (i.e., $\Delta k_{\text{BTMA}}/k_{\text{uracil}}$ is near equal for columns 8-11). At w^w pH 3.0 (**Figure 2.5C**), all zwitterionic phases (8-11) showed minimal change in cation exchange activity (i.e., $\Delta k_{\text{BTMA}}/k_{\text{uracil}} \approx 0$).

Overall, the hydrophilicity behavior of the zwitterionic phases in response to buffer concentration was complex. At w^w pH 6.8 and 5.0 (**Figures 2.5A** and **2.5B**), all zwitterionic phases (8-11) displayed minimal changes in $k_{\text{cytosine}}/k_{\text{uracil}}$. At w^w pH 3.0 (**Figure 2.5C**), the $k_{\text{cytosine}}/k_{\text{uracil}}$ of the zwitterionic phases was more variable but likely compromised due to cytosine protonation.

The amide phases (brown diamonds, 12 and 13) under all pH conditions experienced a small reduction in $k_{\text{BTMA}}/k_{\text{uracil}}$ when the buffer concentration was increased from 5 to 25 mM (**Figures 2.5A-C**). The decrease is attributed to ionic shielding of the

interactions between BTMA and the underlying silanols. This effect was small as the bonded groups or polymeric layer block most silanols.^{15,54} The hydroxylated phases (pink open triangles, 14-16) and PolyHYDROXYETHYL A (black asterisk, 21) behaved similarly, except at w pH 3.0/25 mM (**Figure 2.5C**), where a small increase in cation exchange activity was observed. As noted in **Section 2.3.1**, these hydroxylated phases (14-16) show multiple interactions beyond ion exchange.¹⁵ It is probable that the observed ion interaction behavior of the hydroxylated phases (14-16) is due to other interactions not studied in this work.

The hydrophilicity of the amide (12, 13), hydroxylated phases (14-16), and PolyHYDROXYETHYL A (21) was generally unaffected by increased buffer concentration across all pH's tested. However, the Ascentis Express OH5 (15), FRULIC-N (16) and PolyHYDROXYETHYL A (21) phases did show increased $k_{\text{cytosine}}/k_{\text{uracil}}$ in **Figure 2.5C**.

The Acclaim HILIC-10 (18) showed no consistent trend in ion exchange or hydrophilicity with increased buffer concentration (**Figures 2.5A-C**). **Table 2.5** summarizes the effects of buffer concentration on this phase at the three pH conditions. As noted in **Section 2.3.1**, the proprietary nature of this phase prohibits the rationalization of this column's behavior.

Table 2.5. Summary of selectivity changes of the Acclaim HILIC-10 (column 18) as the buffer concentration is increased at different pH values.

w pH	Effect of increased [buffer]	
	Ion Interaction	Hydrophilicity
6.8	- CE	--
5.0	0	-
3.0	+++ CE	+++

^aLegend: ++++/---- very strong increase/decrease, +++/--- strong increase/decrease, ++/-- moderate increase/decrease, +/- weak increase/decrease, 0 no effect, CE cation exchange, AE anion exchange.

Lastly, as observed by Dinh et al.,¹⁵ PolySULFOETHYL A (22) showed significantly reduced cation exchange activity at all pH's with increased buffer concentration (**Figures 2.5A-C**). This loss in ion interaction may be attributed to shielding of the electrostatic interaction between the anionic sulfonate groups and BTMA. Accordingly, BTMA experienced a > 2-fold reduction in retention at both w pH 6.8 and 5.0 when a 25 mM buffer was used (**Table 2.3**). Further, at w pH 3.0/25 mM the PolySULFOETHYL A exhibited a sharp decrease in $k_{\text{cytosine}}/k_{\text{uracil}}$, arising from a significant decrease in electrostatic retention of cationic cytosine relative to w pH 3.0/5 mM buffer ($k = 17.6$ vs. 9.5).

Along with a summary of the pH-dependent effects on selectivity discussed in **Section 2.3.1**, **Table 2.2** also summarizes the effects of buffer concentration on HILIC selectivity behaviors of various columns as detailed above in this section. Once again the magnitude of the changes in ion exchange and hydrophilicity in response to increasing buffer concentration are graded on a scale of 0 (no change) to ++++/---- (very strong increase/decrease). Those phases which displayed behaviours too complex to adequately summarize using the above scheme are listed as “complex.”

2.4 Conclusions

This work is the one of the first systematic investigations of selectivity effects on many different HILIC phases across a wide range of pH values using different buffer concentrations. I have investigated and plotted the hydrophilicity vs. ion interaction selectivity behavior of 19 HILIC columns. Plots of the changes in selectivity between different pH values and buffer concentrations pinpoint the effect of mobile phase conditions on column interactions. From these difference plots several trends emerge. At $w^w\text{pH} \geq 5$, only minor changes in selectivity are observed. Increasing buffer concentration at $w^w\text{pH} \geq 5$ resulted in a general muting of ionic interactions due to ionic shielding by the buffer salt. Lowering the $w^w\text{pH}$ below 5 caused large changes in the ionic interaction selectivity (especially in phases that utilize ion exchange as part of their retention mechanism) due to protonation of the silanols. Lowering $w^w\text{pH}$ to 3 also resulted in some HILIC phases appearing to increase their hydrophilicity. These observations were supported by additional measurements of representative columns at $w^w\text{pH}$ 3.7 where cytosine is uncharged (as determined by UV absorbance spectra).

2.5 References

- (1) Alpert, A. J. *J. Chromatogr. A* **1990**, *499*, 177–196.
- (2) Tang, D.-Q.; Zou, L.; Yin, X.-X.; Ong, C. N. *Mass Spectrom. Rev.* **2014**.
- (3) Majors, R. E. *LC-GC North Am.* **2012**, *30*, 20–34.
- (4) Buszewski, B.; Noga, S. *Anal. Bioanal. Chem.* **2012**, *402*, 231–247.

- (5) Nováková, L.; Havlíková, L.; Vlčková, H. *TrAC Trends Anal. Chem.* **2014**, *63*, 55–64.
- (6) Hemström, P.; Jonsson, T.; Appelblad, P.; Jiang, W. *Chromatogr. Today* **2011**, 4–8.
- (7) Hemström, P.; Irgum, K. *J. Sep. Sci.* **2006**, *29*, 1784–1821.
- (8) Jandera, P. *Anal. Chim. Acta* **2011**, *692*, 1–25.
- (9) Guo, Y. *Analyst* **2015**, *140*, 6452–6466.
- (10) Guo, Y. In *Hydrophilic Interaction Liquid Chromatography (HILIC) and Advanced Applications*; Wang, P. G.; He, W., Eds.; CRC Press: Boca Raton, FL, 2011; pp. 401–426.
- (11) Guo, Y.; Gaiki, S. *J. Chromatogr. A* **2011**, *1218*, 5920–5938.
- (12) Schuster, G.; Lindner, W. *J. Chromatogr. A* **2013**, *1301*, 98–110.
- (13) Periat, A.; Debrus, B.; Rudaz, S.; Guillarme, D. *J. Chromatogr. A* **2013**, *1282*, 72–83.
- (14) Wang, J.; Guo, Z.; Shen, A.; Yu, L.; Xiao, Y.; Xue, X.; Zhang, X.; Liang, X. *J. Chromatogr. A* **2015**, *1398*, 29–46.
- (15) Dinh, N. P.; Jonsson, T.; Irgum, K. *J. Chromatogr. A* **2011**, *1218*, 5880–5591.
- (16) Zhang, R.; Watson, D. G.; Wang, L.; Westrop, G. D.; Coombs, G. H.; Zhang, T. *J. Chromatogr. A* **2014**, *1362*, 168–179.

- (17) Gika, H. G.; Theodoridis, G. A.; Vrhovsek, U.; Mattivi, F. *J. Chromatogr. A* **2012**, *1259*, 121–127.
- (18) Isokawa, M.; Kanamori, T.; Funatsu, T.; Tsunoda, M. *Bioanalysis* **2014**, *6*, 2421–2439.
- (19) Kahsay, G.; Song, H.; Van Schepdael, A.; Cabooter, D.; Adams, E. *J. Pharm. Biomed. Anal.* **2014**, *87*, 142–154.
- (20) Mercier, T.; Tissot, F.; Gardiol, C.; Corti, N.; Wehrli, S.; Guidi, M.; Csajka, C.; Buclin, T.; Couet, W.; Marchetti, O.; Decosterd, L. A. *J. Chromatogr. A* **2014**, *1369*, 52–63.
- (21) Zhou, Z.; Wu, X.; Wei, Q.; Liu, Y.; Liu, P.; Ma, A.; Zou, F. *Anal. Bioanal. Chem.* **2013**, *405*, 6323–6335.
- (22) Nemoto, T.; Lee, X.-P.; Kumazawa, T.; Hasegawa, C.; Fujishiro, M.; Marumo, A.; Shouji, Y.; Inagaki, K.; Sato, K. *J. Pharm. Biomed. Anal.* **2014**, *88*, 71–80.
- (23) Zhu, R.-H.; Li, H.-D.; Cai, H.-L.; Jiang, Z.-P.; Xu, P.; Dai, L.-B.; Peng, W.-X. *J. Pharm. Biomed. Anal.* **2014**, *96*, 31–36.
- (24) Guo, S.; Duan, J.; Qian, D.; Tang, Y.; Qian, Y.; Wu, D.; Su, S.; Shang, E. *J. Agric. Food Chem.* **2013**, *61*, 2709–2719.
- (25) Karatapanis, A. E.; Fiamegos, Y. C.; Stalikas, C. D. *J. Sep. Sci.* **2009**, *32*, 909–917.
- (26) Spackova, V.; Pazourek, J. *Chem. Pap.* **2013**, *67*, 357–364.

- (27) Xiong, Y.; Zhao, Y.-Y.; Goruk, S.; Oilund, K.; Field, C. J.; Jacobs, R. L.; Curtis, J. *M. J. Chromatogr. B* **2012**, *911*, 170–179.
- (28) Bernal, J.; Ares, A. M.; Pol, J.; Wiedmer, S. K. *J. Chromatogr. A* **2011**, *1218*, 7438–7452.
- (29) van Nuijs, A. L. N.; Tarcomnicu, I.; Covaci, A. *J. Chromatogr. A* **2011**, *1218*, 5964–5974.
- (30) Schlichtherle-Cerny, H.; Affolter, M.; Cerny, C. *Anal. Chem.* **2003**, *75*, 2349–2354.
- (31) Koupparis, M. A.; Megoulas, N. C.; Gremilogianni, A. M. *Chem. Anal.* **2013**, *177*, 239–264.
- (32) Melmer, M.; Stangler, T.; Premstaller, A.; Lindner, W. *J. Chromatogr. A* **2011**, *1218*, 118–123.
- (33) Adamczyk, B.; Struwe, W. B.; Ercan, A.; Nigrovic, P. A.; Rudd, P. M. *J. Proteome Res.* **2013**, *12*, 444–454.
- (34) Tao, S.; Huang, Y.; Boyes, B. E.; Orlando, R. *Anal. Chem.* **2014**, *86*, 10584–10590.
- (35) Horie, K.; Kamakura, T.; Ikegami, T.; Wakabayashi, M.; Kato, T.; Tanaka, N.; Ishihama, Y. *Anal. Chem.* **2014**, *86*, 3817–3824.
- (36) Li, X.; Jiang, J.; Zhao, X.; Wang, J.; Han, H.; Zhao, Y.; Peng, B.; Zhong, R.; Ying, W.; Qian, X. *PLoS One* **2013**, *8*, e81921/1–e81921/15, 15 pp.

- (37) Longworth, J.; Noirel, J.; Pandhal, J.; Wright, P. C.; Vaidyanathan, S. *J. Proteome Res.* **2012**, *11*, 5959–5971.
- (38) Di Palma, S.; Mohammed, S.; Heck, A. J. R. *Nat. Protoc.* **2012**, *7*, 2041–2055.
- (39) Ibrahim, M. E. A.; Lucy, C. A. In *Hydrophilic Interaction Chromatography: A Guide for Practitioners*; Olsen, B. A.; Pack, B. W., Eds.; John Wiley & Sons: Hoboken, NJ, 2013; Vol. 177, pp. 43–85.
- (40) Dinh, N. P.; Jonsson, T.; Irgum, K. *J. Chromatogr. A* **2013**, *1320*, 33–47.
- (41) Soukup, J.; Jandera, P. *J. Chromatogr. A* **2014**, *1374*, 102–111.
- (42) Gritti, F.; Hölzel, A.; Tallarek, U.; Guiochon, G. *J. Chromatogr. A* **2015**, *1376*, 112–125.
- (43) McCalley, D. V. *J. Chromatogr. A* **2010**, *1217*, 3408–3417.
- (44) Neue, U. D. *J. Sep. Sci.* **2007**, *30*, 1611–1627.
- (45) Neue, U. D.; VanTran, K.; Iraneta, P. C.; Alden, B. A. *J. Sep. Sci.* **2003**, *26*, 174–186.
- (46) Ibrahim, M. E. A.; Liu, Y.; Lucy, C. A. *J. Chromatogr. A* **2012**, *1260*, 126–131.
- (47) Nawrocki, J. *J. Chromatogr. A* **1997**, *779*, 29–71.
- (48) Greco, G.; Grosse, S.; Letzel, T. *J. Chromatogr. A* **2012**, *1235*, 60–67.
- (49) Kumar, A.; Heaton, J. C.; McCalley, D. V. *J. Chromatogr. A* **2013**, *1276*, 33–46.

- (50) Heaton, J. C.; McCalley, D. V. *J. Chromatogr. A* **2014**, *1371*, 106–116.
- (51) Heaton, J. C.; Russell, J. J.; Underwood, T.; Boughtflower, R.; McCalley, D. V. *J. Chromatogr. A* **2014**, *1347*, 39–48.
- (52) Ikegami, T.; Tomomatsu, K.; Takubo, H.; Horie, K.; Tanaka, N. *J. Chromatogr. A* **2008**, *1184*, 474–503.
- (53) Calculated from ACD labs software, V11.02, 2014.
- (54) Kawachi, Y.; Ikegami, T.; Takubo, H.; Ikegami, Y.; Miyamoto, M.; Tanaka, N. *J. Chromatogr. A* **2011**, *1218*, 5903–5919.
- (55) Wahab, M. F.; Ibrahim, M. E. A.; Lucy, C. A. *Anal. Chem.* **2013**, *85*, 5684–5691.
- (56) Alpert, A. J. *Anal. Chem.* **2008**, *80*, 62–76.
- (57) Subirats, X.; Rosés, M.; Bosch, E. *Sep. Purif. Rev.* **2007**, *36*, 231–255.
- (58) Schwer, C.; Kenndler, E. *Anal. Chem.* **1991**, *63*, 1801–1807.
- (59) Billingham, B. E.; Oladepo, S. A.; Loppnow, G. R. *J. Phys. Chem. B* **2009**, *113*, 7392–7397.
- (60) Guo, Y.; Gaiki, S. *J. Chromatogr. A* **2005**, *1074*, 71–80.
- (61) Chirita, R.-I.; West, C.; Zubrzycki, S.; Finaru, A.-L.; Elfakir, C. *J. Chromatogr. A* **2011**, *1218*, 5939–5963.
- (62) Jiang, W.; Irgum, K. *Anal. Chem.* **1999**, *71*, 333–344.

- (63) Wang, X.; Lin, X.; Xie, Z.; Giesy, J. P. *J. Chromatogr. A* **2009**, *1216*, 4611–4617.
- (64) Qiu, H.; Loukotková, L.; Sun, P.; Tesařová, E.; Bosáková, Z.; Armstrong, D. W. *J. Chromatogr. A* **2011**, *1218*, 270–279.

CHAPTER 3: Aniline-Modified Porous Graphitic Carbon for Hydrophilic Interaction and Attenuated Reverse Phase Liquid Chromatographyⁱⁱ

3.1 Introduction

As noted in Chapter 1, a multitude of silica based phases with different selectivities are commercially available for RPLC and HILIC. These include hydrophobic C₈ and C₁₈ columns for RPLC,¹⁻⁴ and a variety of positively and negatively charged, zwitterionic, and neutral polar bonded phases on silica for HILIC.⁵⁻⁷

However, traditional silica based phases are limited with respect to pH and temperature. Above pH 8, the silica backbone solubilizes, while below pH 2 the bonded material hydrolyzes.^{8,9} Both degradation processes are accentuated by increased column temperature such that manufacturers generally recommend temperatures no higher than 60 °C.^{10,11}

Knox *et al.*¹² developed porous graphitic carbon (PGC) particles as an alternative to traditional silica HPLC phases. These columns have been commercialized by Thermo Scientific under the trade-name Hypercarb with 3 and 5 μm PGC particles available.¹³

PGC is stable over pH 0-14 and can withstand temperatures > 200 °C, thereby enabling use of extreme separation conditions.^{13,14} Furthermore, PGC has been called the ultimate reversed phase material, since 20-40% more ACN is required to elute compounds on PGC than from a comparable C₁₈ phase.¹⁵ Thus, PGC is often used as the second column in comprehensive and heart cutting 2D-LC separations.¹⁶⁻¹⁹

ⁱⁱ A version of this chapter has been previously published as Iverson, C. D.; Lucy, C. A. *J. Chromatogr. A*, **2014**, *1373*, 17-24. See the Preface for further details.

Modification of the carbon surface of PGC is desirable for two reasons. First, the stability of PGC would be useful for other modes of HPLC such as HILIC. However, although unmodified PGC shows increased retention of polar compounds as compared to ODS bonded phases, relative to many commercial silica-based HILIC phases the retention of most high polarity compounds is weak.^{20,21} Second, while the high retention noted above can be beneficial, it can also be a curse. Compounds may be so strongly retained by PGC that long analysis times and lower efficiency result. Harsh elution conditions may be used,²² but even then some compounds are irreversibly retained.²³

PGC is difficult to covalently modify.²⁴ Most approaches to increasing the hydrophilicity of PGC involve strong oxidizing agents such as nitric acid²⁵ or permanganate.²⁶ Alternatively, PGC has been functionalized *in situ* with di-*tert*-amylperoxide.²⁷ Relative to unfunctionalized PGC, the di-*tert*-amylperoxide modification decreased RPLC retention on average by 7% and increased column efficiency by ~20%.²⁷ Several non-covalent modifications which can also passivate the retentivity of PGC, such as the adsorption of polyethylene glycol, have been noted in a recent review.¹³

Recently, the Lucy Group has used aryl diazonium chemistry to modify PGC for ion chromatography and HILIC.²⁸⁻³⁰ Introduction of carboxylates to the PGC surface yielded novel HILIC selectivity and a ~5-fold increase in hydrophilicity.²⁸ In this chapter, I report the preparation and characterization of two aniline modified PGC phases; one of which demonstrated both HILIC and attenuated reverse phase properties.

3.2 Experimental

3.2.1 Chemicals and Reagents

Porous graphitic carbon (PGC, 5 μm spherical particles comprised of pure graphitic carbon, 250 \AA , 120 m^2/g , lot no. PGC593; O/C ratio of 2 %, see **Table 3.1**) was from Thermo Fisher Scientific. Deionized water ($> 17.7 \text{ M}\Omega$) was from a Barnstead E-pure system (Marietta, OH, USA). Sodium nitrite, sodium borohydride, sodium hydroxide, 4-nitroaniline, N,N-dimethyl-*p*-phenylenediamine HCl, HPLC grade ammonium formate, and LC-MS grade water, acetonitrile, and formic acid were from Sigma Aldrich (St. Louis, MO, USA). Hydrochloric acid (37 %), potassium hydroxide, N,N-dimethylformamide (DMF), and dimethylsulfoxide (DMSO) were from Caledon Laboratory Chemicals (Georgetown, ON, Canada). HPLC grade ammonium acetate, iron powder ($< 10 \mu\text{m}$, 99.9 %), and reagent grade ammonium chloride were from Alfa Aesar (Wardtown, MA, USA). Anhydrous ethanol, Optima grade acetonitrile, methanol, acetone, and salicylic acid ($> 99\%$) were from Fisher Scientific (Fair Lawn, NJ, USA). Benzyltrimethylammonium chloride (BTMA) was from ACROS Organics (Fair Lawn, NJ). Phenol (ACS reagent, 99%) was from ACP (Montreal, QC, Canada) and phlorglucinol was from Fluka (Buchs, Switzerland). All other chromatographic standards were from Sigma Aldrich and had $\geq 99\%$ purity. The structures of all test compounds are shown in **Figure 3.1**. Log P and pK_a data for the test compounds are given in **Appendix 2**

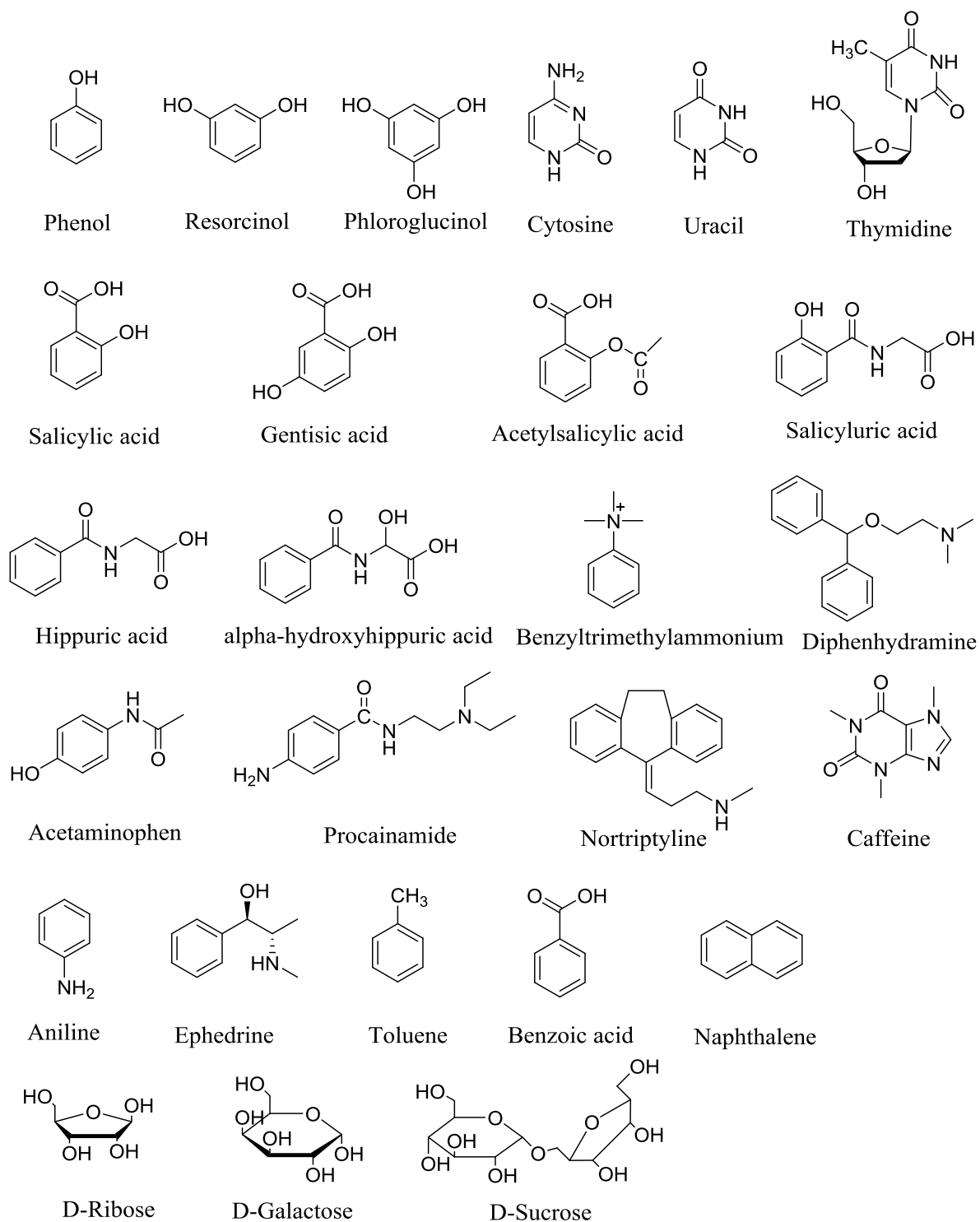
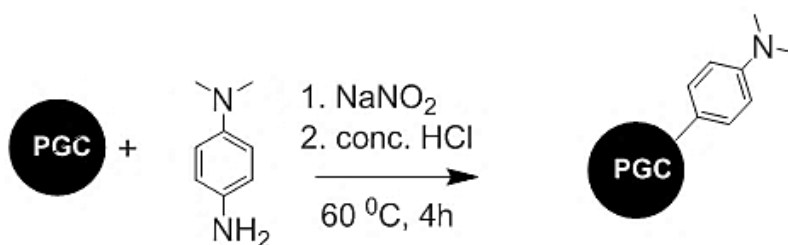


Figure 3.1. Structures of analytes used to characterize the Dimethylaniline-PGC and Aniline-PGC stationary phases. Log P and pK_a data for the test compounds are given in **Appendix 2**.

3.2.2 Synthesis of Dimethylaniline-PGC

Diazonium chemistry with N, N-dimethyl-*p*-phenylenediamine (**Figure 3.2**) was used to introduce N,N-dimethylaniline onto the PGC surface as per Chambers et al.²⁹ As X-ray photoelectron spectroscopic (XPS, Section 2.5) analysis of this material indicated low nitrogen surface concentration (0.3 atomic % \equiv 0.3 molecules/nm²), a second round of functionalization was performed following the method of Wahab et al.²⁸

First Grafting:



Second Grafting:

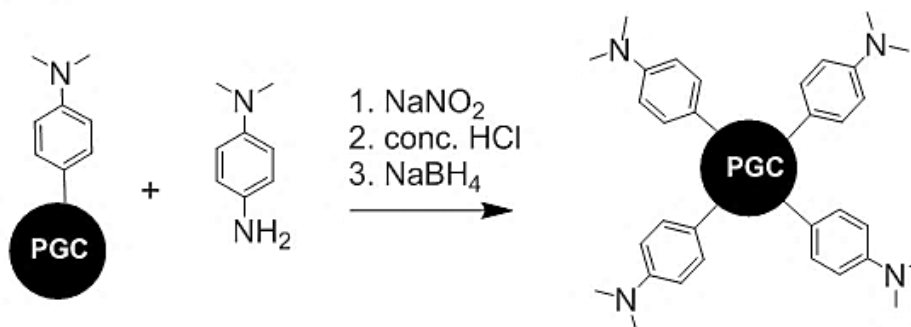


Figure 3.2. Reaction scheme for the synthesis of Dimethylaniline-PGC.

3.2.3 Synthesis of Aniline-PGC

Synthesis of the Aniline-PGC phase (**Figure 3.3**) was based on previous syntheses in the Lucy group,^{28,29} with several modifications. 50 mmol of 4-nitroaniline was added to a 1 L beaker containing 45 mL (540 mmol) conc. HCl, 35 mL DMSO, and 15 mL deionized water. The mixture was warmed to dissolve the aniline and then cooled to room temperature. 1.8 g of porous graphitic carbon (PGC) suspended in 30 mL DMSO was added, and the mixture was stirred at room temperature for 15 min, and then at 5-10 °C for 30 min. To this suspension, 50 mmol of NaNO₂ in 50 mL of 50 % DMSO_(aq) was added quickly and stirred at 5-10 °C for 2 h. Sodium borohydride (120 mmol in 50 mL 40% DMSO_(aq)) was added dropwise over 10 min with vigorous stirring at 5-10 °C to yield the nitrobenzene modified PGC (*Caution: the reaction is vigorous due to the evolution of both hydrogen and nitrogen gas*). After stirring for an additional 20 min at 5-10 °C, the suspension was diluted in methanol and filtered using a 0.22 µm nylon filter. The solid material was successively washed with DMSO, DMF, deionized water, 1 % KOH, ethanol, acetone, and methanol until no color was observed. This material was characterized by XPS (**Sections 3.2.5 and 3.3.2**). The grafting procedure was then repeated a second time and the particles were dried under vacuum overnight.

The nitro group of the grafted nitrobenzene was reduced to the amine as per a previously reported method.³¹ In a 250 mL 3-neck flask, 250 mmol spherical iron powder (<10 µm) was suspended in 80 mL ethanol. 2.1 mL (25 mmol) conc. HCl was added to the stirred solution, and the mixture was warmed to 65 °C over 30-45 min and then stirred at 65 °C for 2 h. After cooling to 55-60 °C over 10 min, 40 mL (187 mmol) 25 % NH₄Cl solution was added. The temperature was increased to 75 °C and the modified

PGC material was added in portions over 15 min. The suspension was stirred at 65 °C for 3 h and cooled to room temperature to yield the Aniline-PGC. The bulk iron was removed magnetically. Residual iron was removed by addition of 800 mL 2 M HCl and stirring at room temperature for 60 h. The acidified solution was diluted 4-fold in deionized water (to prevent the supernatant from dissolving the membrane filters) and filtered using a 0.22 µm nylon filter. The particles were washed with 2 L of 0.15 M HCl to remove dissolved residual iron from the previous step, followed by sequential washings with water, ethanol, DMSO, DMF, acetone, and methanol to remove any adsorbed species from the particles. The Aniline-PGC particles were dried over suction for 2 h and defined three times by sedimentation (18 h each) in ~900 mL deionized water, yielding 1.7 g of modified particles.

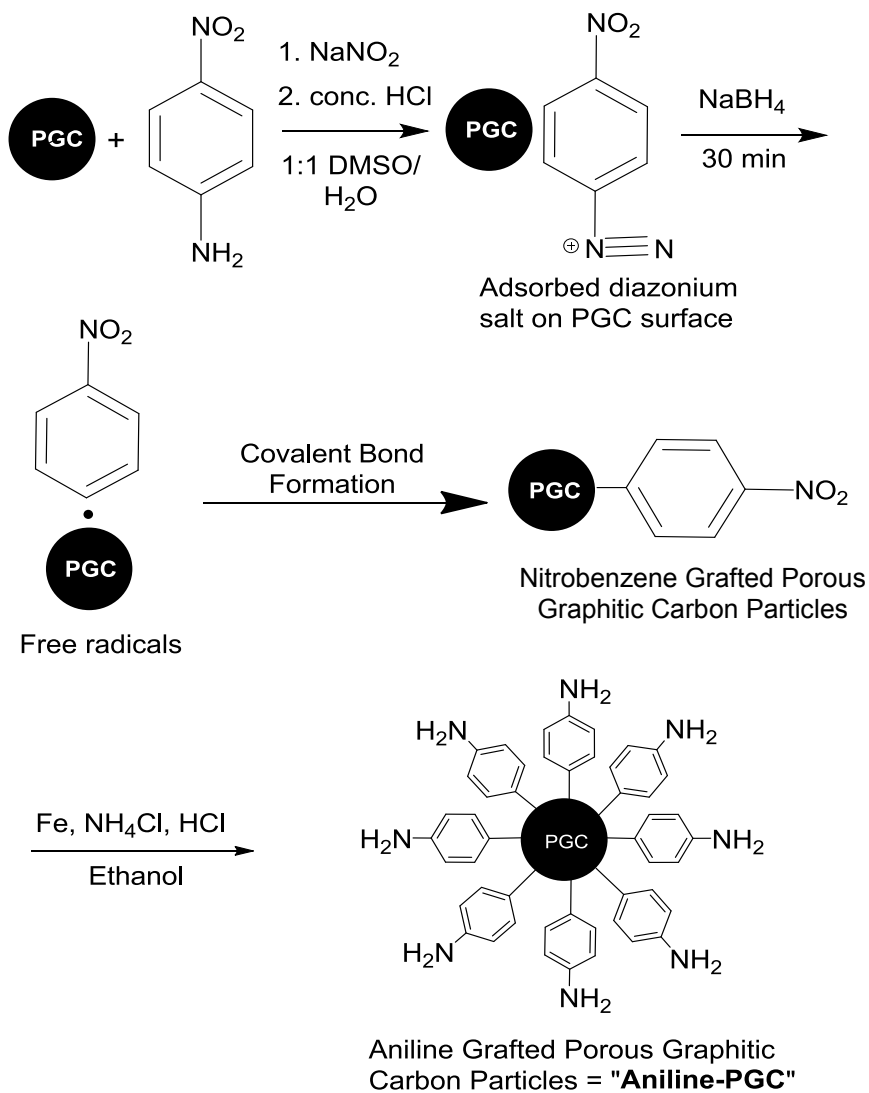


Figure 3.3. Scheme for the addition of aniline functionalities onto the surface of PGC by using an *in situ* generated nitrobenzene diazonium salt. Once grafted, the aniline is generated via the reduction of the nitro group using iron powder under acidic conditions.

3.2.4 Packing

Columns were packed at constant pressure using a Haskel pump (DSF-122-87153, Burbank, CA, USA) driven by N₂ gas (Praxair Inc., Edmonton, AB, Canada). 1 g of Dimethylaniline-PGC or 1.7 g of Aniline-PGC from above was slurried in 35 mL deionized water and placed into a 40 mL slurry reservoir (Lab Alliance, State College, PA, USA). The remaining 5 mL of the final rinse from the container was added to the reservoir to fully fill the slurry reservoir. The particles were packed in a downward direction into a 50 mm x 4 mm ID (Dimethylaniline-PGC) or a 150 mm × 3 mm ID (Aniline-PGC) polyether ether ketone (PEEK) column fitted with a Ti outlet frit. Pressure was maintained at 35 MPa for 1.5 h using deionized water as the driving solvent. The columns were detached from the packing assembly and were washed with mixtures of ACN-NaOH (0.1-0.2 M) until the baseline at 254 nm became stable. After washing, PEEK screw caps with ultrahigh molecular weight polyethylene frits (UHMWPE) and 0.2 μm Zitex membranes (Thermo Fisher Scientific, Sunnyvale, CA, USA) were installed on both ends. Prior to the first separation, the columns were washed with 50 % aqueous ACN and neat ACN.

3.2.5 Characterization of the PGC Phases

X-ray photoelectron spectroscopy (XPS) was performed on an AXIS 165 spectrometer (Kratos Analytical, NY). XPS spectra of the unmodified PGC were collected on the raw material as received. Dimethylaniline-PGC and Aniline-PGC particles were washed with methanol and dried under house vacuum for two days prior to XPS analysis. Thermogravimetric (TGA) analyses were done on a Perkin Elmer TGA

analyzer (Norwalk, CT, USA) under a nitrogen atmosphere from ambient temperature to 900 °C at 10 °C/min.

3.2.6 Chromatographic Separations

Chromatographic studies (except for the chemical reactivity study, see **Section 3.2.7**) were performed on a Waters (Mississauga, ON, Canada) Acquity UPLC system consisting of a binary solvent manager, a thermostated (5 °C) sample manager equipped with a 10 µL loop (all injections were 5 µL partial loop), thermostated column compartment, and a tunable UV detector. The instrument was controlled using Empower software (Waters). Except where noted, the column temperature was 25 °C. Separations were performed at flow rates of 0.5-1.0 mL/min. Data were collected at 20 Hz at 254 or 268 nm.

The mobile phase was a mixture of ACN, ammonium acetate or ammonium formate, and water. The pH was adjusted with NaOH or HCl. Aqueous stock ammonium acetate/ammonium formate solutions (2 M) at the desired pH were made and refrigerated. The reported buffer concentration is the final concentration in the eluent after mixing with ACN. The reported pH of the buffer is the final pH of aqueous diluted buffer prior to adding acetonitrile. The percentage of ACN in this work represents the volume of ACN relative to the total volume of the solvents including buffer and ACN.

An unmodified PGC (100 × 4.6 mm ID, 5 µm, Thermo Scientific, USA) and an Epic HILIC-PI column (aniline bound to silica, 100 × 4.6 mm ID, 5 µm, gifted by ES Industries, West Berlin, NJ, USA) were used as controls to assess the performance of the Dimethylaniline-PGC and/or Aniline-PGC phase.

3.2.7 Evaluation of the Chemical Reactivity of Aniline-PGC

LC-MS Separations on Aniline-PGC were performed on an Agilent (Mississauga, ON, Canada) 1100 series LC system consisting of a binary pump, autosampler, and thermostated column compartment. Detection was via an Agilent 1100 series MSD in the positive ion mode. The source gas temperature was 350 °C, and the capillary and fragmentor voltages were 4000 V and 80 V, respectively. The instrument was controlled using Chem Station software (Agilent).

8 µL injections of a 0.5 mM mixture of D-ribose, D-galactose, and D-sucrose (prepared in 90% ACN) were loaded onto the Aniline-PGC column. Separations were performed at 30, 40, and 50 °C (after 1 hour thermal equilibration) using 0.1 % formic acid in 90 % ACN at 0.55 mL/min. Data analysis was performed using Mass Hunter Qualitative Analysis v. 5.0 software (Agilent). Peak integration was done using the software's "general integration" parameters.

3.3 Results and Discussion

Porous graphitic carbon (PGC) is a very stable HPLC phase. Unfortunately the PGC surface can be too retentive in RPLC^{15,32} and often shows only weak HILIC retention.^{15,21,33} In this chapter, I investigate aniline-functionalization of PGC to create phases for HILIC and/or as a means to attenuate the reversed phase retention character of PGC. Previously, the Lucy lab used diazonium chemistry to introduce carboxylate functionalities to PGC to increase its hydrophilicity.²⁸

3.3.1 Synthesis of Phases

Previously, an N,N-dimethylaniline carbon phase was synthesized and characterized for ion chromatography.²⁹ Herein I re-explored the phase for HILIC behavior. However, the synthesis based on previous work in the Lucy group^{28,29} (**Figure 3.2, Section 3.2.2**) resulted in only 1 atomic % N (0.9 molecules/nm²) being introduced to the PGC surface (**Table 3.1**). This is within the 0.5-4.0 atomic % N previously reported.²⁹ This is less than 50 % of the maximum surface coverage.³⁴

During preliminary chromatographic characterization of this phase, only a minimal increase in HILIC character was observed over unmodified PGC in the separation of phenolic solutes (**Figure 3.4**). The weak HILIC character may be due to the low surface coverage and/or disruption of the water layer by the nonpolar substituents on the nitrogen.³⁵

Attempts to graft primary benzylamine functionalities directly onto the PGC surface posed several synthetic challenges. Use of *p*-phenylenediamine yielded 0.3 % nitrogen (elemental analysis) on porous 3 μm carbon clad zirconia.³⁶ *p*-phenylenediamine may also form two diazonium moieties which makes the reaction difficult to reproduce.³⁷ Alternatively, one could use *p*-aminobenzylamine. However, the benzyl amine readily oxidizes to the hydroxyl in the presence of aqueous NaNO₂ and HCl.³⁸ This oxidation can be circumvented via the use of a suitable protecting group such as a fluoroenylmethyloxycarbonyl (Fmoc)³⁹ but this resulted in only 0.5 atomic % N (0.35 molecules/nm²) grafted, perhaps due to steric hindrance.

Thus, the synthetic route used herein (**Figure 3.3**) involved the grafting of *p*-nitroaniline onto the PGC surface. This grafting proceeded smoothly without side

reactions. Further, the nitro group should enhance diazonium salt formation.⁴⁰ Following the grafting, the desired aniline was obtained using a modified Bechamp iron reduction.³¹

Table 3.1. Surface composition from XPS survey scans of PGC, Dimethylaniline-PGC (DMA-PGC), and Aniline-PGC.

Element	Peak (eV)	FWHM (PGC)	Peak area (PGC) ^c	% Atomic conc. (PGC) ^a	FWHM (DMA-PGC)	Peak area (DMA-PGC)	% Atomic conc. (DMA-PGC) ^b	FWHM (Aniline-PGC)	Peak area (Aniline-PGC)	% Atomic conc. (Aniline-PGC) ^b
Carbon	1s 285.0	2.64	85480	98.1	2.65	2255093	94.1	2.86	67040	93.5
Nitrogen	1s 400.0	—	0	0	3.49	4581	1.10	2.53	3054	2.45
Oxygen	1s 535.0	3.10	265	1.19	3.13	32790	4.75	4.39	8469	4.09
Iron	2p 720.0	—	n/a	n/a	—	n/a	n/a	—	0	0 ^d

^a The composition was calculated from the peak areas in the spectra using the CasaXPS (version 2.3) with Scofield values of relative sensitivity factors (RSF). Shirley background correction was applied in the measurement of all peaks.

^b The values reported are after the second modification reaction.

^cbased on the measured peak areas from the survey spectrum of unmodified PGC, this material has an O/C ratio of 2 %.

^d Iron was absent in the high resolution scans indicating that the washing steps after the nitro reduction were successful.

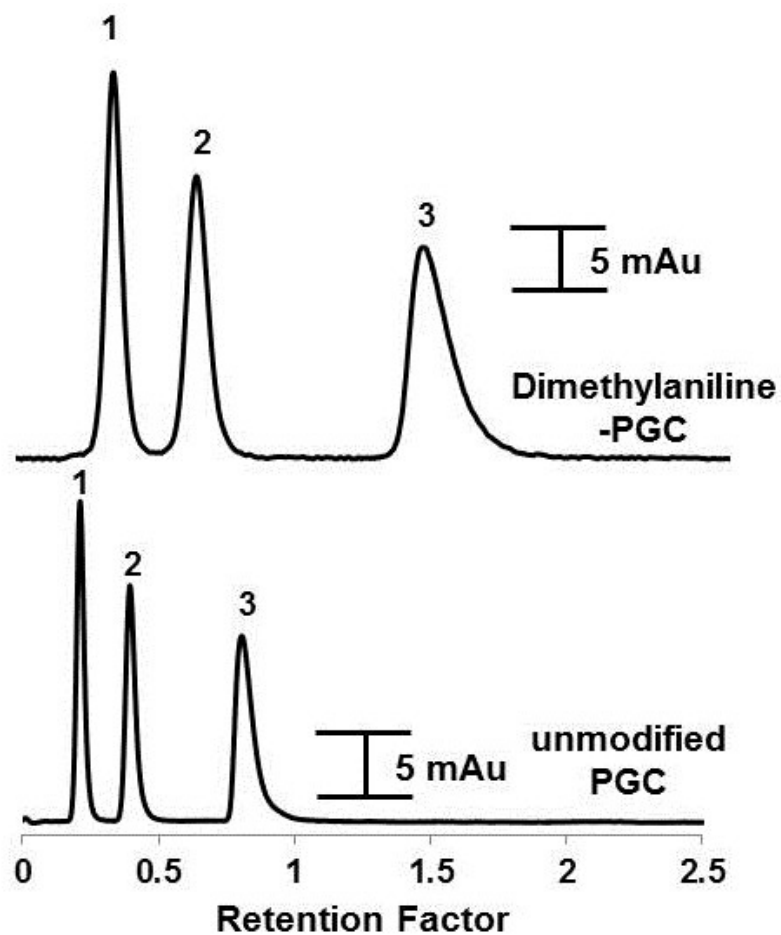


Figure 3.4. Comparison of the HILIC separation of 3 phenolic compounds by Dimethylaniline-PGC and unmodified PGC. Conditions: columns, Dimethylaniline-PGC (50 mm x 4 mm ID, 5 μ m) and unmodified PGC (100 mm x 4.6 mm ID, 5 μ m); 1 mL/min; eluent, 20 mM ammonium acetate (pH = 5.0) in 90 % ACN; analytes, 0.1-0.5 mM of (1) phenol, (2) resorcinol, and (3) phloroglucinol prepared in 90 % ACN; 25 $^{\circ}$ C. UV detection at 268 nm with a 5 μ L injection.

3.3.2 Characterization of Aniline-PGC

An indicator of reaction success was the increased wettability of the material. Prior to functionalization, PGC does not disperse in water without significant agitation. After functionalization, the material disperses readily (**Figure 3.5**). The increased wettability is promising as a HILIC phase must promote water layer formation.

Two rounds of grafting the nitrobenzene moiety introduced 2.6 atomic % N onto PGC based on XPS. After reduction of the nitro groups to the desired aniline, XPS showed 2.5 atomic % N (**Table 3.1**). I conservatively estimate a final aniline surface concentration of 2 molecules/nm², which is double the surface coverage obtained on the Dimethylaniline-PGC phase. This value is in line with similar modifications, which provided grafting concentrations of 1.9-2.6 molecules/nm².^{34,41} XPS also indicated successful removal of residual iron from the PGC material (no peaks in the 705-735 eV range).⁴² Thermogravimetric analysis showed only a 0.2 % mass loss (under nitrogen) at 200 °C, confirming that there were no surface impurities and demonstrating the thermal stability of the functionalized PGC.

The high resolution XPS spectrum (**Figure 3.6**) provided structural insights into the nature of the nitrogen groups on the PGC surface. After covalent addition of nitrobenzene, a dominant peak at 407 eV was observed (**Figure 3.6A**) corresponding to a -NO₂ functionality.^{34,41} Additional small peaks at 403 and 400 eV were evident. The peak at 403 eV (NH₂⁺/NH₃⁺) is believed to be an artifact generated by the XPS instrument during the analysis.^{43,44} It is possible, however, that this peak may have arisen from partial reduction of the nitro group by NaBH₄. Accordingly, some groups have opted for the use of milder reducing agents such as ascorbic acid.⁴⁵ The identity of the

peak at 400 eV may correspond to neutral amine moieties generated by the instrument as above, or to grafted molecules retaining their azo linkage (i.e., PGC–N=N–aniline),^{46,47} or most likely to a mixture of both. Residual azo linkers are a relatively common occurrence in diazonium carbon modifications.^{46,47} Following reduction with Fe, the -NO₂ peak disappeared and the intensity of the NH₂⁺/NH₃⁺ and 400 eV peaks increased (**Figure 3.6B**), indicating a successful reaction.

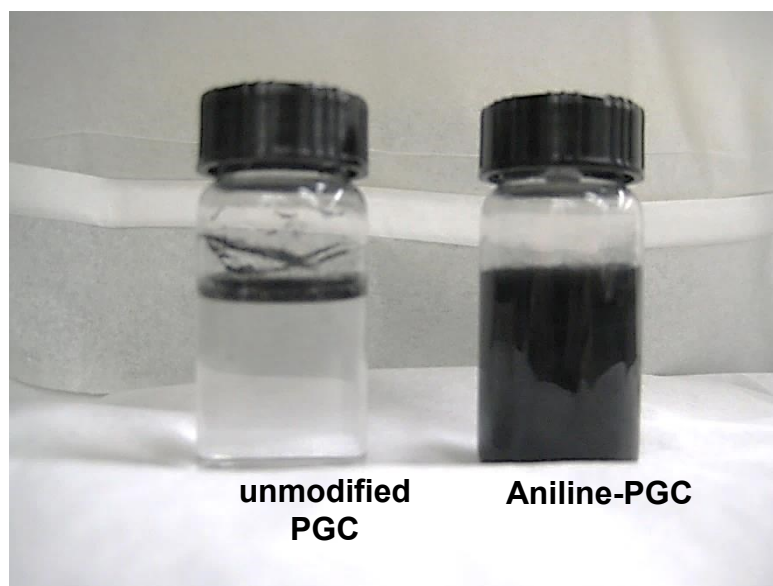


Figure 3.5. Photograph of the difference in wettability between unmodified-PGC and Aniline-PGC. Picture was taken immediately after 30 s sonication of vial.

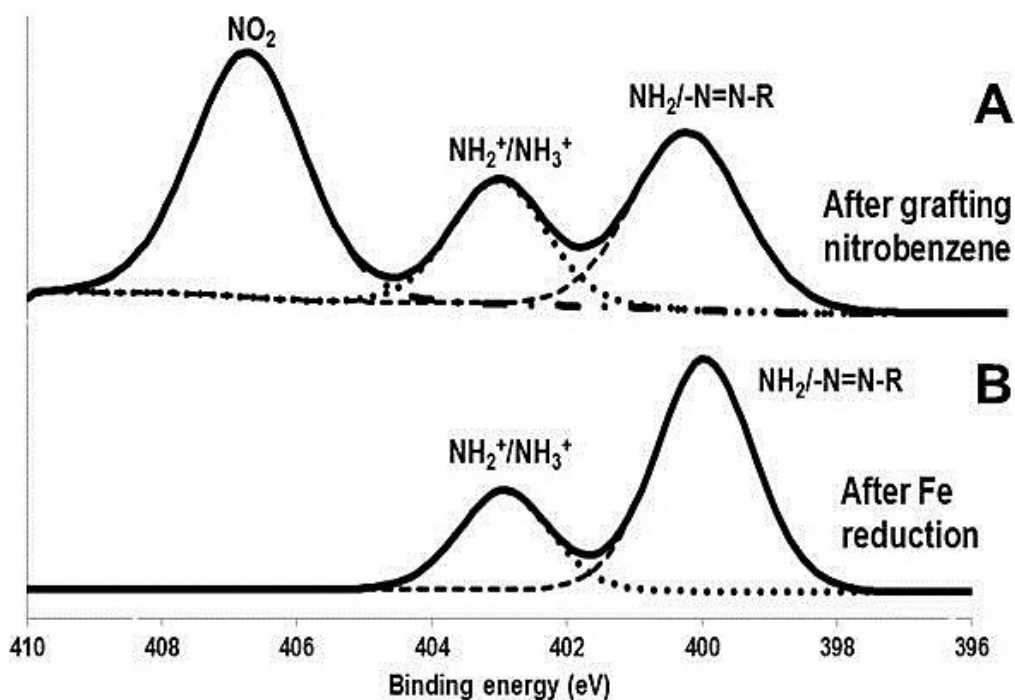


Figure 3.6. Curve-fitted high-resolution XPS spectra of the N 1s region (A) after the grafting of nitrobenzene and (B) after the iron powder reduction of the nitro group to the aniline. XPS measurements were performed on an AXIS 165 spectrometer. The base pressure in the analytical chamber was lower than 3×10^{-8} Pa. A monochromatic Al $K\alpha$ source ($h\nu = 1486.6$ eV) was used at a power of 210 W. The analysis spot was 400×700 μm . High resolution scans were collected for binding energies of 396-410 eV with an analyzer pass energy of 20 eV and a step of 0.1 eV.

3.3.3 HILIC Properties of Aniline-PGC

Figure 3.7 shows the separation of uracil, thymidine and cytosine on the Aniline-PGC phase and on a commercial silica phase with an aniline functionality (Epic HILIC-PI, ES Industries). The Aniline-PGC phase displays greater retention for all three compounds compared to the Epic phase, especially for thymidine ($k = 2.35$ vs. 1.42 , respectively) and cytosine ($k = 5.35$ vs. 0.78). Also, the Aniline-PGC and Epic phases exhibit different selectivity for cytosine vs. uracil ($\alpha = 5.2$ and 1.1 , respectively).

As shown in **Figure 3.8**, retention of cytosine and thymidine increased with increasing % ACN on both the Aniline-PGC and Epic phase, consistent with HILIC behavior. As in **Figure 3.7**, both compounds were less retained on the Epic phase than on the Aniline-PGC phase. The difference in retention was especially evident at pH 3.

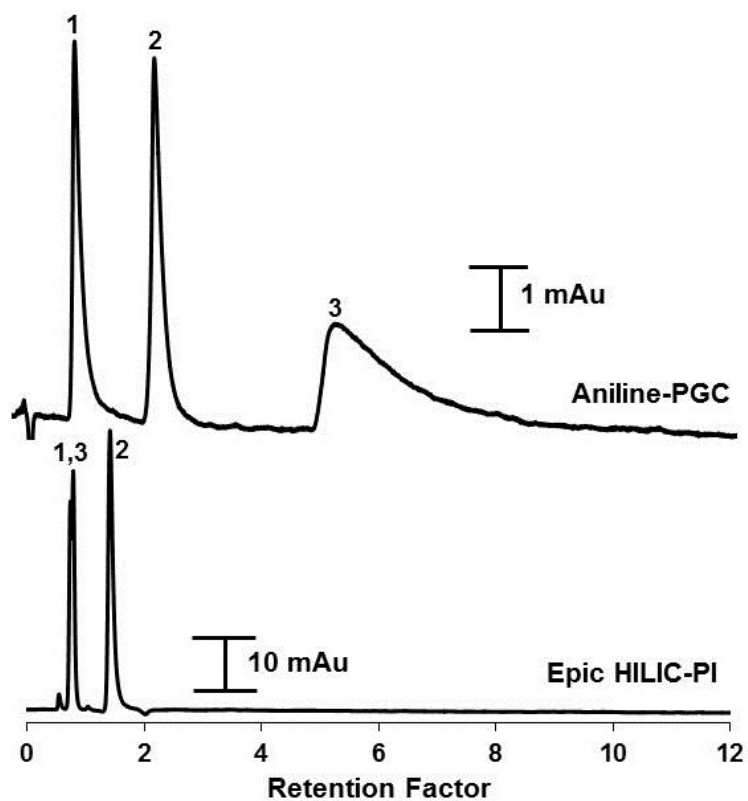


Figure 3.7. HILIC separation of 3 nucleobases on the amine-PGC and Epic HILIC-PI columns. Conditions: columns, Aniline-PGC (150 mm x 3 mm ID., 5 μ m) and Epic HILIC-PI (100 mm x 4.6 mm ID, 5 μ m); 0.5 mL/min; eluent, 10 mM ammonium formate (pH = 3.0) in 95 % ACN; analytes, 0.06-0.3 mM of (1) uracil, (2) thymidine, and (3) cytosine. UV detection at 254 nm with a 5 μ L injection.

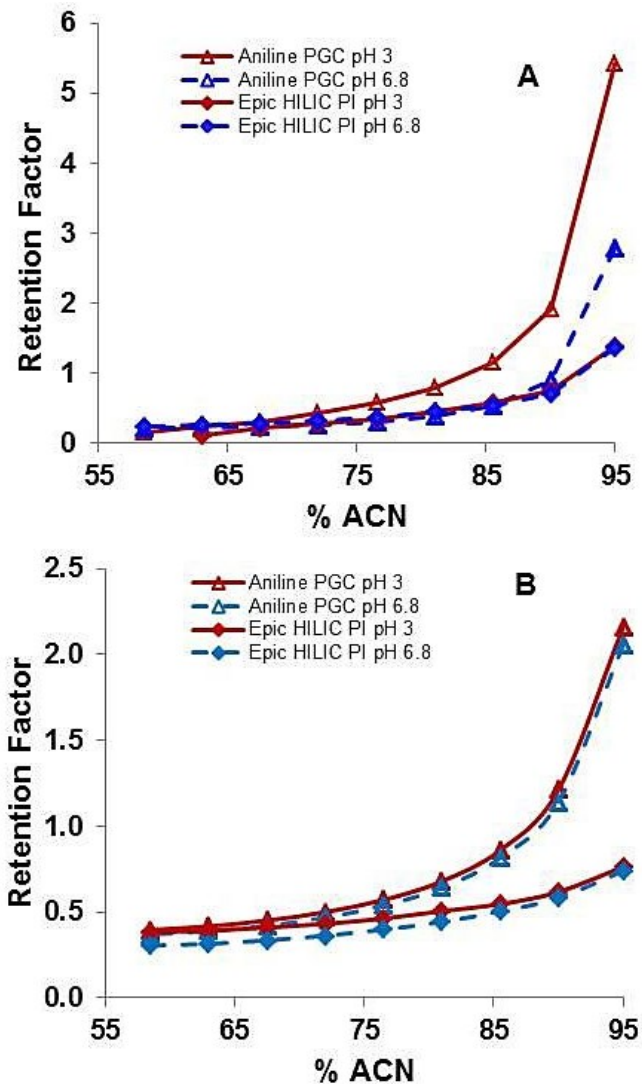


Figure 3.8. Retention behavior of (A) cytosine and (B) thymidine on Aniline-PGC and Epic HILIC PI as a function of % ACN in the eluent, measured at two different pH values. Conditions: columns, Aniline-PGC (150 mm x 3 mm ID, 5 μ m) and Epic HILIC-PI (100 mm x 4.6 mm ID., 5 μ m); 0.5 mL/min; eluents, 10 mM ammonium formate (pH = 3.0) or 10 mM ammonium acetate (pH = 6.8) in 57 to 95 % ACN; analytes, 0.25 mM cytosine and thymidine in 10 mM ammonium acetate (pH = 6.8):ACN (20:80). UV detection at 254 nm with a 5 μ L injection.

To further evaluate the HILIC selectivity of the Aniline-PGC phase, a separation of six carboxylic acids was performed (**Figure 3.9**). This test set has been utilized previously⁴⁸ to compare the selectivity of several different classes of silica-based HILIC phases. Literature retention data⁴⁸ are indicated by the peak numbers situated over markers placed along the line at the appropriate retention time in **Figure 3.9**. **Figure 3.9** also includes retention data for unmodified PGC, the Epic column, and the Carboxylate-PGC phase.²⁸ The Aniline-PGC phase shows completely different selectivity and retention order for these aromatic carboxylic acids. For instance, acetylsalicylic acid (ASA) elutes third on most HILIC phases, but is least retained on the Aniline-PGC. Compared to unmodified PGC and the EPIC phase, the Aniline-PGC displays improved resolution.

Figure 3.9 also demonstrates how the shape selectivity properties of the PGC backbone permit the resolution of structurally similar compounds. For example, salicylic acid (peak 4, **Figure 3.9**) and α -OH-hippuric acid (peak 6, **Figure 3.9**) differ only in the position of a hydroxyl group (**Figure 3.1**). The selectivity between peaks 4 and 6 is greater on Aniline-PGC ($\alpha = 3.6$) than on any of the silica phases ($\alpha = 0.7-0.92$, **Figure 3.9**). However, greater selectivity was observed with Carboxylate-PGC ($\alpha = 14$).²⁸

As discussed in **Chapter 2**, based on the extensive work of Dinh *et al.*,⁴⁹ Ibrahim *et al.*⁵⁰ presented a simple graphical plot to categorize HILIC phases according to their hydrophilicity (based on the relative retention of cytosine to uracil) and ionic character (relative retention of benzyltrimethylammonium (BTMA) to cytosine). These selectivities cluster HILIC column groups such as diol, zwitterion, bare silica, and amine phases. Unfortunately, the mobile phase pH of 6.8 used by Ibrahim *et al.*⁵⁰ is well above the

typical $w^w pK_a$ of anilines (~ 5).⁵¹ Hence aniline phases would be expected to be uncharged at $w^w pH$ 6.8. As a result, both Aniline-PGC and Epic HILIC PI exhibit low hydrophilicity at $w^w pH$ 6.8 (**Figure 3.10**). More hydrophilic character would be expected at lower pH where the aniline is protonated, as was observed in **Figure 3.7**.

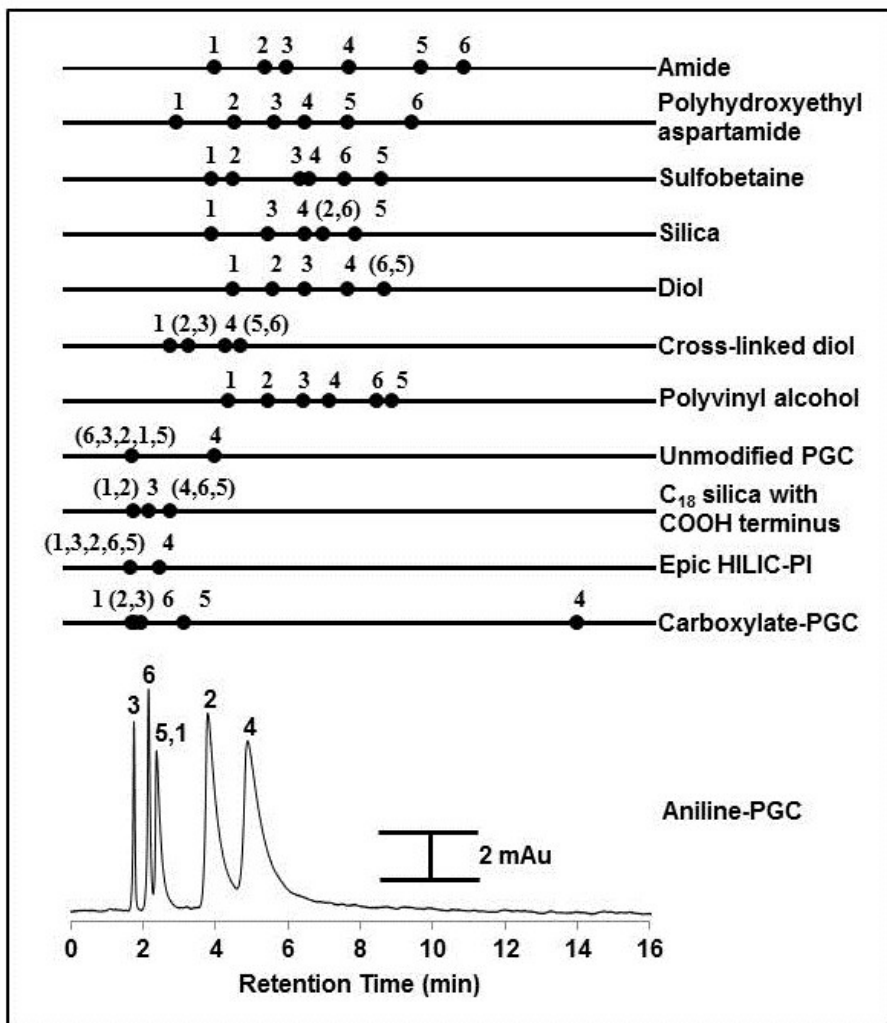


Figure 3.9. Comparison of the selectivity of six aromatic carboxylic acids on eleven different column chemistries versus Aniline-PGC under HILIC mode conditions. Bracketed analytes co-elute. The positions of the markers along the line reflect the actual retention time of the analytes. Conditions: columns, Aniline-PGC (150 mm x 3 mm ID, 5 μ m), Epic HILIC-PI (100 mm x 4.6 mm ID, 5 μ m) and HypercarbTM (100 mm x 4.6 mm ID, 5 μ m); 1.0 mL/min; eluent, 20 mM ammonium acetate in 85 % ACN; analytes, 0.10-0.40 mM of (1) salicylic acid, (2) gentisic acid, (3) acetylsalicylic acid, (4) salicylic acid, (5) hippuric acid, and (6) α -hydroxyhippuric acid. UV detection at 254 nm with a 5 μ L injection. Retention data for carboxylate-PGC from Wahab *et al.*²⁸ Retention data for all remaining columns from Guo *et al.*⁴⁸

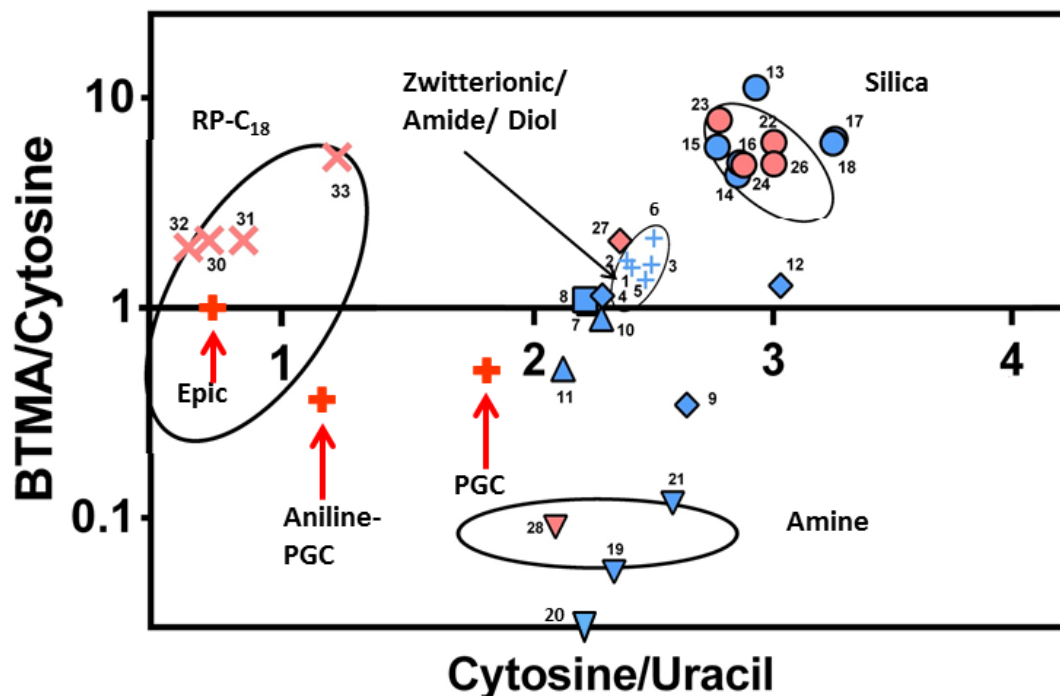


Figure 3.10. HILIC selectivity plot displaying selectivity behavior of Aniline-PGC, Epic HILIC-PI, and unmodified PGC (Hypercarb) with respect to 33 commercial columns (see **Table 3.2** for column identities). Symbols: bare silica (\bullet), amide (\blacksquare), diol (\blacktriangle), amine and/or triazole (\blacktriangledown), polymer substrate and/or polymer coated silica (\blacklozenge), zwitterionic ($+$), RPLC (\times), other phases (boldface $+$). Conditions: 0.5 mL/min; eluent, 5 mM ammonium acetate (pH = 6.8) in 80 % ACN; analytes, 0.062-1.25 mM BTMA, cytosine, and uracil in 80 % ACN; UV detection at 254 nm with a 5 μ L injection. (Adapted from Ibrahim *et al.*⁵⁰).

Table 3.2. Characteristics of tested stationary phases in **Figure 3.10** (Data from Ibrahim *et al.*⁵⁰)

Col. #	Brand name	Manufacturer	Support	Functionality	Particle size (µm)	Pore size (Å)	Surface area (m ² /g)	Column length (mm)	Column diameter (mm)
1	ZIC-HILIC	Merck	Silica	Polymeric sulfoalkylbetaine zwitterionic	5	200	135	100	4.6
2	ZIC-HILIC	Merck	Silica	Polymeric sulfoalkylbetaine zwitterionic	3.5	200	135	150	4.6
3	ZIC-HILIC	Merck	Silica	Polymeric sulfoalkylbetaine zwitterionic	3.5	100	180	150	4.6
4	ZIC-pHILIC	Merck	Porous polymer	Polymeric sulfoalkylbetaine zwitterionic	5	-	-	50	4.6
5	Nucleodur HILIC	Macherey-Nagel	Silica	Sulfoalkylbetaine zwitterionic	5	110	340	100	4.6
6	PC HILIC	Shiseido	Silica	Phosphorylcholine zwitterionic	5	100	450	100	4.6
7	TSKgel Amide 80	Tosoh Bioscience	Silica	Amide (polymeric carbamoyl)	5	80	450	100	4.6
8	TSKgel Amide 80	Tosoh Bioscience	Silica	Amide (polymeric carbamoyl)	3	80	450	50	4.6
9	Poly-Hydroxyethyl A	PolyLC	Silica	Poly(2-hydroxyethyl aspartamide)	5	200	188	100	4.6
10	LiChrospher 100 Diol	Merck	Silica	2,3-Dihydroxypropyl	5	100	350	125	4.0
11	Luna HILIC	Phenomenex	Silica	Cross-linked diol	5	200	185	100	4.6
12	Poly-Sulfoethyl A	PolyLC	Silica	Poly(2-sulfoethyl aspartamide)	5	200	188	100	4.6
13	Chromolith Si	Merck	Silica monolith	Underivatized	N/A	130	300	100	4.6
14	Atlantis HILIC Si	Waters	Silica	Underivatized	5	100	330	100	4.6
16	LiChrospher Si 100	Merck	Silica	Underivatized	5	100	400	125	4.0
15	Purospher STAR Si	Merck	Silica	Underivatized	5	120	330	125	4.0
17	LiChrospher Si 60	Merck	Silica	Underivatized	5	60	700	125	4.0
18	Cogent Type C Silica	Microsolv	Silica	Silica hydride ("Type C" silica)	4	100	350	100	4.6
19	LiChrospher 100 NH ₂	Merck	Silica	3-Aminopropyl	5	100	350	125	4.0

Table 3.2 continued.

Col. #	Brand name	Manufacturer	Support	Functionality	Particle size (µm)	Pore size (Å)	Surface area (m ² /g)	Column length (mm)	Column diameter (mm)
20	Purospher STAR NH ₂	Merck	Silica	3-Aminopropyl	5	120	330	125	4.0
21	TSKgel NH ₂ -100	Tosoh Bioscience	Silica	Aminoalkyl	3	100	450	50	4.6
22	Atlantis HILIC	Waters	Silica	Underivatized	3	100	330	50	1.0
23	Onyx silica monolith	Phenomenex	Silica monolith	Underivatized	N/A	130	300	100	4.6
24	Zorbax HILIC plus	Agilent	Silica	Underivatized	3.5	95	160	100	4.6
25	Silica monolith coated with AS9-SC	homemade	Silica monolith	Silica – cationic nanoparticle	N/A	130	300	80	4.6
26	Zorbax RRHD HILIC plus	Agilent	Silica	Underivatized	1.8	95	160	100	3.0
27	Acclaim Trinity P1	Dionex	Silica	Silica-cationic nanoparticle	3	-	-	150	3.0
28	Cosmosil HILIC	Nacalai	Silica	Triazole	5	120	300	150	4.6
29	Acclaim HILIC-10	Dionex-Thermo Scientific	Silica	Proprietary neutral polar functionality	3	120	300	150	4.6
30	Zorbax Eclipse XDB-C18	Agilent	Silica	Octadecyl	5	80	180	150	4.6
31	XBridge C18	Waters	silica (BEH)	Octadecyl	5	130	185	150	4.6
32	YMC Pro C18	YMC	silica	Octadecyl	3	120	340	150	2.0
33	Zorbax SB-aq	Agilent	silica	Octadecyl	3.5	80	180	150	2.1
	Hypercarb™	ThermoFisher	carbon	Underivatized	5	250	120	100	4.6
	EPIC HILIC-PI	ES Industries	silica	Aniline	5	120	350-	100	4.6
	Aniline-PGC	Home made	carbon	Aniline	5	250	120	150	3.0

3.3.4 Attenuated Reversed Phase Properties of Aniline-PGC

Owing to the extra retentivity provided by PGC,^{15,32} this material is often used as the second column in comprehensive and heart cutting 2D-LC separations.¹⁶⁻¹⁹ Additionally, the adsorptive character of PGC enables structural isomer separations not possible on traditional C₁₈ phases.⁵²⁻⁵⁵ However, the strong retentive character can also extend run times and result in poor efficiencies.²⁷ In extreme cases some compounds are irreversibly retained.^{23,56} Here I investigate whether introduction of an aniline functionality to the PGC surface can moderate the strong RPLC character of PGC.

Figure 3.11 compares the reversed-phase separation of diphenhydramine, acetaminophen, procainamide, nortriptyline and caffeine on Aniline-PGC and unmodified PGC. These compounds are moderately hydrophilic pharmaceuticals used previously to probe the selectivity of both HILIC and RP stationary phases.⁵⁷⁻⁵⁹ Using 63% ACN, the reversed-phase separation of these compounds on unmodified PGC (**Figure 3.11B**) required nearly *80 minutes*, with procainamide and nortriptyline so severely broadened that they were hardly visible above the baseline. In contrast, the separation on the Aniline-PGC column under the same mobile phase conditions (**Figure 3.11A**) was completed in 14 min. Separation efficiencies (N) up to 2600 plates on the home-packed Aniline-PGC and up to 6500 plates on the commercially prepared unmodified PGC were observed (**Table 3.3**). Nevertheless, the Aniline-PGC phase provided a significant improvement in the efficiency of procainamide (N = 600 vs. 100, 6-fold improvement) and nortriptyline (N = 300 vs. 100, 3-fold improvement) over unmodified PGC.

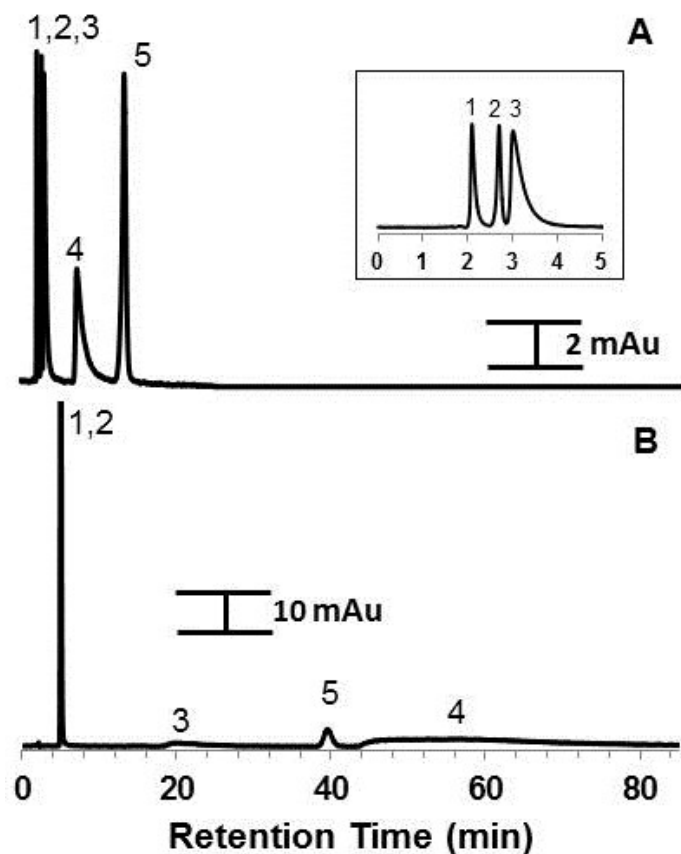


Figure 3.11. Comparison of the reversed phase separation of five alkaline pharmaceuticals on (A) Aniline-PGC and (B) unmodified PGC. The inset in A shows an expanded view of the first three peaks of separation A. Conditions: columns, Aniline-PGC (150 mm x 3 mm ID, 5 μ m) and unmodified PGC (100 mm x 4.6 mm ID, 5 μ m); 0.6 mL/min; eluent, 25 mM ammonium acetate (pH = 5.0) in 63 % ACN; analytes, 0.02-0.9 mM of (1) diphenhydramine, (2) acetaminophen, (3) procainamide, (4) nortriptyline, and (5) caffeine prepared in 63 % ACN. UV detection at 254 nm with a 5 μ L injection.

Table 3.3. Comparison of separation efficiencies attained by Aniline-PGC and unmodified PGC in the separation of 5 alkaline pharmaceuticals. Conditions: columns, Aniline-PGC (150 mm x 3 mm ID, 5 μ m) and unmodified PGC (100 mm x 4.6 mm ID, 5 μ m); 0.6 mL/min; eluent, 25 mM ammonium acetate (pH = 5.0) in 63 % ACN; analytes, 0.02-0.9 mM of diphenhydramine, acetaminophen, procainamide, nortriptyline, and caffeine prepared in 63 % ACN. UV detection at 254 nm with a 5 μ L injection.

Compound	Separation efficiency (N) Aniline-PGC	Separation efficiency (N) unmodified PGC
diphenhydramine	2000	5500
acetaminophen	2200	5500
procainamide	600	100
nortriptyline	300	100
caffeine	2600	6500

3.3.5 Low pH Separation

Currently, the majority of commercial silica-based HPLC stationary phases are only useable between pH 2-8. Below pH 2 the bonded material is hydrolyzed and above pH 8 the aqueous solubility of the silica backbone dramatically increases.^{8,9,11,60} PGC, conversely, is stable at pH 0-14. The alkaline stability of a carboxylate-modified PGC phase had been previously demonstrated for eluents such as 0.1 M NaOH.²⁸ Here I demonstrate the performance of Aniline-PGC at pH 2.

Figure 3.12 compares the mixed-mode separation of an acid, two bases, and two neutral compounds performed under the same conditions on the Aniline-PGC phase and unmodified PGC. On both phases the two charged amines (aniline and ephedrine) show little retention, while the hydrophobic naphthalene is the most retained due to strong π - π interactions with the PGC surface. There is a greater than 50% reduction in the retention of naphthalene with the Aniline-PGC column.

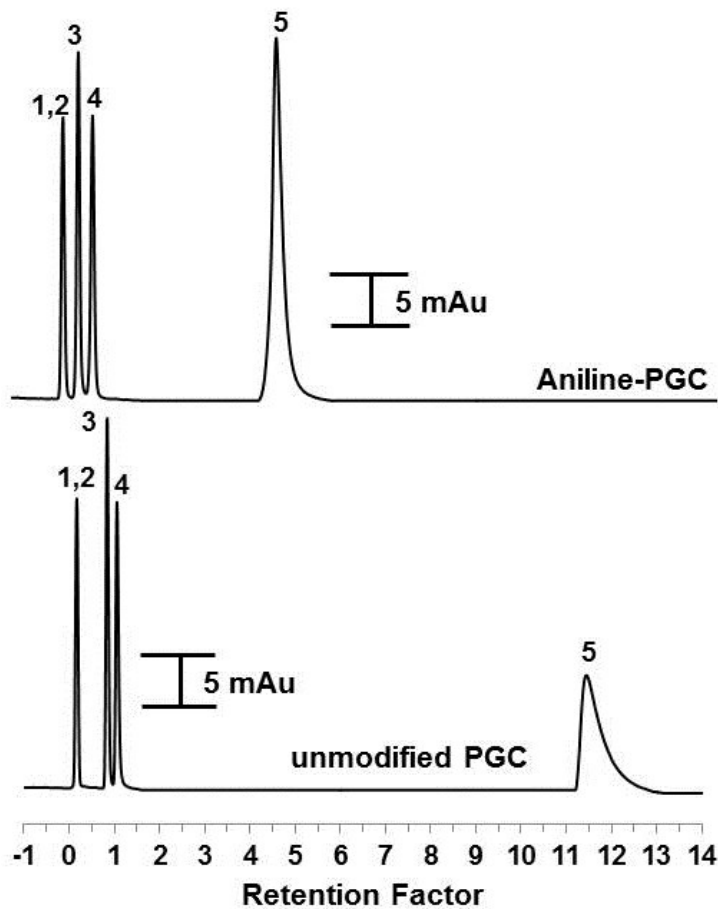


Figure 3.12. Comparison of the low pH mixed-mode separation of five organic compounds by Aniline-PGC and unmodified PGC. Conditions: columns, Aniline-PGC (150 mm x 3 mm ID, 5 μ m) and unmodified PGC (100 mm x 4.6 mm ID, 5 μ m); 0.75 mL/min; eluent, 25 mM ammonium formate (pH = 2.0) in 75 % ACN; analytes, 0.3-0.8 mM of (1) ephedrine, (2) aniline, (3) benzoic acid, (4) toluene, and (5) naphthalene prepared in 75 % ACN; 30 $^{\circ}$ C. UV detection at 254 nm with a 5 μ L injection.

The naphthalene peak also had a lower plate height (105 μm vs. 210 μm) and was much less tailed ($A_s = 1.2$ vs. 4.3) on the Aniline-PGC phase.

Interestingly, both aniline and ephedrine elute prior to the void volume of the Aniline-PGC column. Both compounds are protonated at the eluent pH. Likewise the surface anilines would be protonated. Thus aniline and ephedrine experience Donnan exclusion.

Lastly, the stability of Aniline-PGC under acidic conditions was tested using 40 mM ammonium formate (pH 2.0) in 75 % ACN. After 4000 column volumes, the retention times of benzoic acid and naphthalene showed only a minor drift of 0.03 min (2.1 %) and 0.35 min (5.6 %), respectively (**Figure 3.13**). Further, it is noteworthy that the column had previously been subjected to a variety of mobile phase conditions over 18 months.

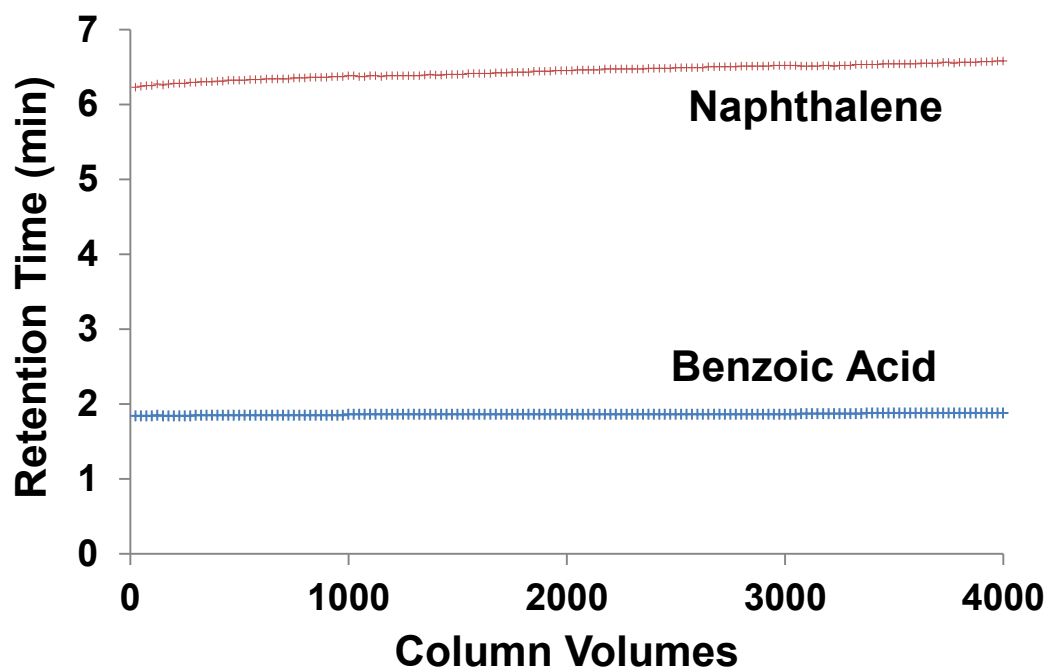


Figure 3.13. Stability of Aniline-PGC under acidic conditions. Separations were performed every 25 column volumes. Conditions: column, Aniline-PGC (150 mm x 3 mm ID, 5 μ m); 0.75 mL/min; eluent, 40 mM ammonium formate (pH = 2.0) in 75 % ACN; analytes, 0.25 mM of benzoic acid and naphthalene prepared in 75 % ACN; 30 °C. UV detection at 254 nm with a 5 μ L injection.

3.3.6 Evaluation of the Chemical Reactivity of Aniline-PGC

Primary amine functionalized stationary phases can react with solutes such as reducing sugars to form Schiff bases, resulting in significant loss in signal.^{61,62} This reaction is greatly enhanced at elevated temperatures.⁶² To evaluate the propensity of Aniline-PGC towards Schiff base formation, LC-MS separations under HILIC conditions (**Section 3.2.7**) of a mixture of two reducing sugars (D-ribose and D-galactose) and one non-reducing sugar (D-sucrose) were performed at 30, 40, and 50 °C. Given that the peak areas of these compounds remained relatively constant with an increase in separation temperature (**Table 3.4**), Aniline-PGC therefore shows no propensity towards Schiff base formation.

Table 3.4. Measured peak areas of 3 sugars separated by Aniline-PGC at different temperatures. Conditions: column, Aniline-PGC (150 mm x 3 mm ID, 5 µm); 0.55 mL/min; eluent, 0.1 % formic acid in 90 % ACN; analytes, 0.5 mM of D-ribose, D-galactose, and D-sucrose prepared in 90 % ACN; 30, 40, and 50 °C. Positive MS detection (see **Section 3.2.7**) with an 8 µL injection.

Temperature (°C)	Peak Area (x 10 ⁵)		
	D-Ribose	D-Galactose	D-Sucrose
30	5.4	6.2	58.7
40	6.3	7.2	61.3
50	6.3	6.3	63.1

3.4 Conclusions

PGC is an attractive material for HPLC due to its different retention mechanism, pH stability, and thermal stability. The PGC surface was modified with aniline groups using aryl diazonium chemistry to produce a phase which displayed both HILIC and attenuated reversed phase properties. As a HILIC phase, Aniline-PGC demonstrated increased retention of nucleobases compared to a commercial aniline silica HILIC column. The Aniline-PGC phase also displayed selectivity that was different from 10 other HILIC columns. As an attenuated reversed phase, the Aniline-PGC phase reduced the separation time for a mixture of basic pharmaceuticals more than 5-fold and increased the separation efficiency up to 6-fold compared to unmodified PGC. The effectiveness and stability of the Aniline-PGC column under low pH conditions was also demonstrated. Lastly, the Aniline-PGC material was shown to be resistive towards Schiff base formation. This is the first report of a diazonium-modified PGC column which displays both HILIC and attenuated reversed phase properties.

3.5 References

- (1) Carr, P.; Snyder, L.; Dolan, J. W.; Majors, R. E. *LCGC North Am.* **2010**, *28*, 418–430.
- (2) Sanjay Kumar, D.; Harish Kumar, D. R. *Int. J. Pharm. Sci. Res.* **2012**, *3*, 4626–4633.
- (3) Borges, E. M.; Rostagno, M. A.; Meireles, M. A. A. *RSC Adv.* **2014**, *4*, 22875–22887.

- (4) Chester, T. L. *Anal. Chem.* **2013**, *85*, 579–589.
- (5) Buszewski, B.; Noga, S. *Anal. Bioanal. Chem.* **2012**, *402*, 231–247.
- (6) Jandera, P. *Anal. Chim. Acta* **2011**, *692*, 1–25.
- (7) Ibrahim, M. E. A.; Lucy, C. A. In *Hydrophilic Interaction Chromatography: A Guide for Practitioners*; Olsen, B. A.; Pack, B. W., Eds.; John Wiley & Sons: Hoboken, NJ, 2013; Vol. 177, pp. 43–85.
- (8) Kirkland, J. J.; van Straten, M. A.; Claessens, H. A. *J. Chromatogr. A* **1995**, *691*, 3–19.
- (9) Kirkland, J. J. *J. Chromatogr. Sci.* **1996**, *34*, 309–313.
- (10) Borges, E. M.; Collins, C. H. *J. Chromatogr. A* **2012**, *1227*, 174–180.
- (11) Claessens, H. A.; van Straten, M. A. *J. Chromatogr. A* **2004**, *1060*, 23–41.
- (12) Knox, J. H.; Kaur, B.; Millward, G. R. *J. Chromatogr. A* **1986**, *352*, 3–25.
- (13) West, C.; Elfakir, C.; Lafosse, M. *J. Chromatogr. A* **2010**, *1217*, 3201–3216.
- (14) Pereira, L.; Aspey, S.; Ritchie, H. *J. Sep. Sci.* **2007**, *30*, 1115–1124.
- (15) Forgács, E. *J. Chromatogr. A* **2002**, *975*, 229–243.
- (16) Haun, J.; Leonhardt, J.; Portner, C.; Hetzel, T.; Tuerk, J.; Teutenberg, T.; Schmidt, T. C. *Anal. Chem.* **2013**, *85*, 10083–10091.
- (17) Moretton, C.; Crétier, G.; Nigay, H.; Rocca, J.-L. *J. Chromatogr. A* **2008**, *1198*, 73–79.
- (18) Sakhi, A. K.; Russnes, K. M.; Smeland, S.; Blomhoff, R.; Gundersen, T. E. *J.*

- Chromatogr. A* **2006**, *1104*, 179–189.
- (19) Thiébaud, D.; Vial, J.; Michel, M.; Hennion, M.-C.; Greibrokk, T. *J. Chromatogr. A* **2006**, *1122*, 97–104.
- (20) De Matteis, C. I.; Simpson, D. A.; Euerby, M. R.; Shaw, P. N.; Barrett, D. A. *J. Chromatogr. A* **2012**, *1229*, 95–106.
- (21) Pereira, L. *LC-GC North Am.* **2011**, *29*, 262–269.
- (22) Shen, W.; Li, Z.; Liu, Y. *Recent Patents Chem. Eng.* **2008**, *1*, 27–40.
- (23) Pabst, M.; Grass, J.; Fischl, R.; Léonard, R.; Jin, C.; Hinterkörner, G.; Borth, N.; Altmann, F. *Anal. Chem.* **2010**, *82*, 9782–9788.
- (24) Knox, J. H.; Wan, Q.-H. *Chromatographia* **1996**, *42*, 83–88.
- (25) Zhang, N.; Wang, L.; Liu, H.; Cai, Q.-K. *Surf. Interface Anal.* **2008**, *40*, 1190–1194.
- (26) Tornkvist, A.; Markides, K. E.; Nyholm, L. *Analyst* **2003**, *128*, 844.
- (27) Jensen, D. S.; Gupta, V.; Olsen, R. E.; Miller, A. T.; Davis, R. C.; Ess, D. H.; Zhu, Z.; Vail, M. A.; Dadson, A. E.; Linford, M. R. *J. Chromatogr. A* **2011**, *1218*, 8362–8369.
- (28) Wahab, M. F.; Ibrahim, M. E. A.; Lucy, C. A. *Anal. Chem.* **2013**, *85*, 5684–5691.
- (29) Chambers, S. D.; McDermott, M. T.; Lucy, C. A. *Analyst* **2009**, *134*, 2273–2280.
- (30) Wahab, M. F.; Pohl, C. A.; Lucy, C. A. *Analyst* **2011**, *136*, 3113–3120.
- (31) Liu, Y.; Lu, Y.; Prashad, M.; Repic, O.; Blacklock, T. J. *Adv. Synth. Catal.* **2005**,

347, 217–219.

- (32) Michel, M.; Buszewski, B. *Adsorption* **2009**, *15*, 193–202.
- (33) Ross, P.; Knox, J. H. *Adv. Chromatogr.* **1997**, *37*, 121–162.
- (34) Liu, Y.-C.; McCreery, R. L. *J. Am. Chem. Soc.* **1995**, *117*, 11254–11259.
- (35) Noga, S.; Bocian, S.; Buszewski, B. *J. Chromatogr. A* **2013**, *1278*, 89–97.
- (36) Baergen, A. C.; Chambers, S. D.; Lucy, C. A. Preparation of a carbon based aniline Stationary phase for high performance liquid chromatography (Poster Presentation), presented at the 91st Canadian Chemistry Conference and Exhibition, 2008.
- (37) Chambers, S. D. Personal Communication, 2014.
- (38) Smith, M. B. *March's Advanced Organic Chemistry: Reactions, Mechanisms, and Structure*; 7th ed.; John Wiley & Sons: Hoboken, NJ, 2013.
- (39) Wuts, P. G. M.; Greene, T. W. *Greene's Protective Groups in Organic Synthesis*; 4th ed.; John Wiley & Sons: Hoboken, NJ, 2012.
- (40) Lebègue, E.; Brousse, T.; Gaubicher, J.; Cougnon, C. *Electrochim. Acta* **2013**, *88*, 680–687.
- (41) Masheter, A. T.; Wildgoose, G. G.; Crossley, A.; Jones, J. H.; Compton, R. G. *J. Mater. Chem.* **2007**, *17*, 3008–3014.
- (42) Moulder, J. F.; Chastain, J.; King, R. C. *Handbook of x-ray photoelectron spectroscopy: a reference book of standard spectra for identification and interpretation of XPS data*; Physical Electronics: Eden Prairie, MN., 1995.

- (43) Roodenko, K.; Gensch, M.; Rappich, J.; Hinrichs, K.; Esser, N.; Hunger, R. *J. Phys. Chem. B* **2007**, *111*, 7541–7549.
- (44) Iqbal, P.; Critchley, K.; Attwood, D.; Tunnicliffe, D.; Evans, S. D.; Preece, J. A. *Langmuir* **2008**, *24*, 13969–13976.
- (45) Zheng, W.; Du, R.; Cao, Y.; Mohammad, M.; Dew, S.; McDermott, M.; Evoy, S. *Sensors* **2015**, *15*, 18724–18741.
- (46) Benjamin, O. D.; Weissmann, M.; Bélanger, D. *Electrochim. Acta* **2014**, *122*, 210–217.
- (47) Lebègue, E.; Brousse, T.; Gaubicher, J.; Cougnon, C. *Electrochem. commun.* **2013**, *34*, 14–17.
- (48) Guo, Y. In *Hydrophilic Interaction Liquid Chromatography (HILIC) and Advanced Applications*; Wang, P. G.; He, W., Eds.; CRC Press: Boca Raton, FL, 2011; pp. 401–426.
- (49) Dinh, N. P.; Jonsson, T.; Irgum, K. *J. Chromatogr. A* **2011**, *1218*, 5880–5591.
- (50) Ibrahim, M. E. A.; Liu, Y.; Lucy, C. A. *J. Chromatogr. A* **2012**, *1260*, 126–131.
- (51) Canals, I.; Valkó, K.; Bosch, E.; Hill, a P.; Rosés, M. *Anal. Chem.* **2001**, *73*, 4937–4945.
- (52) Barrett, D. A.; Pawula, M.; Knaggs, R. D.; Shaw, P. N. *Chromatographia* **1998**, *47*, 667–672.
- (53) Pietrogrande, M. C.; Benvenuti, A.; Previato, S.; Dondi, F. *Chromatographia* **2000**, *52*, 425–432.

- (54) Peacock, K. S.; Ruhaak, L. R.; Tsui, M. K.; Mills, D. A.; Lebrilla, C. B. *J. Agric. Food Chem.* **2013**, *61*, 12612–12619.
- (55) Pereira, L. *J. Liq. Chromatogr. Relat. Technol.* **2008**, *31*, 1687–1731.
- (56) Pabst, M.; Altmann, F. *Anal. Chem.* **2008**, *80*, 7534–7542.
- (57) Kumar, A.; Heaton, J. C.; McCalley, D. V. *J. Chromatogr. A* **2013**, *1276*, 33–46.
- (58) Periat, A.; Kohler, I.; Bugey, A.; Bieri, S.; Versace, F.; Staub, C.; Guillarme, D. *J. Chromatogr. A* **2014**.
- (59) McCalley, D. V. *J. Chromatogr. A* **2007**, *1171*, 46–55.
- (60) Teutenberg, T.; Hollebekkers, K.; Wiese, S.; Boergers, A. *J. Sep. Sci.* **2009**, *32*, 1262–1274.
- (61) Hutchinson, J. P.; Remenyi, T.; Nesterenko, P.; Farrell, W.; Groeber, E.; Szucs, R.; Dicinoski, G.; Haddad, P. R. *Anal. Chim. Acta* **2012**, *750*, 199–206.
- (62) Brons, C.; Olieman, C. *Anal. Chim. Acta* **1983**, *259*, 79–86.

CHAPTER 4: Diazonium Modification of Porous Graphitic Carbon with Catechol and Amide Groups for Hydrophilic Interaction and Attenuated Reversed Phase Liquid Chromatographyⁱⁱⁱ

4.1 Introduction

As demonstrated previously¹⁻⁵ and in **Chapter 3**, diazonium modification is an attractive means to increase the hydrophilicity of the chemically and thermally stable porous graphitic carbon. Concurrently, diazonium modification is also a means to reduce the excessive retentivity of PGC in the RPLC mode.⁶ In **Chapter 3**, introduction of aniline groups to the PGC surface yielded a hydrophilic mixed-mode PGC phase which, relative to unmodified PGC, demonstrated a nearly 7-fold increase in HILIC retention and up to 5.5-fold reduction in RPLC retentivity. Hence, as part of the Lucy group's effort to build a library of modified PGC phases with unique selectivities, this chapter continues from **Chapter 3** by investigating the chromatographic behavior of PGC modified separately with catechol and with amide groups.

4.2 Experimental

4.2.1 Chemicals and Reagents

Porous graphitic carbon (PGC, 5 μm spherical particles comprised of pure graphitic carbon, 250 \AA , 120 m^2/g lot no. PGC593) was from Thermo Fisher Scientific (Sunnyvale, CA, USA). Deionized water ($> 17.7 \text{ M}\Omega$) was from a Barnstead E-pure

ⁱⁱⁱ A version of this chapter has been previously published as Iverson, C. D; Zhang, Y.; Lucy, C. A. *J. Chromatogr. A.* **2015**, *1422*, 186-193. See the Preface for a description of individual contributions to this work.

system (Marietta, OH, USA). Sodium nitrite, sodium borohydride, sodium hydroxide, anhydrous dichloromethane (DCM), boron tribromide (1 M solution in DCM), 3,4-dimethoxyaniline, and 4-aminoacetanilide were from Sigma Aldrich (St. Louis, MO, USA). Hydrochloric acid (37 %), potassium hydroxide, and N,N-dimethylformamide (DMF) were from Caledon Laboratory Chemicals (Georgetown, ON, Canada). Anhydrous ethanol, anhydrous diethyl ether, HPLC grade ammonium acetate, and Optima grade acetonitrile, methanol, and acetone were from Fisher Scientific (Fair Lawn, NJ, USA). Phenol (ACS reagent, 99 %) was from ACP (Montreal, QC, Canada) and phloroglucinol was from Fluka (Buchs, Switzerland). All other chromatographic standards were from Sigma Aldrich and had ≥ 99 % purity. The structures of all test compounds are shown in **Figure 4.1**. Log P and pK_a values for all test compounds are given in **Appendix 2**.

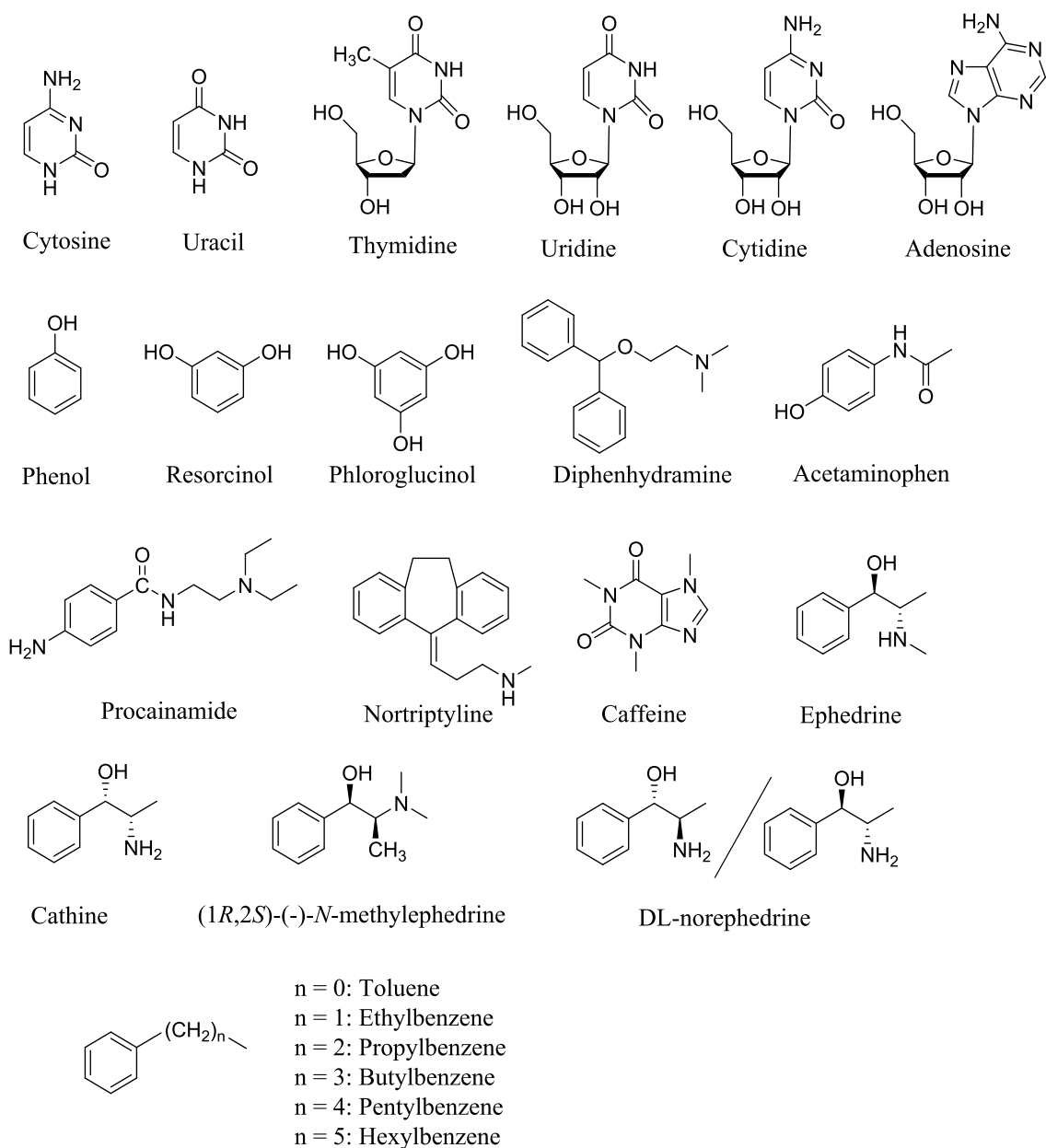


Figure 4.1. Structures of analytes used to characterize the Catechol-PGC and Amide-PGC phases. Log *P* and p*K*_a data for the test compounds are given in **Appendix 2**.

4.2.2 Synthesis of 4-Aminocatechol

4-Aminocatechol was prepared by scaling up the method described by Pognon et al.⁷ with slight modification (**Figure 4.2**). In a dry 1000 mL round bottom flask, 100 mmol of 3,4-dimethoxyaniline was dissolved in 100 mL anhydrous DCM under nitrogen at room temperature. The solution was cooled to 0 °C and 250 mL of 1 M boron tribromide solution (2.5 eq.) was added (*Caution: solution is extremely corrosive and reactive upon exposure to air and moisture, handle with appropriate technique; see Leonard et al.⁸ for instructions on how to handle such reagents.*) After warming to room temperature the mixture was stirred for 6 h. Then methanol (230 mL) was slowly added to the mixture to quench the remaining BBr₃ (*Caution: ensure reaction vessel is adequately vented during this step.*) The crude product was concentrated under reduced pressure to a residue which was recrystallized by dissolving in a minimum volume of methanol (~75-100 mL) and precipitating with diethyl ether (1800 mL). The precipitate was washed by stirring it in 2 x 900 mL portions of diethyl ether to afford 4-aminocatechol as a light blue powder. Yield: 12.36 g, 99 %. Based on higher field 1D- and 2D-NMR data (**Figures 4.3** and **4.4**) I have adjusted the chemical shift assignments reported by Pognon et al.⁷ ¹H NMR (700 MHz, CD₃OD): 6.85 (1H, d, H-2, *J* 8.4 Hz), 6.84 (2H, br s, -NH₂), 6.83 (1H, d, H-5, *J* 2.6 Hz), 6.71 (1H, dd, H-3, *J* 2.6 and 8.4 Hz), 4.80 (2H, br s, -OH). ¹³C NMR (100 MHz, CD₃OD): 147.2 (C-6), 146.7 (C-1), 122.5 (C-4), 116.3 (C-3), 114.3 (C-2), 110.6 (C-5). HRESIMS [M+H]⁺ expected 126.0550, found 126.0550.

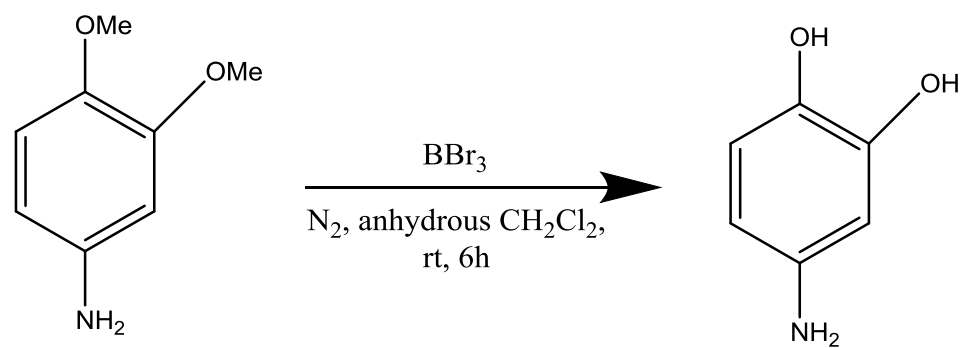


Figure 4.2. Scheme for the synthesis of 4-aminocatechol.

699.771 MHz H1 PRESAT in cd3od (ref. to CD3OD @ 3.30 ppm), temp 27.5 C -> actual temp = 27.0 C, coldid probe

date: Apr 21 2015 sweep width: 8389Hz acq.time: 3.0s relax.time: 2.1s # scans: 16 dig.res.: 0.1 Hz/pt hz/mm:0.9
spectrometer:d401 file:/mnt/d600/home12/gennmr/nmrdata/HUCY/Chad/2015.04/2015.04.21.v7_4aminocatechol_higher_field_loc67_14.59_H1_ID

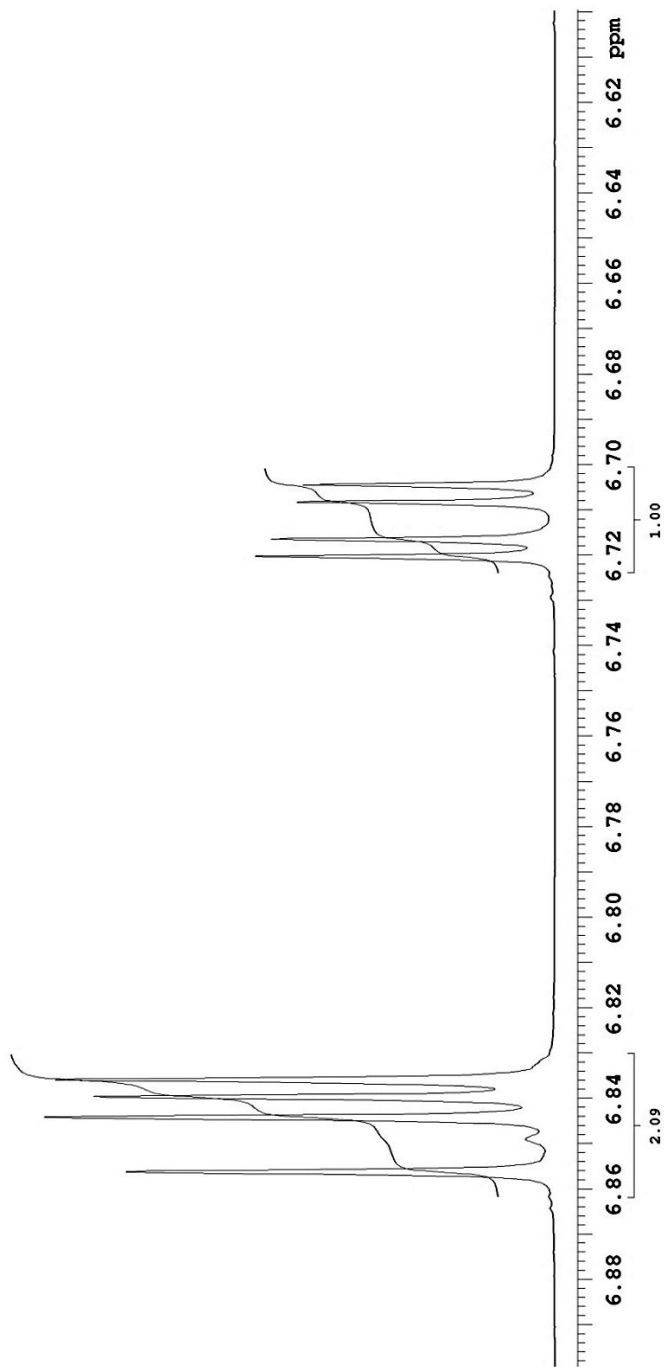


Figure 4.3. Expanded ¹H-NMR spectrum (700 MHz, CD₃OD) showing the aromatic region of the compound synthesized in **Section 4.2.2**.

699.773 MHz H1 gHSQCAD in cd3od (ref. to CD3OD @ 3.30 ppm), temp 27.5 C -> actual temp = 27.0 C, coldidid probe

Temp. 27.5 C / 300.6 K
Sample #67, Operator: IUCY

Relax. delay 1.750 sec

Acq. time 0.125 sec

Width 2097.3 Hz

2D Width 8798.0 Hz

2 repetitions

2 x 64 increments

OBSERVE H1, 699.7679963 MHz

DECOUPLE C13, 175.9787982 MHz

Power 41 dB

on during acquisition

off during delay

W40_coldidid modulated

DATA PROCESSING

Gauss apodization 0.058 sec

F1 DATA PROCESSING

Sq. sine bell 0.007 sec

Shifted by -0.007 sec

FT size 8192 x 1024

Total time 8 min 23 sec

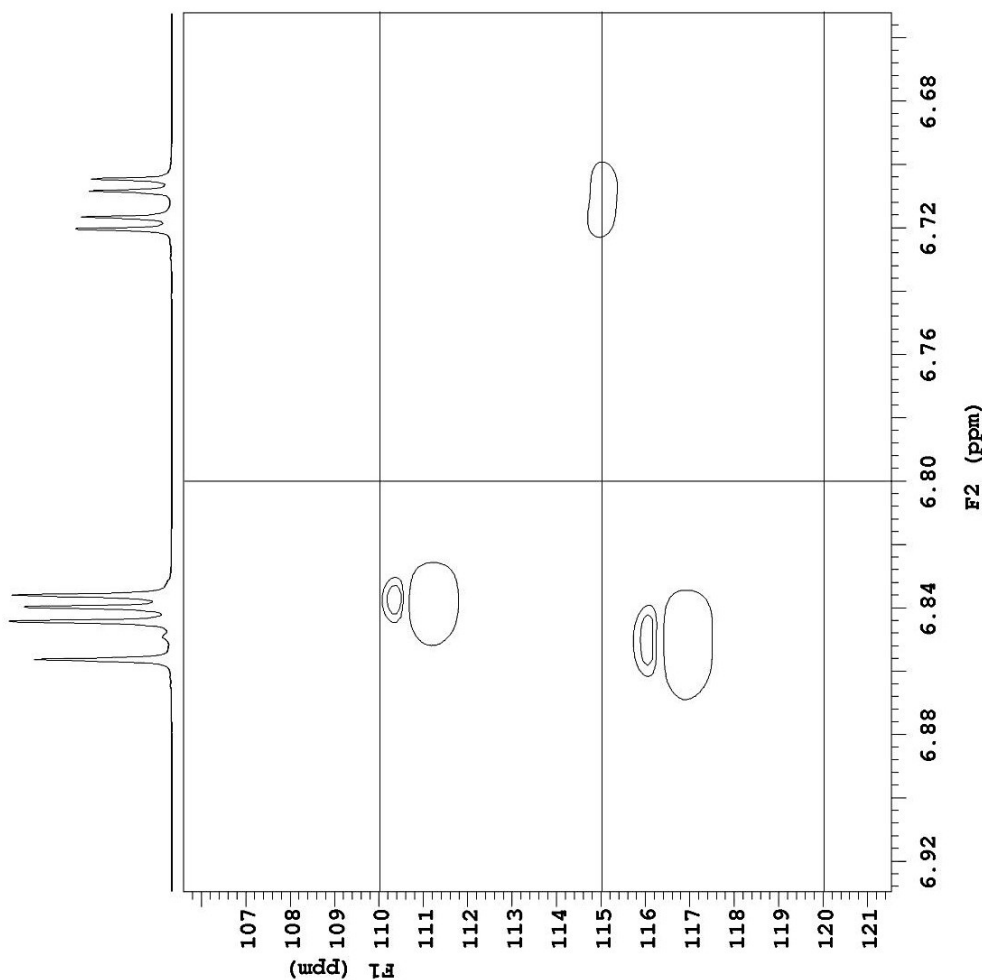


Figure 4.4. Expanded HSQC spectrum (700 MHz, CD₃OD) showing the aromatic regions of the compound synthesized in **Section 4.2.2.**

4.2.3 Synthesis of Catechol-PGC

Synthesis of the Catechol-PGC phase (**Figure 4.5**) was based on that performed in **Chapter 3** with several modifications. 45 mmol of 4-aminocatechol (**Section 4.2.2**) was added to a 1 L beaker containing 40 mL (480 mmol) conc. HCl and 75 mL deionized water. 1.85 g of porous graphitic carbon (PGC) suspended in 30 mL 50 % EtOH_(aq) was added, and the mixture was stirred at 5 °C for 60 min. To this suspension, 45 mmol of NaNO₂ in 50 mL H₂O was added quickly and stirred at 5 °C for 3 h. Sodium borohydride (110 mmol in 50 mL H₂O) was added dropwise over 10 min with vigorous stirring at 5 °C to yield the catechol modified PGC (*Caution: the reaction is vigorous due to the evolution of both hydrogen and nitrogen gas.*) After stirring for 25 min at room temperature, the suspension was diluted in water and filtered using a 0.22 μm nylon filter. The solid material was successively washed with deionized water, 1 % KOH, methanol, DMF, acetonitrile, and acetone until no color was observed in the filtrate. The grafting procedure was then repeated twice more (see **Section 4.3.1.1**) and the particles were characterized by X-ray photoelectron spectroscopy (XPS) as per **Sections 4.2.6** and **4.3.1.1**. Prior to packing, the Catechol-PGC particles were defined twice by sedimentation (36 h each) in ~900 mL 20 % ACN_(aq), yielding 1.7 g of modified particles.

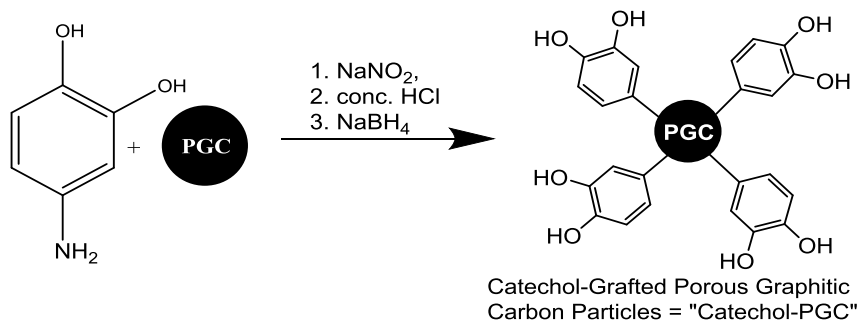
4.2.4 Synthesis of Amide-PGC

The synthesis of the Amide-PGC phase (**Figure 4.5**) was performed by Ms. Ya Zhang similarly to **Section 4.2.3**. The following procedure was repeated three times to yield sufficient modified PGC to prepare one column. 12.5 mmol of 4-aminoacetanilide

was dissolved in 100 mL of deionized water and added into a 1 L beaker. 0.6 g of PGC powder was then suspended into the solution by stirring for 10 min at room temperature. The solution was cooled to 0 °C and 12.4 mmol of NaNO₂ in 15 mL deionized water was added dropwise. The solution was stirred for 5 min, and then 3.75 mL of 37 % HCl (37.5 mmol) was added dropwise over 5 min followed by continued stirring at 0 °C for 30 min. 31.3 mmol of NaBH₄ in 30 mL deionized water was slowly added drop wise over 10 min with vigorous stirring. (*Caution: the reaction is vigorous due to the evolution of both hydrogen and nitrogen gas.*) The mixture was subsequently warmed to room temperature, and after stirring for 30 min the suspension was diluted and filtered using a 0.22 µm nylon membrane filter. The modified particles were successively washed with deionized water, 1 % NaOH, additional deionized water, and anhydrous ethyl alcohol until no color persisted in the filtrate. The functionalization procedure was then repeated a second time.

After all three batches had been prepared, they were combined and the Amide-PGC particles were de-fined once by sedimentation in deionized water for 18 hours. The overall procedure yielded 1.3 g of modified particles. This material was characterized by XPS as described in **Sections 4.2.6** and **4.3.1.2**.

Catechol-PGC



Amide-PGC

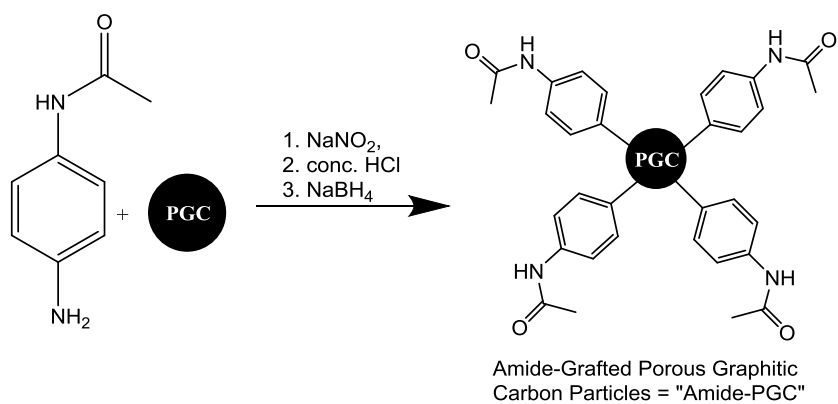


Figure 4.5. Reaction schemes for the *in situ* diazonium modification of PGC particles with catechol and amide groups.

4.2.5 Packing

Columns were packed at constant pressure using a Haskel pump (DSF-122-87153, Burbank, CA, USA) driven by N₂ gas (Praxair Inc., Edmonton, AB, Canada). 1.7 g of Catechol-PGC or 1.3 g Amide-PGC from above was slurried in 35 mL of 10 % ACN_(aq) (Catechol-PGC) or deionized water (Amide-PGC) and placed into a 40 mL slurry reservoir (Lab Alliance, State College, PA, USA). The remaining 5 mL of the final rinse from the container was added to the reservoir to fully fill the slurry reservoir. The particles were packed in a downward direction into a 150 mm x 3 mm ID polyether ether ketone (PEEK) column fitted with a Ti outlet frit. Pressure was maintained at 35 MPa for 1.5 h using 10 % ACN_(aq) (Catechol-PGC) or deionized water (Amide-PGC) as the driving solvent. The columns were detached from the packing assembly and PEEK screw caps with Ultrahigh Molecular Weight Polyethylene frits (UHMWPE) and 0.2 μm Zitex membranes (Thermo Fisher Scientific) were installed on both ends. Prior to the first separation, the columns were flushed with 50 % ACN_(aq) and neat ACN at 1 mL/min for 1 h each.

4.2.6 Characterization of the PGC Phases

X-ray photoelectron spectroscopy (XPS) was performed on an AXIS 165 spectrometer (Kratos Analytical, NY). Catechol-PGC and Amide-PGC particles were washed with methanol and dried under house vacuum for two days prior to XPS analysis.

4.2.7 Chromatographic Separations

Chromatographic studies of the Catechol-PGC phase were performed on a Waters (Mississauga, ON, Canada) Acquity UPLC system consisting of: a binary solvent manager; a thermostated (5 °C) sample manager equipped with a 10 µL loop (injections were done in either partial or full loop fill mode); thermostated column compartment; and a tunable UV detector. The instrument was controlled using Empower software (Waters). Separations were performed at ambient temperature or 60 °C at flow rates of 0.5-1.0 mL/min. Data were collected at 20 Hz at 210, 254 or 268 nm.

Chromatographic studies of the Amide-PGC phase were performed on a Varian HPLC system consisting of: a Prostar 210 pump (Varian, part of Agilent Technologies, Santa Clara, CA, USA); a Varian Prostar 410 autosampler equipped with a 40 µL loop (injections done in either partial loop or full loop mode); and a Knauer UV detector 2500 (Berlin, Germany) set at 220 or 254 nm. Data was collected at 5 Hz using the Varian Star Chromatography Workstation Version 6.20. Separations were performed at ambient temperature at flow rates of 0.5-0.6 mL/min.

The mobile phase was a mixture of ACN, water, and (where necessary) ammonium acetate or ammonium formate. The pH was adjusted with NaOH or HCl. Aqueous stock ammonium acetate/ammonium formate solutions (2 M) at the desired pH were made and refrigerated. The reported buffer concentration is the final concentration in the eluent after mixing with ACN. The reported pH of the buffer is the final pH of aqueous diluted buffer prior to adding acetonitrile. The percentage of ACN in this work represents the volume of ACN relative to the total volume of the solvents including buffer and ACN.

An unmodified PGC (Hypercarb, 100 x 4.6 mm ID, 5 μ m, Thermo Scientific) column was used as a control to assess the performance of the Catechol and Amide-PGC phases.

4.3 Results and Discussion

Porous graphitic carbon (PGC) is a stable and unique HPLC phase. Unfortunately the PGC surface can be too retentive in RPLC^{9,10} and often shows weak HILIC retention.^{9,11,12} In this chapter, I investigate catechol and amide functionalization of PGC to create phases for HILIC and/or as a means to attenuate the reversed phase retention character of PGC. Previously, the Lucy lab used diazonium chemistry to introduce carboxylate and aniline functionalities to PGC to increase its hydrophilicity.^{3,6}

4.3.1 Synthesis and Characterization of Phases

4.3.1.1 Catechol-PGC

In 2012 Pognon et al.⁷ reported the diazonium modification of black pearls carbon with catechol groups as a means to generate a new electrocapacitive material. Inspired by this work, I desired to functionalize the catechol moiety onto PGC as a means to generate the carbon equivalent of a diol phase (see **Table 1.1** for the representative structure of a diol phase).

The gram-scale demethylation of 3,4-dimethoxyaniline proceeded smoothly to generate the desired 4-aminocatechol in a 99 % yield. Following the general methodology utilized in **Chapter 3**, PGC particles were initially subjected to two rounds of functionalization with the catechol. As demonstrated in **Chapter 3**, a useful means to

judge grafting success is to suspend the material in water. Unmodified PGC is strongly hydrophobic and floats on the water surface. After two rounds of catechol functionalization as described in **Section 4.2.3**, ~ 70 % of the modified PGC dispersed in water, indicating that the hydrophilicity of the phase had increased. Functionalizing PGC a third time with 4-aminocatechol resulted in ~90 % dispersion of the Catechol-PGC. For comparison, two derivatizations resulted in full dispersion of Carboxylate-PGC³ and Aniline-PGC (**Chapter 3**). Addition of ACN to a 10–20 % final concentration facilitated full dispersion of Catechol-PGC particles. The difficulty of grafting catechol moieties onto carbon has been previously noted.^{7,13}

XPS analysis of the final trice modified Catechol-PGC particles showed that the surface oxygen concentration had increased from 2.0 atomic % (unmodified PGC)³ to 4.9 % (**Table 4.1**; no peak was observed in the N 1s region). The 2.9 atomic % increase in oxygen content is comparable to the 3.3 atomic % increase in oxygen observed previously for the 2X catechol modification of black pearls carbon.⁷ Due to the nature of the mixed surface oxides present on the surface of PGC¹⁴ it is difficult to selectively quantify catechol loading onto the surface of PGC by XPS using the O 1s signal. Catechol loading on black pearls carbon was previously estimated using cyclic voltammetry.⁷ Based on these measurements I estimate a surface grafting concentration of 0.2 molecules/nm². As mentioned above, the grafting of catechol moieties onto carbon is known to occur with low efficiency as compared to other aryl diazonium compounds.

^{7,13}

Table 4.1. Surface composition from XPS scans of Catechol-PGC and Amide-PGC.

Element	Peak, eV	FWHM (Catechol-PGC)	Peak Area (Catechol-PGC)	% Atomic Conc. (Catechol-PGC)^b	FWHM (Amide-PGC)	Peak Area (Amide-PGC)	% Atomic Conc. (Amide-PGC)^c
Carbon	1s 284.0	2.77	132570	95.16	3.35	41750	93.26
Nitrogen	1s 399.6	0.00	0	0.00	2.95	1956	2.43
Oxygen	1s 532.6	3.17	18903	4.84	—	—	—
Oxygen	1s 531.6	—	—	—	4.06	5658	4.31

^a The composition was calculated from the peak areas in the survey spectra using the CasaXPS (version 2.3) with Scofield values of relative sensitivity factors (RSF). Shirley background correction was applied in the measurement of all peaks.

^b The values reported are after the third modification reaction.

^c The values reported are of the combined material after the second modification reaction.

As an alternative method of quantification, Belanger and co-workers¹⁵ have used halogen tags to facilitate XPS quantification of the grafting of anthroquinones onto carbon particles. Accordingly, numerous attempts were made over the course of three months to synthesize a 4-amino-5-bromocatechol analogue, but were not successful. While the trifluoroacetate protection of compound **1** (**Figure 4.6**) and subsequent bromination and deprotection of compound **2** proceeded relatively smoothly in 89 % or better yields (reaction performance monitored by GC-MS), the demethylation of compound **3** did not. This last reaction afforded a mixture of products consisting of < 20 % of the desired compound (compound **4**, **Figure 4.6**).

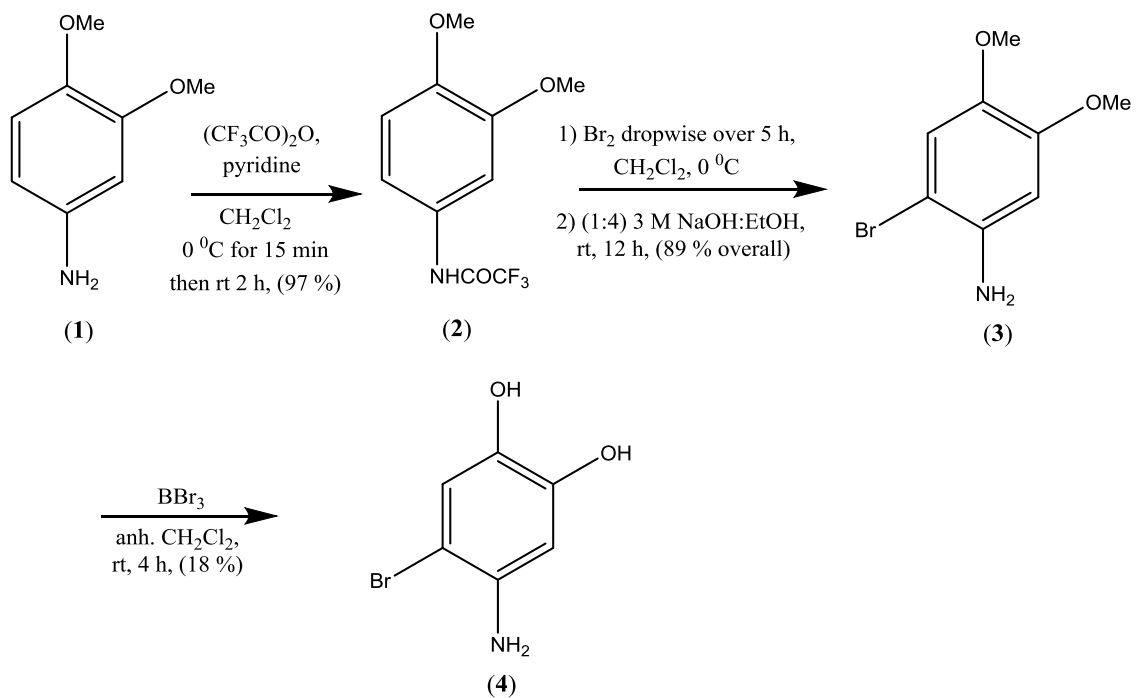


Figure 4.6. Scheme for the synthesis of 4-amino-5-bromocatechol (compound **4**).

4.3.1.2 Amide-PGC

Synthesis of Amide-PGC by Ms. Ya Zhang proceeded more readily than the Catechol-PGC. After two rounds of functionalization, the material dispersed in water without requiring addition of acetonitrile.

The high resolution XPS spectrum of the N 1s band (**Figure 4.7**) showed a peak centered at 399.7, consistent with an amide group bonded to carbon.¹⁶ Integration of the peak in the XPS survey spectrum indicated that 2.43 atomic % N (**Table 4.1**) had been introduced to the Amide-PGC surface (nitrogen was absent on unmodified PGC⁶). Assuming that the population of carbon atoms on PGC is 7.3×10^{-9} mol/cm²,¹⁷ I conservatively estimate a surface grafting concentration of 2.1 molecules/nm². This is a comparable level of grafting efficiency to the Aniline-PGC phase (**Chapter 3**).

4.3.2 Chromatographic Retention Behavior of Catechol-PGC and Amide PGC

Figure 4.8 shows the effect of acetonitrile concentration in the mobile phase on the retention of hydrophilic resorcinol and DL-norephedrine by Catechol-PGC. The retention of both compounds increased with increasing % ACN, consistent with HILIC behavior. Similarly, Amide-PGC displayed HILIC behavior for cytosine and uracil as hydrophilic test probes (**Figure 4.9**). The Amide-PGC phase at pH 6.8 provided a greater than 3-fold increase in the retention of cytosine compared to Aniline-PGC (**Chapter 3**).

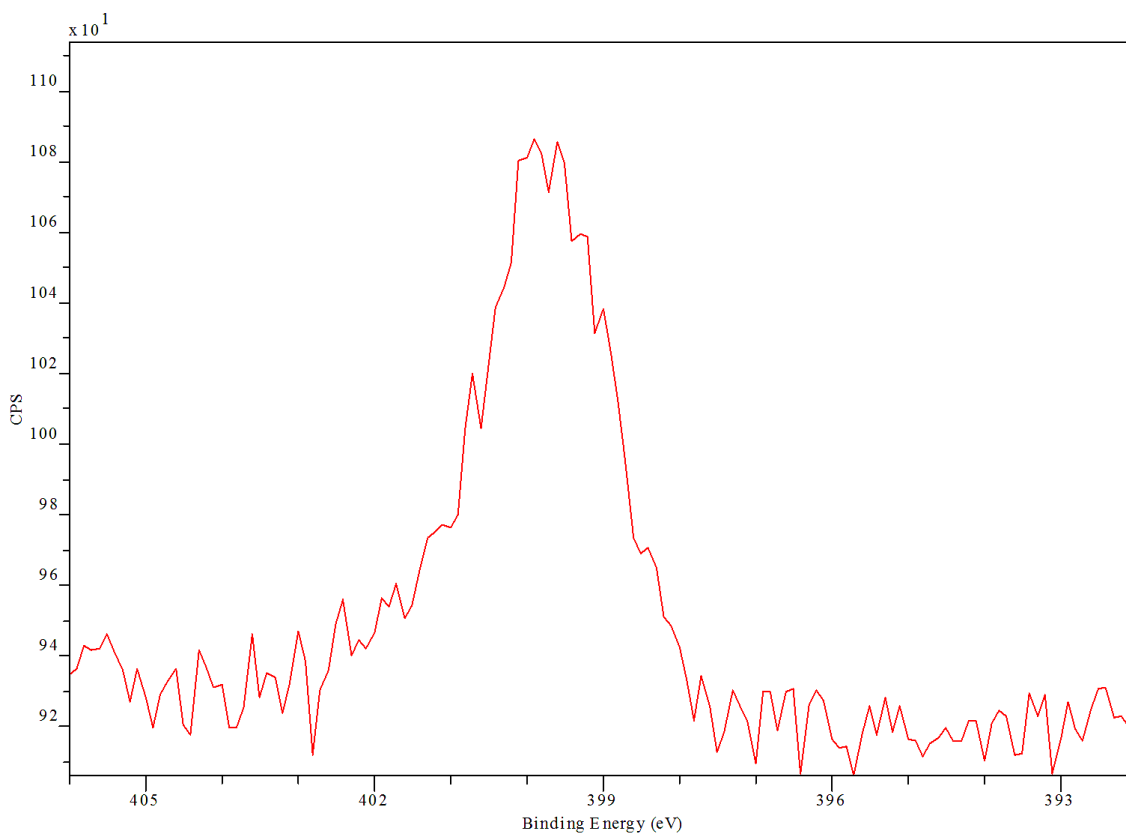


Figure 4.7. Raw high-resolution N 1s XPS spectrum of Amide-PGC. XPS measurements were performed on an AXIS 165 spectrometer. The base pressure in the analytical chamber was $< 3 \times 10^{-8}$ Pa. A monochromatic Al K α source ($h\nu = 1486.6$ eV) was used at a power of 210 W. The analysis spot was $400 \times 700 \mu\text{m}$. High resolution scans were collected for binding energies of 392-406 eV with an analyzer pass energy of 20 eV and a step of 0.1 eV.

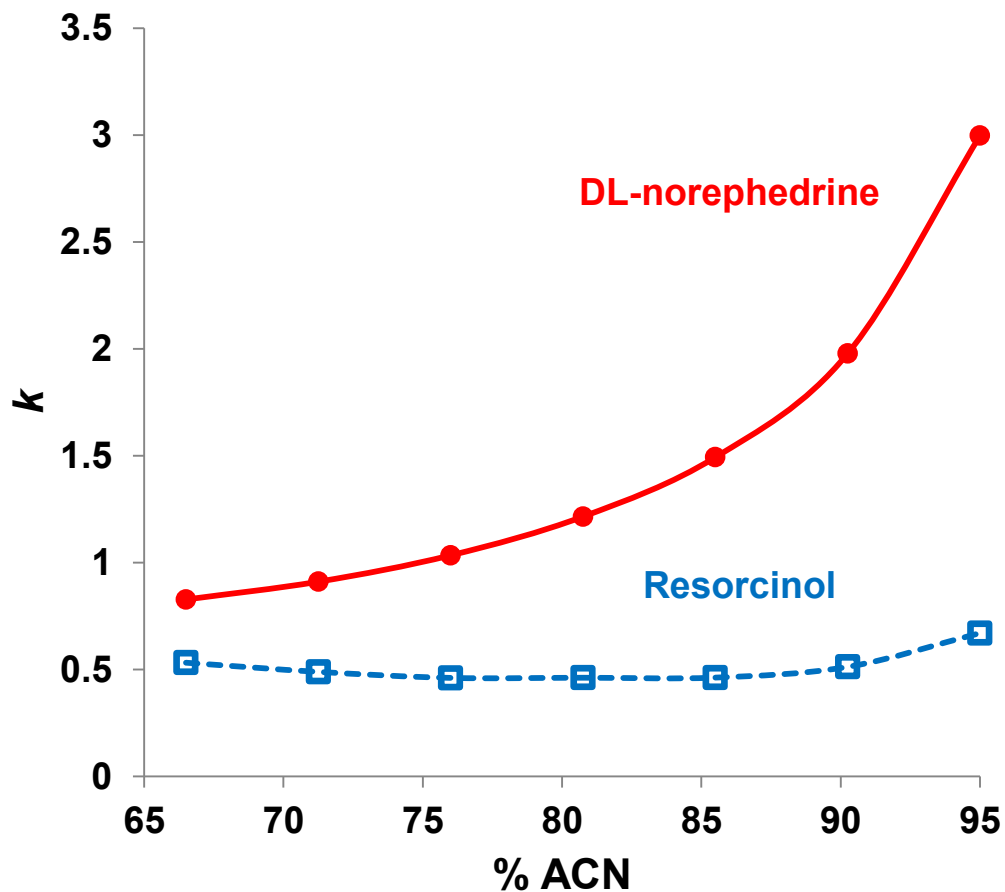


Figure 4.8. Retention behavior of phenylpropanolamine and resorcinol on Catechol-PGC as a function of % ACN in the eluent. Conditions: column, Catechol-PGC (150 mm x 3 mm ID, 5 μ m); eluent, 10 mM ammonium formate (pH = 3.1) in 66 to 95 % ACN at 0.6 mL/min; analytes, 0.25 mM DL-norephedrine and resorcinol in ACN:10 mM ammonium formate (pH = 3.1, 95:5). UV detection at 210 nm with a 5 μ L injection.

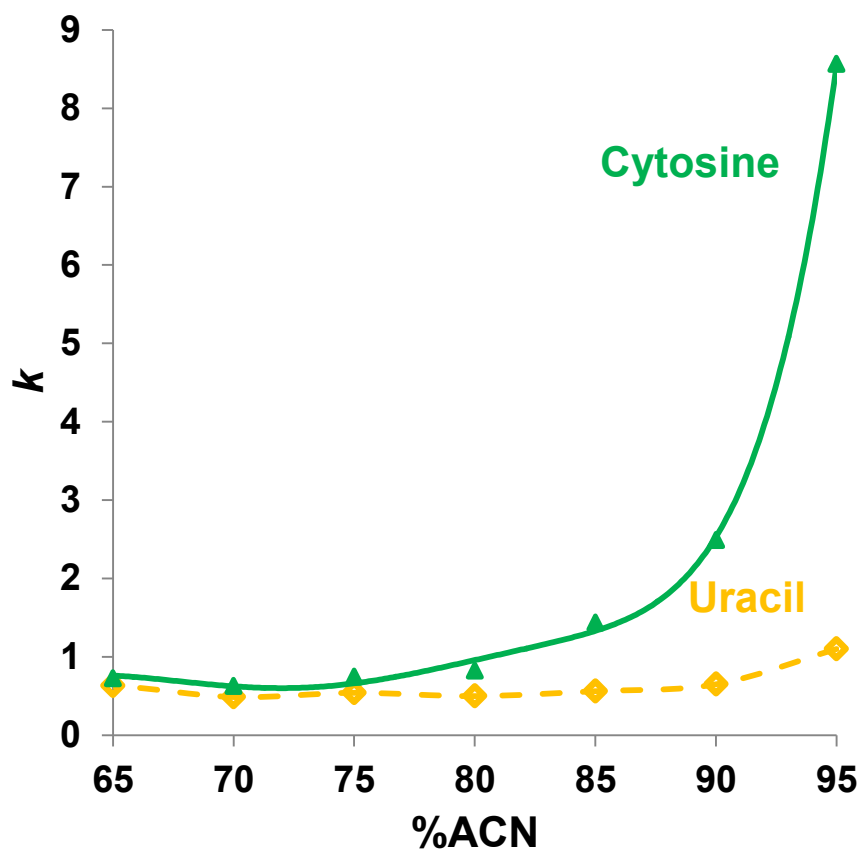


Figure 4.9. Retention behavior of cytosine and uracil on Amide-PGC as a function of % ACN in the eluent. Conditions: column, Amide-PGC (150 mm x 3 mm ID, 5 μ m); eluent, 10 mM ammonium acetate (pH = 6.8) in 66 to 95 % ACN at 0.5 mL/min; analytes, 0.4-0.5 mM cytosine and uracil in 10 mM ammonium acetate (pH = 6.8):ACN (5:95). UV detection at 254 nm with a 40 μ L injection.

Originally, HILIC retention was attributed to partitioning into an adsorbed water layer.¹⁸ Under this mechanism, $\log k$ should be related to the % water. Hemström and Irgum,¹⁹ as well as Gritti et al.²⁰ have since shown that many “HILIC” separations are not truly partitioning in nature, but rather also have adsorptive character. A simple test developed by Hemström and Irgum¹⁹ to pinpoint which type of retention was dominant was to plot both $\log k$ vs. % water (partitioning mechanism) and $\log k$ vs. \log % water (adsorption mechanism). Whichever plot was more linear was viewed to be the dominant retention mechanism.

Figure 4.10 plots the retention data of phenylpropanolamine and resorcinol for Catechol-PGC (from **Figure 4.8**), and cytosine and uracil for Amide-PGC (from **Figure 4.9**), to test whether retention is via partitioning (**Figures 4.10A** and **4.10C**) or adsorption (**Figures 4.10B** and **4.10D**). The $\log k$ vs. \log % water plot is notably more linear for both analytes for the Amide-PGC (**Figure 4.10D** vs. **4.10C**), indicative of primarily adsorptive retention.

The primary HILIC mechanism for Catechol-PGC, however, is more difficult to discern. For DL-norephedrine both the partitioning plot ($R^2 > 0.98$, **Figure 4.10A**) and adsorption plot ($R^2 > 0.99$, **Figure 4.10B**) show comparable good linearity. Hence, it is likely the retention of this compound is influenced significantly by both partitioning and adsorption. Resorcinol, on the other hand, shows a curved retention pattern in both **Figures 4.10A** and **4.10B**, albeit a significant increase in linearity is observed in the adsorption plot. Thus it is likely that while partitioning behavior is present, the retention of resorcinol is more greatly influenced by adsorption. Such compound-dependent

variability in retention behavior as seen above has previously been demonstrated on a BEH Silica phase.²⁰

Determination of HILIC selectivity behavior by means of the HILIC selectivity plot (as in **Figure 3.10** for Aniline-PGC) was not done for these phases, due to their significant adsorptive character as described above. Such excessive adsorptive behavior may bias the retention of the probe compounds, resulting in higher retention ratios than truly warranted.³

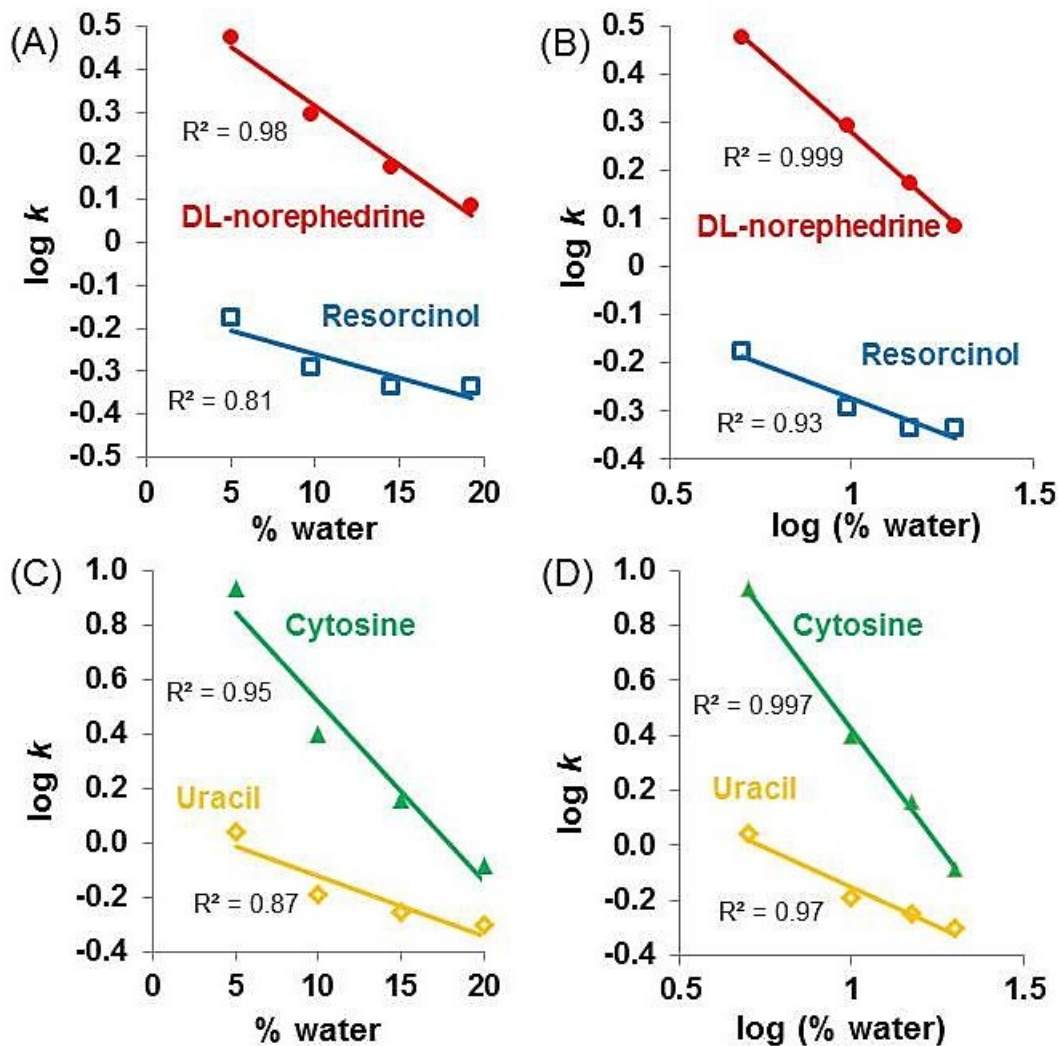


Figure 4.10. Partitioning versus adsorption behavior on (A,B) Catechol-PGC and (C,D) Amide-PGC. Conditions: columns, (A,B) Catechol-PGC (150 mm x 3 mm ID, 5 μm) and (C,D) Amide-PGC (150 mm x 3 mm ID, 5 μm); eluents, (A,B) 10 mM ammonium formate (pH = 3.1) in 80 to 95 % ACN at 0.6 mL/min, (C,D) 10 mM ammonium acetate (pH = 6.8) in 80 to 95 % ACN at 0.5 mL/min; analytes, (A,B) 0.25 mM DL-norephedrine and resorcinol in ACN:10 mM ammonium formate (pH = 3.1, 95:5), (C,D) 0.4-0.5 mM cytosine and uracil in ACN:10 mM ammonium acetate (pH = 6.8, 95:5). UV detection at (A,B) 210 nm, (C,D) 254 nm with an (A,B) 5 μL or (C,D) 40 μL injection.

4.3.3 Applications of Catechol-PGC in HILIC Separations

To illustrate the selectivity behavior of Catechol-PGC, separations of phenols, nucleosides, and ephedrine derivatives were performed under HILIC conditions (**Figure 4.11 A-C**). The retention factors (k) of these test compounds ranged from 0.5 to 13. **Figure 4.11A** shows the HILIC separation of phenol, resorcinol and phloroglucinol in under 2 minutes. The compounds elute in order of their aqueous solubilities (96 g/L, 163 g/L, and 305 g/L, respectively at pH 5²¹), consistent with expected HILIC behavior. Catechol-PGC displayed improved resolution between phenol and resorcinol compared to unmodified PGC ($R_s = 1.14$ for Catechol-PGC vs. 0.74 for unmodified PGC), and increased selectivity between resorcinol and phloroglucinol ($\alpha = 2.13$ vs. 1.48). However, the peak efficiencies (N) obtained with the home-packed Catechol-PGC phase were lower than that of the commercially prepared unmodified PGC phase (**Table 4.2**). Peak asymmetry values (A_s) indicated comparable levels of tailing between the two phases for this separation (**Table 4.2**).

The separation of nucleic acids and analogues are of great importance to genetics, genomics, pharmaceutical sciences, and other fields.²² **Figure 4.11B** shows the separation of four nucleosides (uridine (U), thymidine (T), cytidine (C), and adenosine (A)) on Catechol-PGC under HILIC conditions. Here, Catechol-PGC provided up to 5-fold increased retention of all nucleosides relative to unmodified PGC (data not shown). All compounds, with the exception of adenosine (which perhaps shows stronger retention due to strong adsorptive interactions by the underlying PGC), were baseline resolved ($R_s > 1.5$) in less than 3.5 minutes.

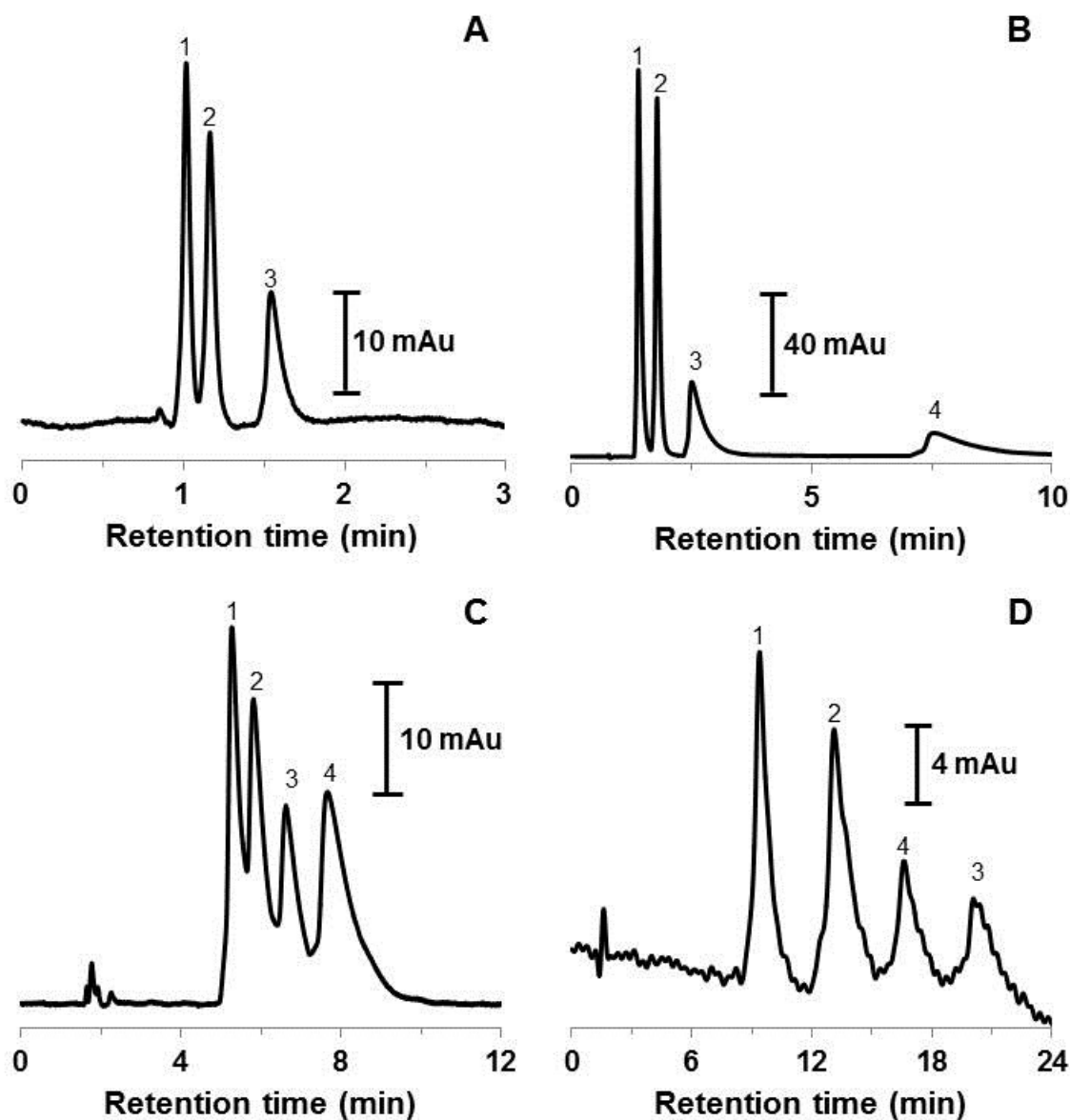


Figure 4.11. HILIC separations of (A) phenols and (B) nucleosides, and the separation of ephedrines in (C) HILIC mode and (D) RP mode. Conditions: column, Catechol-PGC (150 mm x 3 mm ID, 5 μ m); flow rates, (A,B) 1 mL/min, (C,D) 0.6 mL/min; eluents, (A) 20 mM ammonium acetate (pH 5.0) in 90 % ACN, (B) 25 mM ammonium acetate (pH 6.8) in 80 % ACN, (C) 10 mM ammonium formate (pH 3.1) in 87 % ACN, (D) 10 mM ammonium acetate (pH 5.0) in 20 % ACN; analytes, (A) 0.25-0.75 mM of (1) phenol, (2) resorcinol, and (3) phloroglucinol, (B) 0.25 mM of (1) uridine, (2) thymidine, (3) cytidine, and (4) adenosine, (C and D) 0.07 mM of (1) cathine, (2) DL-norephedrine, (3) ephedrine, and (4) (1*R*, 2*S*)-(-)-*N*-methylephedrine, UV detection at (A) 268 nm, (B) 254 nm, (C,D) 210 nm with 10 μ L injection. The data in **Figure 4.11D** was subjected to 30 iterations of a 35 point Savitsky-Golay smooth.

Table 4.2. Comparison of peak efficiencies (N) and asymmetry factors ($A_s = B/A$) between Catechol-PGC and unmodified PGC for the separation of 3 phenolic compounds. Chromatographic conditions are as in **Figure 4.10A**.

Compound	Catechol-PGC		Unmodified PGC	
	N	A_s	N	A_s
Phenol	580	1.0	2010	1.2
Resorcinol	600	1.5	1980	1.4
Phlorglucinol	720	2.7	1520	2.0

The separation of uridine, thymidine, and cytidine on Catechol-PGC is comparable to that performed on a pentahydroxy phase,²³ albeit Catechol-PGC displayed different selectivity and retention order (T<U<A<C on pentahydroxy vs. U<T<C<<A on Catechol-PGC). The selectivity of this overall separation (including adenosine) is also different from that of diol, amide and bare silica phases.^{22,24}

Similar to the phenolic compounds above, the peak efficiencies afforded by the Catechol-PGC phase were lower than on the unmodified PGC column (**Table 4.3**). Additionally, all compounds displayed significant tailing ($A_s \gg 1$, **Table 4.3**) on Catechol-PGC, perhaps due to increased hydrogen bonding interactions between the analytes and the sparsely grafted catechol functionalities. Running the separation at 60 °C reduced peak tailing, but overall peak efficiencies were comparable to the ambient temperature separation (**Table 4.3**).

Table 4.3. Comparison of peak efficiencies (N) and asymmetry factors ($A_s = B/A$) between Catechol-PGC and unmodified PGC for the separation of 4 nucleosides. Chromatographic conditions are as in **Figure 4.10B** with the exception of varying temperature as below.

Compound	Catechol-PGC				Unmodified PGC			
	25 °C		60 °C		25 °C		60 °C	
	N	A_s	N	A_s	N	A_s	N	A_s
Uridine	240	2.3	210	1.4	820	0.5	1800	1.0
Thymidine	440	1.6	400	1.0	1600	0.6	980	0.9
Cytidine	100	4.9	150	2.0	820	0.5	420	2.0
Adenosine	1860	2.2	280	2.7	1230	3.4	760	1.8

In human sport, the World Anti-Doping Agency (WADA) prohibits the use of ephedrine and many of its derivatives since they are regarded as stimulants that may give an athlete an unfair competitive advantage.²⁵ To control use, urine samples from athletes are analysed for the presence of such stimulants, and quantitative analyses are performed where necessary.²⁵ Such analyses require chromatographic separation of these closely related compounds to permit unequivocal identification of the illegal substance. Hence, I first attempted to optimize the HILIC separation of cathine, DL-norephedrine, ephedrine, and (1R,2S)-(-)-N-methylephedrine (**Figure 4.11C**). Although Catechol-PGC provided improved retention and resolution of these closely related compounds relative to unmodified PGC (all compounds co-eluted at the dead time), such a separation would not be adequate for quantitative analysis. Hence, RPLC separations of these stimulants were performed as to be discussed in **Section 4.3.4**.

4.3.4 RPLC Separation of Ephedrine Stimulants by Catechol-PGC

The unique retention mechanism of PGC enables isomer separations.^{1,26–28} The stimulants discussed above in **Section 4.3.3** could not be baseline separated under HILIC

conditions (**Figure 4.11C**). Similarly, this separation is difficult to perform by traditional partition-based RPLC. The separation of these analytes on a sub-2 μm BEH C_{18} required the use of relatively harsh separation conditions which may significantly shorten the lifetime of a column with regular use (i.e., low % B (10 % ACN), alkaline pH (pH 10), and high temperature (60 $^{\circ}\text{C}$)).²⁹ However, under separation conditions more amenable to prolonging column life (i.e., higher % B (20 % ACN), weakly acidic pH (pH 5), and ambient temperature), Catechol-PGC provides satisfactory resolution of these analytes (**Figure 4.11D**). Unmodified PGC was unable to adequately resolve these analytes under the conditions of **Figure 4.11D**.

4.3.5 Attenuated Reversed-Phase Separations by Amide-PGC

The strong retention and unique retention mechanism of PGC is useful in two dimensional separations³⁰⁻³⁵ and, as demonstrated above, in the separation of structural isomers.^{1,26-28} However, the strong retentive character of PGC can also extend run times and yield poor efficiencies.³⁶ In extreme cases compounds may be irreversibly retained.^{37,38} **Chapter 3** demonstrated that introduction of aniline functionalities to PGC significantly reduced the separation time for 5 common pharmaceuticals from >80 minutes (unmodified PGC) to <15 minutes (Aniline-PGC). Furthermore, the efficiencies (N) of the later eluting peaks were greatly improved. Performing the same separation on Amide-PGC (**Figure 4.12**) further reduced the separation time to <8 minutes. The efficiency and the reduction in peak tailing relative to unmodified PGC were comparable to those achieved with the Aniline-PGC phase (**Chapter 3**).

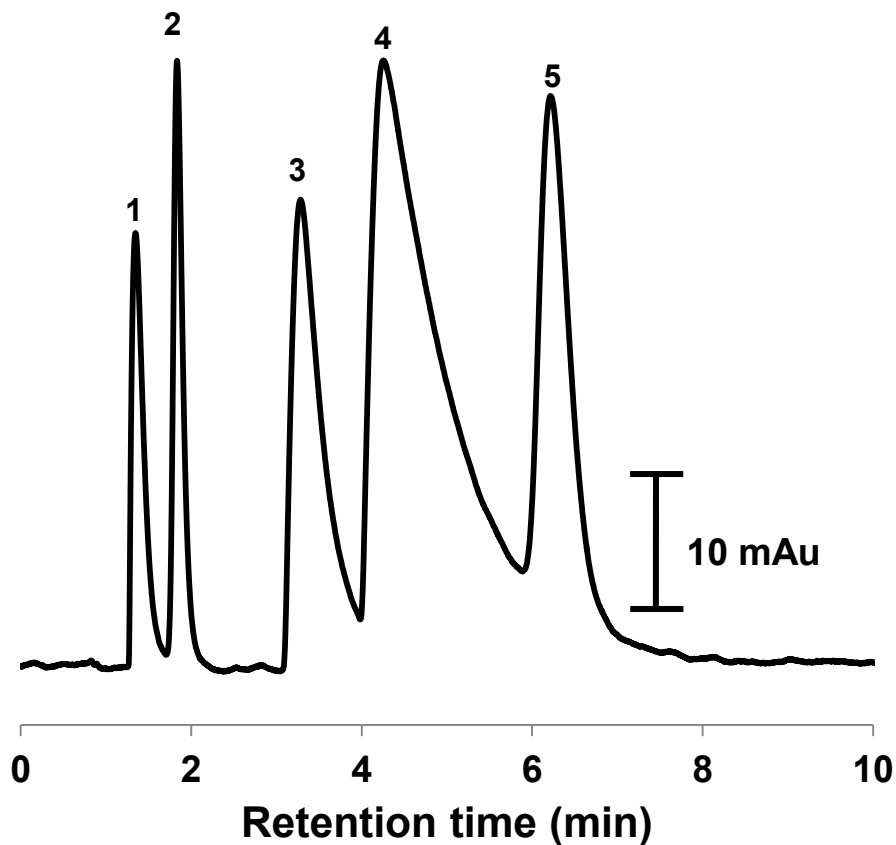


Figure 4.12. Attenuated reversed phase separation of alkaline pharmaceuticals on Amide-PGC. Conditions: column, Amide-PGC (150 mm x 3 mm ID, 5 μ m); eluent, 20 mM ammonium acetate (pH = 5.0) in 63 % ACN at 0.6 mL/min; analytes, 0.2-5 mM of (1) diphenhydramine, (2) acetaminophen, (3) procainamide, (4) nortriptyline and (5) caffeine in 63% ACN. UV detection at 254 nm with a 20 μ L injection.

Interestingly, in **Figure 4.12**, the test analytes do not elute in order of their hydrophobicities. This is not unexpected as the unique dispersive and electronic interactions of PGC promote increased retention of compounds with multiple fused rings and/or multiple polarizable groups.^{1,39-41}

To further investigate the nature of the retention of Amide-PGC under reversed phase conditions, comparative separations of a mixture of n-alkylbenzenes was performed on Amide-PGC and unmodified PGC. Both Amide-PGC and unmodified PGC show comparable patterns of retention (**Figure 4.13**) consistent with that observed previously on PGC.⁴² Retention increased on both phases with increasing alkyl chain length (= increased hydrophobicity). However, similar to **Figure 4.12**, the alkylbenzenes in **Figure 4.13** displayed ten-fold lower retention on Amide-PGC relative to unmodified PGC.

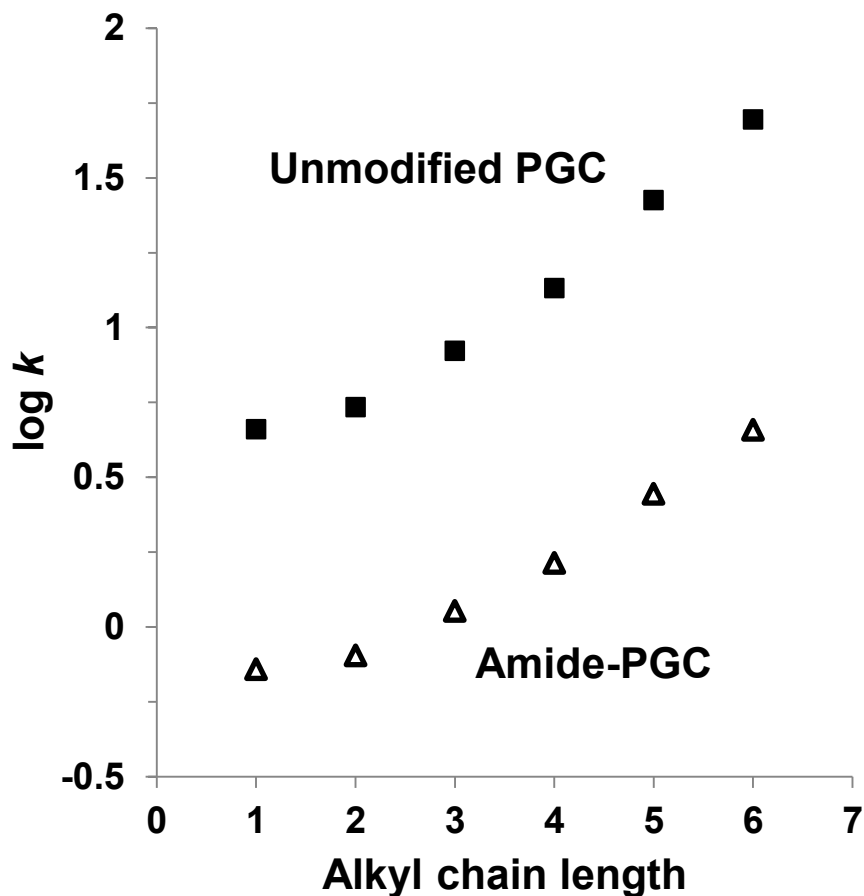


Figure 4.13. Comparison of the retention behavior of C₁-C₆ n-alkylbenzenes under reversed phase conditions on Amide-PGC and unmodified PGC. Markers are the average of duplicate injections. Standard deviations are smaller than the markers. Conditions: columns, Amide-PGC (150 mm x 3 mm ID, 5 μm) and unmodified PGC (Hypercarb, 100 mm x 4.6 mm ID, 5 μm); eluent, unbuffered 60 % ACN at 0.5 (Amide-PGC) or 1.0 mL/min (unmodified PGC); analytes, 0.5 mM of toluene, ethylbenzene, propylbenzene, butylbenzene, pentylbenzene, and hexylbenzene in 60 % ACN. UV detection at 220 nm with a 10 μL injection.

4.4 Conclusions

Diazonium chemistry was used to prepare two new modified PGC phases. Investigations into the retention behaviors of the Catechol-PGC and Amide-PGC phases showed that Catechol-PGC showed mixed partitioning and adsorptive retention of the hydrophilic analytes, while HILIC retention on Amide-PGC was mainly adsorptive. Relative to unmodified PGC, Catechol-PGC exhibits greater HILIC retention of biologically relevant phenolic compounds and nucleosides. As a reversed phase, Catechol-PGC successfully resolved a mixture of ephedrine derivatives under mild eluent conditions. The Amide-PGC phase provided significant attenuation (almost 90 % reduction in k) of the excessive retentivity of PGC for a mixture of common pharmaceuticals. Additionally, a 10-fold reduction in the retention of n-alkylbenzenes was observed on Amide-PGC relative to a separation performed under the same conditions on unmodified PGC.

4.5 References

- (1) West, C.; Elfakir, C.; Lafosse, M. *J. Chromatogr. A* **2010**, *1217*, 3201–3216.
- (2) Harnisch, J. A.; Gazda, D. B.; Anderegg, J. W.; Porter, M. D. *Anal. Chem.* **2001**, *73*, 3954–3959.
- (3) Wahab, M. F.; Ibrahim, M. E. A.; Lucy, C. A. *Anal. Chem.* **2013**, *85*, 5684–5691.
- (4) Chambers, S. D.; McDermott, M. T.; Lucy, C. A. *Analyst* **2009**, *134*, 2273–2280.
- (5) Baergen, A. C.; Chambers, S. D.; Lucy, C. A. Preparation of a carbon based

aniline Stationary phase for high performance liquid chromatography (Poster Presentation), presented at the 91st Canadian Chemistry Conference and Exhibition, 2008.

- (6) Iverson, C. D.; Lucy, C. A. *J. Chromatogr. A* **2014**, *1373*, 17–24.
- (7) Pognon, G.; Cougnon, C.; Mayilukila, D.; Bélanger, D. *ACS Appl. Mater. Interfaces* **2012**, *4*, 3788–3796.
- (8) Leonard, J.; Lygo, B.; Procter, G. *Advanced Practical Organic Chemistry*; 3rd ed.; CRC Press: Boca Raton, FL, 2013.
- (9) Forgács, E. *J. Chromatogr. A* **2002**, *975*, 229–243.
- (10) Michel, M.; Buszewski, B. *Adsorption* **2009**, *15*, 193–202.
- (11) Pereira, L. *LC-GC North Am.* **2011**, *29*, 262–269.
- (12) Ross, P.; Knox, J. H. *Adv. Chromatogr.* **1997**, *37*, 121–162.
- (13) Belanger, D. Modification of materials for energy storage applications, presented at the 97th Canadian Chemistry Conference and Exhibition, 2014.
- (14) McCreery, R. L. *Chem. Rev.* **2008**, *108*, 2646–2687.
- (15) Le Comte, A.; Pognon, G.; Brousse, T.; Belanger, D. *Electrochemistry* **2013**, *81*, 863–866.
- (16) Jansen, R. J. J.; van Bekkum, H. *Carbon N. Y.* **1995**, *33*, 1021–1027.

- (17) Liu, Y.-C.; McCreery, R. L. *J. Am. Chem. Soc.* **1995**, *117*, 11254–11259.
- (18) Alpert, A. J. *J. Chromatogr. A* **1990**, *499*, 177–196.
- (19) Hemström, P.; Irgum, K. *J. Sep. Sci.* **2006**, *29*, 1784–1821.
- (20) Gritti, F.; Höltzel, A.; Tallarek, U.; Guiochon, G. *J. Chromatogr. A* **2015**, *1376*, 112–125.
- (21) Calculated from ACD labs software, V11.02, 2014.
- (22) Marrubini, G.; Mendoza, B. E. C.; Massolini, G. *J. Sep. Sci.* **2010**, *33*, 803–816.
- (23) Tyteca, E.; Guillarme, D.; Desmet, G. *J. Chromatogr. A* **2014**, *1368*, 125–131.
- (24) Schuster, G.; Lindner, W. *Anal. Bioanal. Chem.* **2011**, *400*, 2539–2554.
- (25) World Anti-Doping Agency <http://www.wada-ama.org> (accessed Jan 1, 2015).
- (26) Michael, C.; Rizzi, A. M. *Rapid Commun. Mass Spectrom.* **2015**, *29*, 1268–1278.
- (27) Michael, C.; Rizzi, A. M. *J. Chromatogr. A* **2015**, *1383*, 88–95.
- (28) Verspreet, J.; Holmgaard Hansen, A.; Dornez, E.; Courtin, C. M.; Harrison, S. J. *Anal. Bioanal. Chem.* **2014**, *406*, 4785–4788.
- (29) Heaton, J.; Gray, N.; Cowan, D. A.; Plumb, R. S.; Legido-Quigley, C.; Smith, N. *W. J. Chromatogr. A* **2012**, *1228*, 329–337.
- (30) Haun, J.; Leonhardt, J.; Portner, C.; Hetzel, T.; Tuerk, J.; Teutenberg, T.; Schmidt, T. C. *Anal. Chem.* **2013**, *85*, 10083–10091.

- (31) Moretton, C.; Crétier, G.; Nigay, H.; Rocca, J.-L. *J. Chromatogr. A* **2008**, *1198*, 73–79.
- (32) Sakhi, A. K.; Russnes, K. M.; Smeland, S.; Blomhoff, R.; Gundersen, T. E. *J. Chromatogr. A* **2006**, *1104*, 179–189.
- (33) Thiébaud, D.; Vial, J.; Michel, M.; Hennion, M.-C.; Greibrokk, T. *J. Chromatogr. A* **2006**, *1122*, 97–104.
- (34) Ortmayr, K.; Hann, S.; Koellensperger, G. *Analyst* **2015**, *140*, 3465–3473.
- (35) Zhao, Y.; Szeto, S. S. W.; Kong, R. P. W.; Law, C. H.; Li, G.; Quan, Q.; Zhang, Z.; Wang, Y.; Chu, I. K. *Anal. Chem.* **2014**, *86*, 12172–12179.
- (36) Jensen, D. S.; Gupta, V.; Olsen, R. E.; Miller, A. T.; Davis, R. C.; Ess, D. H.; Zhu, Z.; Vail, M. A.; Dadson, A. E.; Linford, M. R. *J. Chromatogr. A* **2011**, *1218*, 8362–8369.
- (37) Pabst, M.; Grass, J.; Fischl, R.; Léonard, R.; Jin, C.; Hinterkörner, G.; Borth, N.; Altmann, F. *Anal. Chem.* **2010**, *82*, 9782–9788.
- (38) Pabst, M.; Altmann, F. *Anal. Chem.* **2008**, *80*, 7534–7542.
- (39) Kanya, Z.; Cserhati, T.; Forgacs, E. *Chromatographia* **2003**, *57*, 451–456.
- (40) Hennion, M.-C.; Coquart, V.; Guenu, S.; Sella, C. *J. Chromatogr. A* **1995**, *712*, 287–301.
- (41) Forgacs, E.; Cserhati, T. *J. Chromatogr.* **1992**, *600*, 43–49.

- (42) De Matteis, C. I.; Simpson, D. A.; Doughty, S. W.; Euerby, M. R.; Shaw, P. N.; Barrett, D. A. *J. Chromatogr. A* **2010**, *1217*, 6987–6993.

CHAPTER 5: An Exploration of the Use of Ethanol as a HPLC Mobile Phase^{iv}

5.1 Introduction

One current goal of modern Chemistry is to make our craft more environmentally sustainable; specifically by minimizing or eliminating the use of toxic solvents and reagents in our daily work.^{1,2} Applying the concept of *green chemistry* to liquid chromatography, the use of organic solvents may be significantly reduced by utilizing narrow bore columns (reduce flow) in conjunction with smaller particles (maintain efficiency).^{3,4} For example, a 1 hour run on a standard 4.6 mm inner diameter column containing 5 μm particles run at 1 mL/min would consume 60 mL of mobile phase. A 2 mm column containing 2 μm particles run at 0.2 mL/min, on the other hand, would consume 12 mL of mobile phase, reducing consumption by 80 %.

Alternatively, there has been a shift towards the use of less toxic solvents in HPLC. Ethanol, for instance, is one favored solvent due to its lower toxicity and derivation from environmentally friendly sources.³⁻⁶

In a recent paper, Welch et al.⁷ evaluated and successfully demonstrated the use of several distilled spirits as economical and environmentally friendly alternatives to common HPLC grade eluents for quantitative and qualitative RPLC analyses. Specifically, gradient RPLC separations of mixtures of low to medium polarity analytes were performed using five readily available distilled spirits (grain alcohol, vodka, rum, cachaça, and aguardente).⁷ The retention and peak shapes of the analytes afforded by the

^{iv} This is a significantly expanded version of Iverson, C. D.; Wu, D.; Jiang, P.; Stanley, B.; Pappoe, M. B.; Lucy, C. A. *ACS Sustainable Chem. Eng.* **2015**, *3*, 1898. See the Preface for details on individual contributions.

spirits were compared to separations performed using HPLC grade ethanol.⁷ Additionally, LC-MS quantitative analyses of piperidine isomers in black pepper and vitamin C in different food samples were performed as a proof of concept using distilled spirit mobile phases buffered with mixtures of vinegar and ammonia (to yield an ammonium acetate buffer).⁷

In this chapter I shift my focus from the column to other important factors to consider in HPLC method development, such as eluent choice. Specifically, based on my replication of the qualitative spirit-based RPLC separations performed in Welch et al.'s paper⁷ and additional experiments, I will discuss some of the factors related to chromatographic performance that Welch et al.⁷ either undersold or did not properly address in their work. Furthermore in this discussion, I will highlight additional factors beyond their work that one must consider when choosing an appropriate eluent for HPLC.

5.2 Experimental

5.2.1 Beverage Mobile Phases, Chemicals, Reagents, Materials, and Stationary Phase

Deionized water was from a Milli-Q Reference water purification system (EMD Millipore, Bedford, MA, USA). Ethanol (HPLC grade), 1-phenylethanol, and butyl paraben were from Acros Organics (Fair Lawn, NJ, USA). HPLC Chromasolv grade Acetonitrile and Methanol, as well as uracil were from Sigma Aldrich (St. Louis, MO, USA). Caffeine was from BDH Chemicals (Poole, UK). Spirits used as (potential) mobile phases, including Everclear Grain Alcohol (Luxco, Inc., St. Louis, MO, USA), Smirnoff Vodka No. 21 (Smirnoff Co., Norwalk, CT, USA), Absolut Vodka (Absolut Co.,

Stockholm, Sweden), Ketel One Vodka (Nolet Distillery, Schiedham, Holland), Grey Goose Vodka (Grey Goose BMP, Gensac-La-Pallue, France), Stolichnaya Vodka (SPI Sirits, Riga, Latvia), Russian Prince Vodka (Bacardi Canada, Inc., Brampton, ON, Canada), and Alberta Pure Vodka (Alberta Distillers, Ltd., Calgary, AB, Canada) were all purchased from a local liquor store (Edmonton, AB, Canada) and were used directly for analysis after filtration with a 0.2 μm nylon membrane filter. The neat HPLC grade ethanol was diluted with water to 95 % (i.e., 5 % water, 95 % HPLC ethanol) prior to use in chromatographic separations. Brita (Clorox Co., Oakland, CA, USA) pitchers and “advanced” filters were purchased from a local Wal-Mart (Edmonton, AB, Canada). Prior to use, each Brita filter was conditioned with 500 mL of deionized water and 200 mL of vodka. The “Brita filtered Smirnoff” was prepared by sequentially filtering Smirnoff vodka through three new conditioned Brita filters and then passing the 3x filtered vodka *twice* through a 0.2 μm nylon filter (*the latter filtrations are critical as the Brita filters leach fine black particulate*). The Zorbax Eclipse XDB-C8 column (4.6 mm \times 150 mm, 5 μm) used in this study was kindly gifted by Xiaoli Wang of Agilent Technologies (Wilmington, DA, USA)

5.2.2 Instrumentation and Chromatographic Conditions

UV spectra were recorded on a Hewlett Packard 8453 UV-visible spectrometer (Agilent, Palo Alto, CA, USA). Measurements were made using a 1 cm path length quartz cuvette and were referenced against deionized water.

All chromatographic studies were performed on a Waters (Mississauga, ON, Canada) Acquity UPLC system consisting of a binary solvent manager, a sample

manager equipped with a 10 μL loop (all injections were 3 μL partial loop fill), a thermostated column compartment (see below), and a tunable UV detector. The instrument was controlled using Empower 2 software (Waters).

Two mg/mL stock solutions of uracil, caffeine, 1-phenylethanol, and butyl paraben were prepared in 1:1 HPLC ethanol:water. Final 0.1 mg/mL working solutions of these analytes were prepared from the stock solutions in 20 % HPLC ethanol_(aq). Gradient separations of the four-analyte mixture were performed at 25 °C (HPLC grade ethanol and grain alcohol) or 65 °C (vodkas) at a flow rate of 1.2 mL/min (HPLC grade ethanol and grain alcohol) or 1.5 mL/min (vodkas). UV detection was at 210 nm (HPLC grade ethanol and grain alcohol) or 215 nm (vodkas). The gradient programs used were as follows: 1) mobile phase A: water; mobile phase B: 95 % HPLC ethanol_(aq) or neat grain alcohol; 10 % B to 100 % B in 8 min then hold 2 min; 2) mobile phase A: water; mobile phase B: vodka; 20 % B to 100 % B in 5 min then hold 10 min.

5.3 Results and Discussion

Welch et al.⁷ recently described the use of distilled alcohol spirits as an economical and green alternative to traditional HPLC solvents. The authors demonstrated in their work that the spirit-based mobile phases could yield RPLC separations that were of comparable performance (i.e., comparable retention and peak shapes) to commercially prepared HPLC-grade solvents. However, there were several factors related to chromatographic performance that the authors undersold or did not adequately address. Each of these will be discussed in the following subsections.

5.3.1 Eluent Viscosity is the Key: The Backpressure Penalty of Ethanol

One impact of using aqueous ethanol mixtures that was not discussed by Welch et al.⁷ is its significantly higher viscosity than the traditionally used acetonitrile and methanol solvents.^{6,8} **Figure 5.1** compares the viscosities of aqueous mixtures of these three solvents mixed with water.

Recall from **Section 1.2.1.6** that the observed backpressure (ΔP) across a column is proportional to the eluent viscosity (η). Accordingly, given the viscosities in **Figure 5.1**, much higher backpressures were observed during a chromatographic separation with ethanolic eluents than with traditional RPLC eluents. Here, the conditions utilized by Welch et al.⁷ for the HPLC ethanol and grain alcohol eluents typically yielded backpressures of 3700-4200 psi. These pressures are within the maximum operating limits of most HPLC instruments, but above the typical 3000 psi method development target.⁹ Also, continual use of a column at its higher pressure limits may shorten its lifetime.⁹

Moreover, in contrast to acetonitrile where the viscosity/pressure apex is achieved at low % ACN (**Figure 5.1**), aqueous ethanol (as well as methanol) reaches its maximal viscosity/backpressure at a concentration of ~50 %. This may cause unexpected difficulties for a chromatographer developing a gradient method with ethanol, as they may not expect to see such a surge in pressure during the middle of the gradient. In a near worst case scenario, a separation may be halted unexpectedly (trapping the analytes on the column) as the instrument stops eluent flow to protect the column from damage arising from the pressure surge.

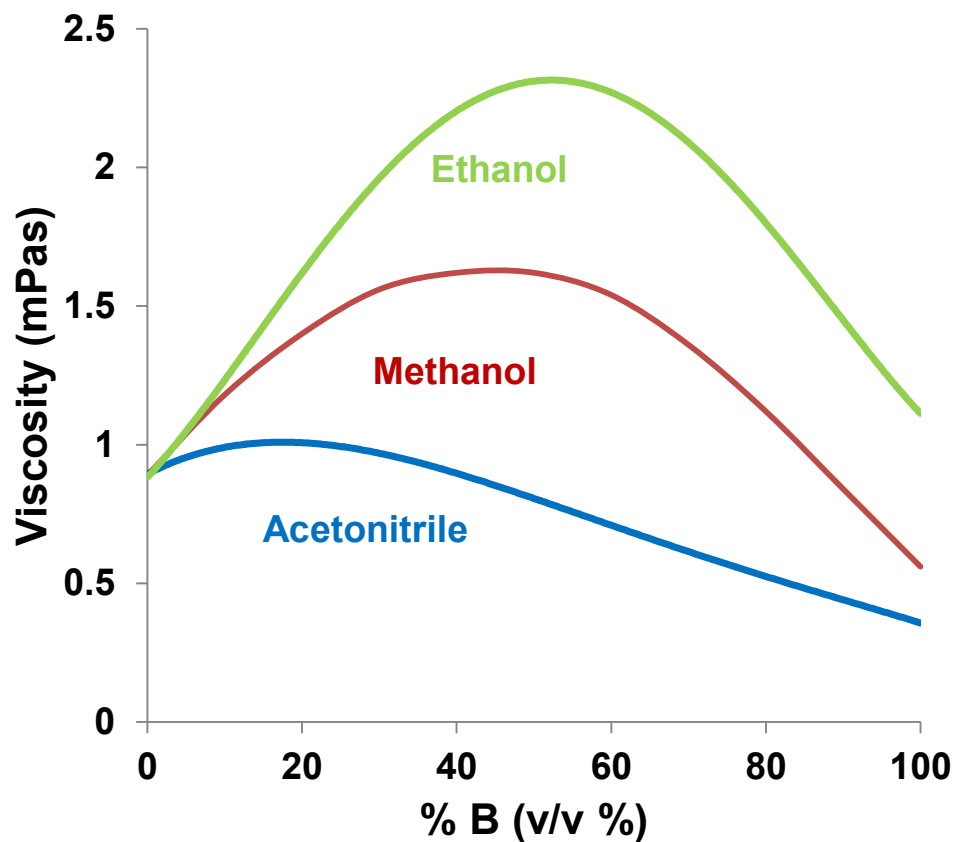


Figure 5.1. Comparison of the viscosities of aqueous mixtures of acetonitrile, methanol, and ethanol. Acetonitrile and methanol data from Snyder et al.¹⁰ Ethanol data adapted from Gonzalez et al.¹¹ Mole fractions of ethanol were converted to (v/v %) using Equations A-5 and A-6 derived in Appendix 1.

5.3.2. Solvent Quality Matters: The Choice of Vodka Brand and Ghost Peaks

Welch et al.⁷ evaluated only one brand of each spirit (e.g., vodka). In this work I evaluated the UV absorbance spectra of seven brands of vodka (**Figure 5.2**). **Figure 5.2** demonstrates that not all brands of vodka are created equal in terms of purity. The presence of UV absorbing impurities may increase detection limits by increasing the baseline signal¹² (see **Section 5.3.3**). **Figure 5.2** also shows that the Smirnoff vodka used by Welch et al.⁷ had the highest UV absorbance (i.e., most impurities) of all of the brands that I studied.

Impurities in the eluent solvent can appear as *ghost peaks* in a gradient separation.¹³ As pre-equilibration proceeds, any mobile phase impurities are absorbed/adsorbed by the stationary phase from the low elution strength mobile phase. Subsequently during the gradient separation the trapped impurities are eluted from the column by the increasingly strong mobile phase, and appear as a peak.¹³ These *ghost peaks* can confound chromatographers due to their variable nature (peak area increases with equilibration time).¹³ In **Figure 5.3** as reproduced from the original Welch et al. paper⁷, a baseline hump is evident at 7.7 min. The authors did not comment on this feature. My replication of this separation yielded two ghost peaks (**Figure 5.4A**). When the separation in **Figure 5.4A** was repeated using a shorter equilibration time (data not shown), the peak area of the ghost peaks was reduced. This observation is a key diagnostic feature of a solvent ghost peak, as a shorter equilibration time allows less of the impurity to collect on the column.

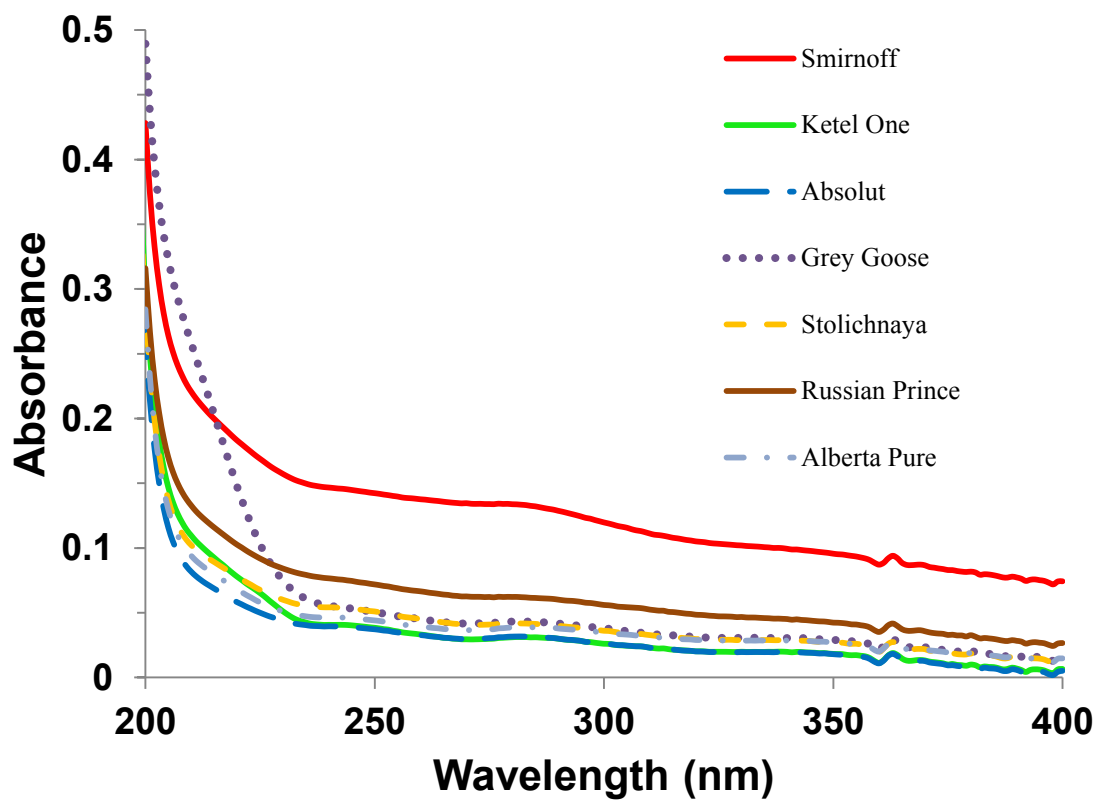


Figure 5.2. UV absorbance spectra of seven brands of vodka.

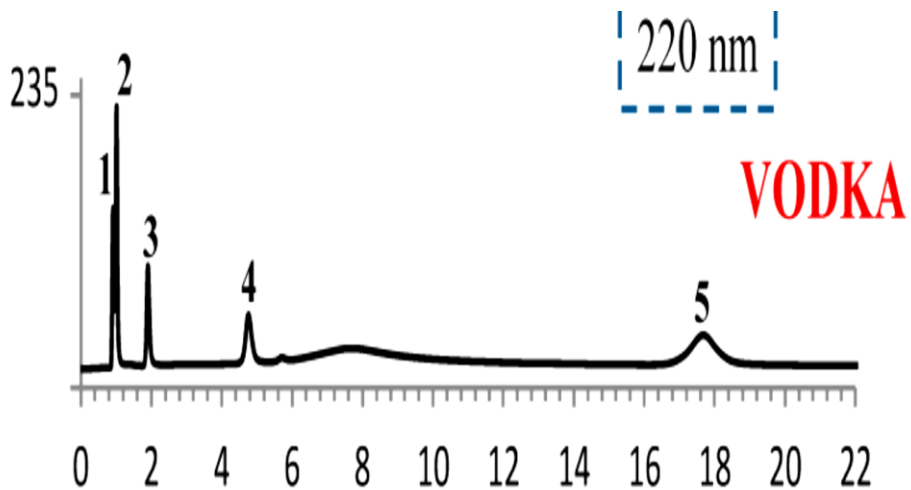


Figure 5.3. Welch et al.'s gradient RPLC separation of a 5-compound mixture using Smirnoff vodka as an eluent. See paper for experimental details. Analytes: (1) uracil, (2) caffeine, (3) 1-phenylethanol, (4) butyl paraben, and (5) anthracene. Reproduced with permission from Welch, C. J.; Nowak, T.; Joyce, L. A.; Regaldo, E. L. *ACS Sustainable Chem. Eng.* **2015**, 3, 1000-1009. Copyright 2015 American Chemical Society.

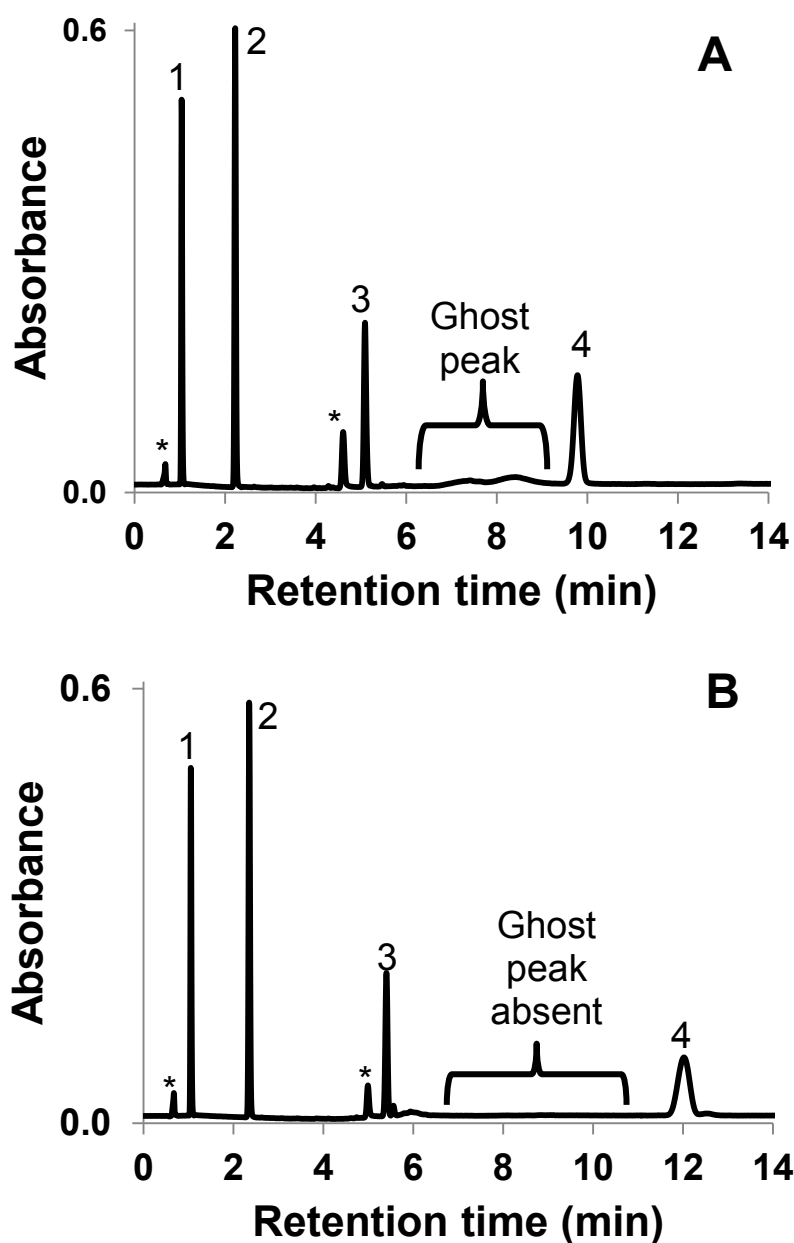


Figure 5.4. Comparison of the gradient separation of four analytes (A) before and (B) after Brita filtration. Chromatographic conditions: column, Zorbax Eclipse XDB C8 (4.6 mm X 150 mm, 5 μ m); eluents, mobile phase A = deionized water, mobile phase B = Smirnoff vodka, or 3x Brita filtered Smirnoff vodka, 20 % to 100 % B in 5 min then hold 9 min; 1.5 mL/min; analytes, 0.1 mg/mL of (1) uracil, (2) caffeine, (3) 1-phenylethanol, and (4) butyl paraben in 20 % EtOH; 65 $^{\circ}$ C; 215 nm. * indicates analyte impurities.

The popular science show *MythBusters* demonstrated that the quality of “cheaper” vodka may be improved by sequential filtration through several Brita filters.¹⁴ Brita filters contain ion exchange resins and activated carbon.¹⁵ Combined, these materials adsorb metals, salts, and organic contaminants from the liquids passed through them to purify those liquids.

To determine whether the MythBusters’ methodology was appropriate to cleanup HPLC solvents, Smirnoff vodka was sequentially filtered through three Brita filters in an attempt to remove the impurities. The Brita filtrations eliminated the ghost peaks (**Figure 5.4B**). However, the retention of all compounds in **Figure 5.4B** increased, suggesting the filters may adsorb some ethanol from the vodka.

The Smirnoff vodka was \$24.68/L and each Brita filter was \$8.00, yielding a cost of \$48.68/L of ethanol eluent. Alternatively one could use a more premium brand of vodka. **Figure 5.5** shows comparable separations (without the ghost peaks) using unfiltered Absolut (\$28.43 /L) and Ketel One (\$36.53 /L) vodka as the eluent. Based on their lower overall cost and reduced need for manual preparation, the use of these higher quality vodkas is preferred over Brita filtration of the lower quality Smirnoff to yield ghost peak free chromatograms.

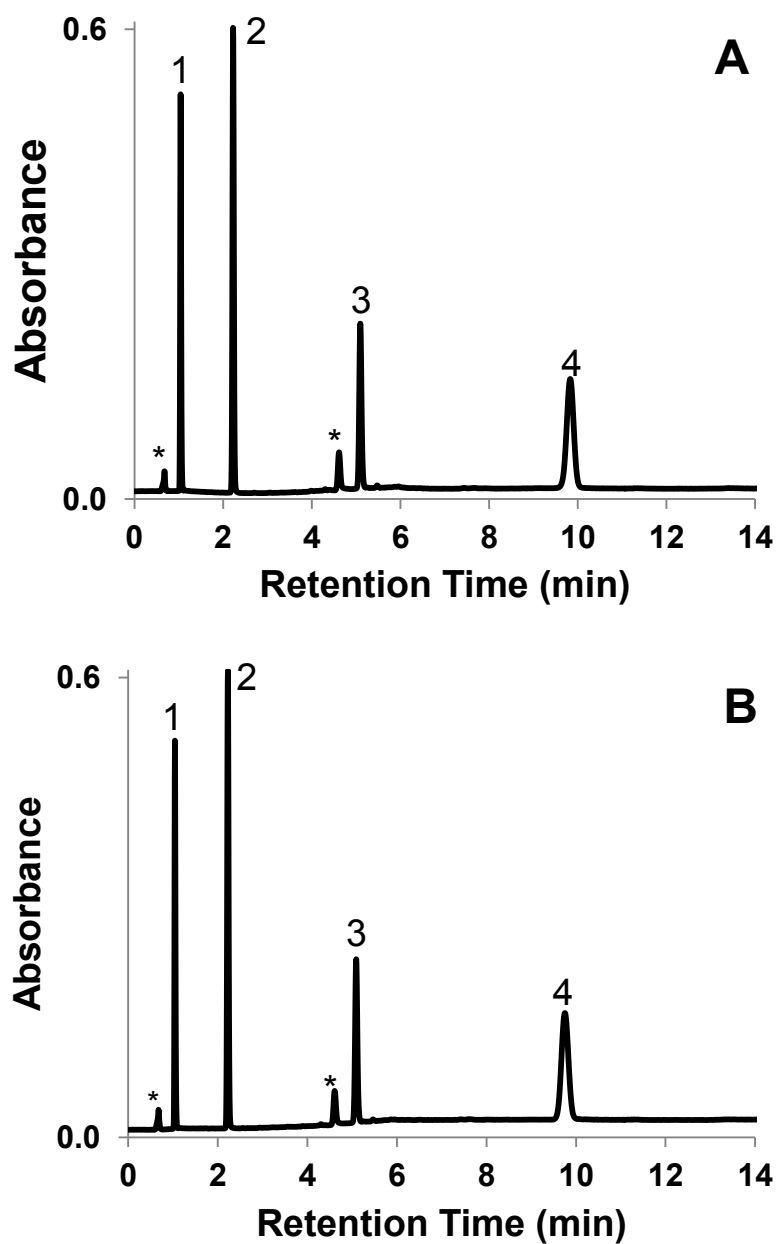


Figure 5.5. Gradient separation of four analytes using (A) Absolut vodka and (B) Ketel One vodka as the organic eluent. Chromatographic conditions: column, Zorbax Eclipse XDB C8 (4.6 mm X 150 mm, 5 μ m); eluents, mobile phase A = deionized water, mobile phase B = Absolut vodka or Ketel One vodka, 20 % to 100 % B in 5 min then hold 9 min; 1.5 mL/min; analytes, 0.1 mg/mL of (1) uracil, (2) caffeine, (3) 1-phenylethanol, and (4) butyl paraben in 20 % EtOH; 65 $^{\circ}$ C; 215 nm. * indicates analyte impurities.

5.3.3. Seeing the Flower Amongst the Weeds: The Importance of Solvent UV Cutoffs

The detection limit is one performance indicator of a HPLC method which is greatly influenced by eluent choice. By definition, the detection limit (DL) is the concentration of analyte which provides a signal that is three times greater than that of the background (**Equation 5.1**).¹⁶

$$DL = \frac{\overline{y_{blank}} + 3s_{blank}}{m} \quad (5.1)$$

where $\overline{y_{blank}}$ is the mean of many (e.g., 20) replicate measurements of the blank signal, s_{blank} is the standard deviation of the many (e.g., 20) replicate measurements, and m is the slope of the calibration curve.

Figure 5.6 shows that not all eluents have the same background absorbance. Methanol and Ethanol display significant absorption up to 230-240 nm, while acetonitrile displays significantly lower absorption at lower wavelengths. The higher absorption of methanol and ethanol at wavelengths below 230 nm (hence higher background signals and higher detection limits) limit the applicability of these eluents for quantitation of low concentration analytes at these lower wavelengths.

The increase in background signal at lower wavelengths with the use of ethanol and methanol eluents is more evident when using gradients. As demonstrated above in **Figure 5.5B**, the baseline signal drifts upward over the course of the gradient as the concentration of the organic eluent is increased. Such baseline drift may significantly affect the precision and/or accuracy of the peak area or height measurement of any trace analyte which elutes over the sloping portion of the baseline (due to increased uncertainty in peak integration).¹⁰

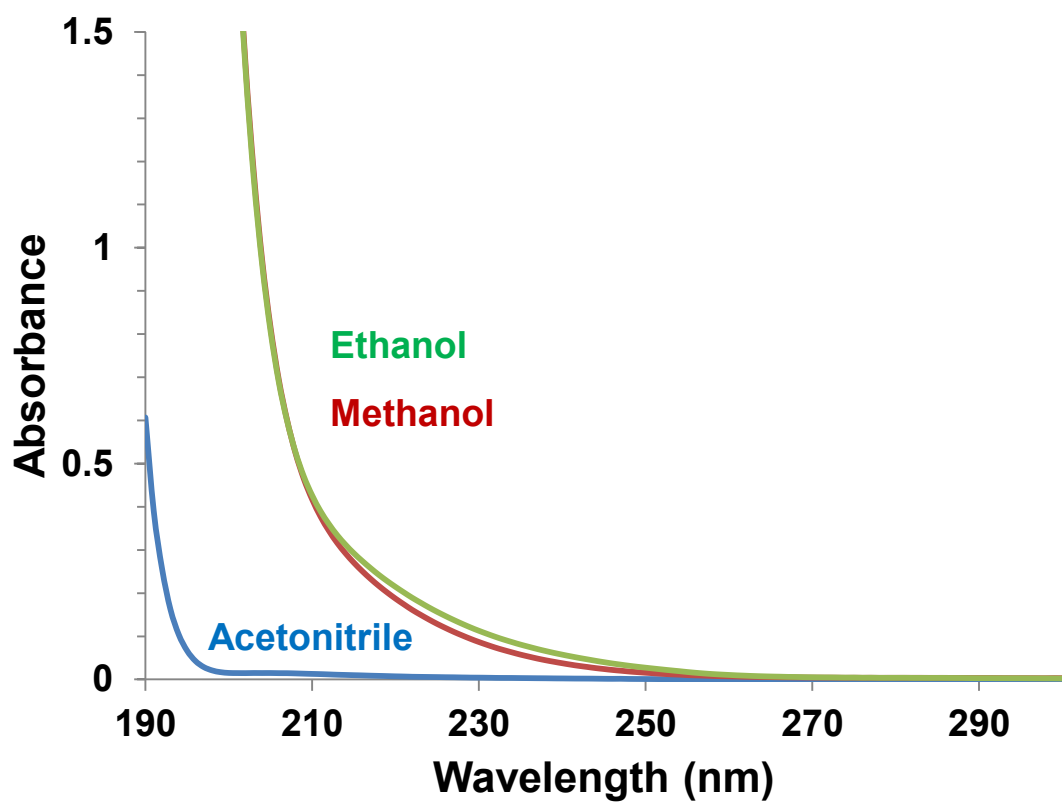


Figure 5.6. UV absorption spectra of HPLC grade acetonitrile, methanol, and ethanol.

5.3.4 Gradient Peak Widths with Grain Alcohol vs. HPLC Grade Ethanol

In any separation, narrow and symmetrical peaks are desired to aid in successful resolution of a mixture in the shortest time possible. In Welch et al.'s⁷ original separation (reproduced in **Figure 5.7**) it appeared that use of grain alcohol caused an increased peak width vs. HPLC grade ethanol. Chromatographic theory does not predict a change in peak width due solely to the source of the eluent.¹⁰ My replication of their separation showed that the peak widths for most of the test compounds were actually equivalent for grain alcohol vs. HPLC grade ethanol (**Table 5.1**). Only the weakly retained uracil showed a difference in peak width, which may be related to extra column effects.

Table 5.1. Measured peak widths of analytes separated under identical conditions using HPLC ethanol and grain alcohol as the organic modifier. Chromatographic conditions: column, Zorbax Eclipse XDB C8 (4.6 mm X 150 mm, 5 μ m); eluents, A = deionized water, B = 95 % HPLC grade ethanol or grain alcohol, 10 % B to 100 % B in 8 min then hold 2 min; 1.2 mL/min; analytes, 0.1 mg/mL of uracil, caffeine, 1-phenylethanol, and butyl paraben in 20 % EtOH; 210 nm.

Analyte	Baseline peak width (s)	
	HPLC ethanol	Grain alcohol
Uracil	49	71
Caffeine	20	23
1-Phenylethanol	21	18
Butyl paraben	16	17

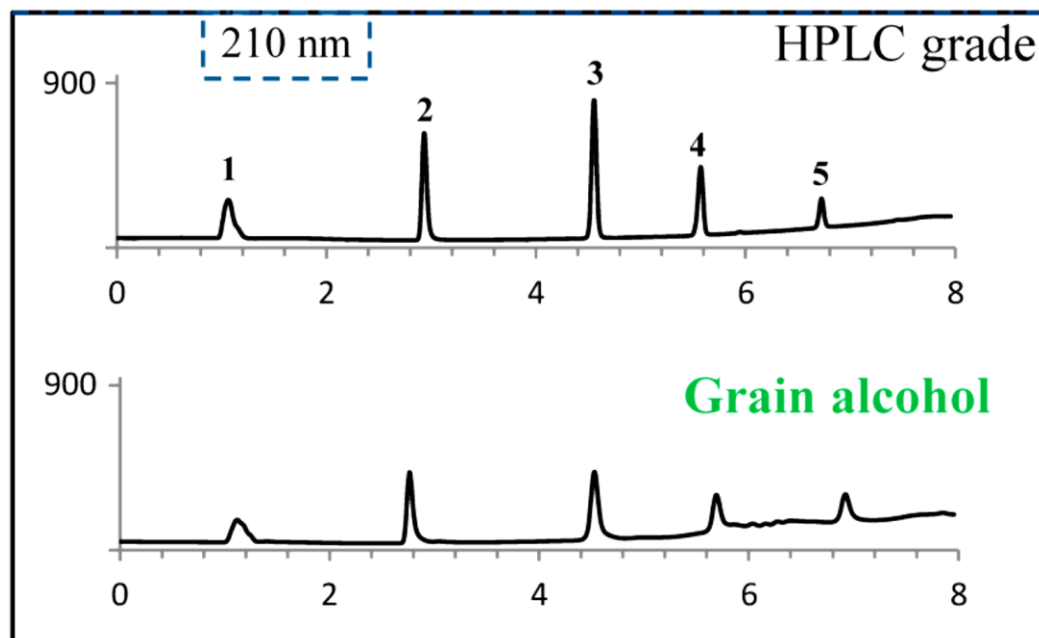


Figure 5.7. Welch et al.'s gradient RPLC separation of a mixture of five analytes using 95 % aqueous HPLC ethanol and grain alcohol as eluents. See paper for experimental details. Analytes: (1) uracil, (2) caffeine, (3) 1-phenylethanol, (4) butyl paraben, and (5) anthracene. Reproduced with permission from Welch, C. J.; Nowak, T.; Joyce, L. A.; Regaldo, E. L. *ACS Sustainable Chem. Eng.* **2015**, *3*, 1000-1009. Copyright 2015 American Chemical Society.

5.4 Conclusions

In commenting on Welch et al.'s⁷ work on “cocktail chromatography,” this chapter has endeavored to discuss some of the key eluent factors that one must consider when developing a separation method. Ethanol is a more environmentally friendly HPLC solvent that provides comparable chromatographic performance to traditional eluents such as acetonitrile and methanol. However, the use of ethanol (particularly if it is sourced from “non-traditional means”) does have drawbacks. Aqueous mixtures with ethanol are more viscous, so the HPLC system must be able to tolerate higher column backpressures. Also, to avoid the appearance of ghost peaks, the analytical method requires use of highly purified solvents. In-lab filter purification of solvents (such as the vodkas) is possible, but perhaps not economical or practical for day to day use. Finally, relative to other solvents such as acetonitrile, ethanol has a significantly higher UV cutoff. At lower wavelengths of detection this can lead to increased background signals and sloping baselines which increase detection limits and reduce method precision and accuracy.

5.5 References

- (1) Gupta, P.; Mahajan, A. *RSC Adv.* **2015**, *5*, 26686–26705.
- (2) Pena-Pereira, F.; Kloskowski, A.; Namiesnik, J. *Green Chem.* **2015**, *17*, 3687–3705.
- (3) Welch, C. J.; Wu, N.; Biba, M.; Hartman, R.; Brkovic, T.; Gong, X.; Helmy, R.; Schafer, W.; Cuff, J.; Pirzada, Z.; Zhou, L. *TrAC, Trends Anal. Chem.* **2010**, *29*,

667–680.

- (4) Shaaban, H.; Gorecki, T. *Talanta* **2015**, *132*, 739–752.
- (5) Welch, C. J.; Brkovic, T.; Schafer, W.; Gong, X. *Green Chem.* **2009**, *11*, 1232–1238.
- (6) Sandra, P.; Sandra, K.; Pereira, A.; Vanhoenacker, G.; David, F. *LC-GC Eur.* **2010**, *23*, 242–259.
- (7) Welch, C. J.; Nowak, T.; Joyce, L. A.; Regalado, E. L. *ACS Sustain. Chem. Eng.* **2015**, *3*, 1000–1009.
- (8) Teutenberg, T.; Wiese, S.; Wagner, P.; Gmehling, J. *J. Chromatogr. A* **2009**, *1216*, 8470–8479.
- (9) Majors, R. E. *LC-GC Eur.* **2008**, *21*, 268–280.
- (10) Snyder, L. R.; Kirkland, J. J.; Dolan, J. W. *Introduction to Modern Liquid Chromatography*; 3rd ed.; John Wiley & Sons: Hoboken, NJ, 2011.
- (11) González, B.; Calvar, N.; Gómez, E.; Domínguez, Á. *J. Chem. Thermodyn.* **2007**, *39*, 1578–1588.
- (12) Nuebauer, M.; Franz, H. *Optimizing and Monitoring Solvent Quality for UV-Vis Absorption, Fluorescence and Charged Aerosol Detectors*; Thermo Scientific, Technical Note 140; Germering, Germany, 2014.

- (13) Sadikin, S.; Zhang, D. D.; Inloes, R.; Redkar, S. *LC-GC North Am.* **2011**, *29*, 394–400.
- (14) Mythbusters. Top Shelf Vodka Myth. Originally aired April 29, 2006.
- (15) Brita Water Filtration Process <https://brita.ca/water-filtration-process/> (accessed Nov 21, 2015).
- (16) Boqué, R.; Heyden, Y. Vander. *LC-GC Eur.* **2009**, *22*, 82–85.

CHAPTER 6: Conclusions and Future Work

6.1 Conclusions

This thesis explored the development and characterization of new stationary phases for hydrophilic interaction liquid chromatography (HILIC) and reversed-phase liquid chromatography (RPLC). **Chapter 2** utilized the hydrophilicity vs. ion interaction plots of Dr. Mohammed Ibrahim¹ to investigate the effect of changing pH and buffer concentration on the selectivity behavior of different HILIC phases. The advantage of using the two dimensional plot is that changes in selectivity are readily observed in a visually appealing and easy to understand format. These plots highlighted changes in selectivity behavior amongst different classes of HILIC phases (e.g., silica, zwitterionic, amine, amide, hydroxylated, etc.), as well as differences within a class of HILIC columns (e.g., different responses to changes in pH by the silica phases due to differences in silanol behavior). These plots allow analytical chemists to predict which column and which mobile phase may be appropriate for their HILIC separation.

Chapters 3 and 4 present the preparation and characterization of three new hydrophilic porous graphitic carbon-based phases (named Aniline-PGC, Catechol-PGC, and Amide-PGC) as a chemically stable alternative to silica. All phases displayed increased HILIC retention (relative to unmodified PGC) and unique selectivity from commercially available HILIC stationary phases. Additionally, the Aniline and Amide modification of attenuated the excessive RPLC retention of PGC by up to 10-fold. The separation times on the modified PGC were greatly reduced and peak efficiencies (N) of later eluting peaks were significantly improved. The stability of Aniline-PGC at pH 2 was also demonstrated.

To date, four different diazonium-modified PGC phases have been prepared by the Lucy group (Amide-PGC,² Aniline-PGC,³ Carboxylate-PGC,⁴ and Catechol-PGC²); all but the Carboxylate-PGC phase are described in this thesis. In comparing the four phases, all have positive and negative aspects in terms of grafting efficiency, hydrophilicity, selectivity, peak efficiency, and peak shape. The phases had an average surface grafting concentration of ~ 2 molecules/nm², with the exception of the Catechol-PGC (**Chapter 4**) which had only ~ 0.2 molecules/nm².

Considering hydrophilicity, all phases displayed increased hydrophilicity after diazonium modification. This was most apparent for the Carboxylate-PGC phase which displayed the greatest overall increase in HILIC retention amongst all of the modified PGC phases, while the other phases had comparable hydrophilicity.

All four phases displayed unique selectivity. Both the Amide-PGC and Aniline-PGC phases displayed mixed-mode retention such that each could operate as a HILIC phase or an attenuated reversed phase. Another interesting aspect of the Aniline and Carboxylate-PGC phases are their pH tunable selectivity. That is, both the aniline and carboxylate columns contain ionisable groups. As such, the selectivity and retention behavior of these two phases changed with changes in mobile phase pH according to the pK_a of the polar groups.

Lastly, turning to peak efficiency and peak shape, all four phases displayed an increased level of tailing for many analytes. A remedy is proposed in **Section 6.2.4** with respect to the Carboxylate-PGC phase. Optimization of the packing procedure may allow for improvements in peak efficiency for these and future modified phases. Taking all of

the above in mind, I believe that the Carboxylate-PGC and Aniline-PGC phases currently stand out as the top performing diazonium-modified PGC phases.

Finally, **Chapter 5** explored the feasibility of ethanol as an alternative eluent for RPLC. Prior research had demonstrated that ethanol can provide comparable retention and peak shape to more commonly used eluents such as acetonitrile and methanol. However there were many aspects of ethanol as an HPLC eluent that had not been clarified. In **Chapter 5** I discussed ethanol's limitations which chromatographers must be aware of, for instance, ethanol/water's higher viscosity results in higher backpressure. Also, ethanolic mobile phases have higher ultraviolet absorbance, which limits its use at low wavelengths. **Chapter 5** also evaluated the use of Brita[®] filters as an alternative means to purify lower grades of solvents for use in HPLC. However, this method may not be practical or economical for regular use.

6.2 Future Work

6.2.1 Investigation of Alternate Test Probes to Measure HILIC Hydrophilic Selectivity

As demonstrated in **Chapter 2**, the pH applicability of $k_{\text{cytosine}}/k_{\text{uracil}}$ is limited under acidic conditions due to the protonation of cytosine. To increase the utility of the selectivity plots for future studies, a probe pair which remains uncharged across a broad pH range is required. Additionally, like cytosine and uracil, an ideal probe pair should use hydrophilic compounds ($\log P < 0$) with similar structures (to negate other interactions) but of differing hydrophilicities ($|\Delta \log P| \geq 0.4$).⁵ Currently, no such gold standard probe pair has been reported in the literature. Considering that beyond its pH limitations, $k_{\text{cytosine}}/k_{\text{uracil}}$ has otherwise been demonstrated as an effective measure of

hydrophilicity,^{1,5} one avenue to explore may be the use of a lower pK_a analogue of cytosine (${}^w pK_a$ 4.4) such as isocytosine (${}^w pK_a$ 4.0), 5-azacytosine (${}^w pK_a$ 3.5), or 6-azacytosine (${}^w pK_a$ 2.8). These compounds have similar structures and comparable hydrophilicities ($\log P = -0.59, -2.50, \text{ and } -1.06, \text{ respectively}$)^{6,7} to cytosine ($\log P = -1.97$),⁶ but lower pK_a values.^{4,7} To validate these compounds as useful probes, studies will be conducted whereby the chromatographic behavior of the potential probes is compared with that of cytosine at ${}^w \text{pH}$ 3.0, 3.7, 5.0, and 6.8 which were studied in **Chapter 2**.

6.2.2 Investigation of Additional Factors Affecting HILIC Selectivity

As noted in a recent review,⁸ many small- and medium-scale studies have been undertaken in order to understand the effects of pH and ionic strength on HILIC selectivity. **Chapter 2** aimed to (and succeeded in) encompass(ing) and add(ing) to these data by investigating a larger number of columns under several pH conditions. However, like many other previous studies, **Chapter 2** focused on the effect of pH while maintaining a constant acetonitrile concentration. By changing the concentration of acetonitrile in a mobile phase of a given ${}^w \text{pH}$, one may drastically alter the acidity of that mobile phase and effect a significant change in the selectivity behavior of a HILIC column.^{5,8-10} To date such mobile phase dependent pH effects on HILIC retention and selectivity have not been comprehensively studied for a large number of HILIC columns. Hence I propose that studies be undertaken on a series of representative HILIC columns to investigate the changes in selectivity behavior at different ${}^w \text{pH}$ values in response to changes in acetonitrile concentration. Specifically, measurements of test probe retention

(both the newly and previously validated probes) would be made at several acetonitrile concentrations and several w pH values for each selected column. To permit effective organization and visualization of the data, these studies would continue to utilize versions of the HILIC selectivity plots and HILIC selectivity *change* plots used in **Chapter 2**.

6.2.3 Zwitterionic Porous Graphitic Carbon for HILIC

As mentioned above, the Lucy group has to date reported four new PGC-based HILIC phases (one previously⁴ and three in this thesis). In the future it is desirable to continue to build our library of PGC phases to provide chemically stable mimics of different classes of commercially available silica-based HILIC phases. Currently, I believe that the next target should be the development of a zwitterionic sulfoalkylbetaine-PGC phase (ZIC-PGC; **Figure 6.1**). The reasoning behind this is two-fold. Firstly, based on the performance of the Carboxylate-PGC⁴ and Aniline-PGC³ (**Chapter 3**) phases it appears that a more hydrophilic PGC phase may be attained by modifying the surface with charged functionalities such as those found within the sulfoalkylbetaine moiety. Secondly, silica-based ZIC phases have previously demonstrated interesting and unique mobile phase dependent selectivities for a variety of polar compounds.^{5,11,12} As such, I believe that the sulfoalkylbetaine moiety combined with the unique retention mode of PGC¹³ will generate a HILIC phase with very different selectivity.

A proposed synthesis of this phase is shown in **Figure 6.1**. All reactions in this scheme utilize relatively inexpensive and readily available reagents. The first two steps in this proposed synthesis have previously given yields of > 85 %.^{14,15} The third step in **Figure 6.1** may require optimization to maximize yield. Structural characterization of all

pre-grafting synthesis products would be accomplished using a combination of mass spectrometry (specifically GC-MS or LC-MS, as appropriate, to allow determination of product purity), and IR and NMR spectroscopy. As in previous chapters, the overall surface concentration of zwitterionic groups on the functionalized PGC will be determined by x-ray photoelectron spectroscopy (XPS, reaction success determined by monitoring the sulfur concentration). Chromatographic characterization of this phase will be performed using a variety of hydrophilic analytes such as nucleotides, nucleosides, carbohydrates, amino acids, and organic acids.

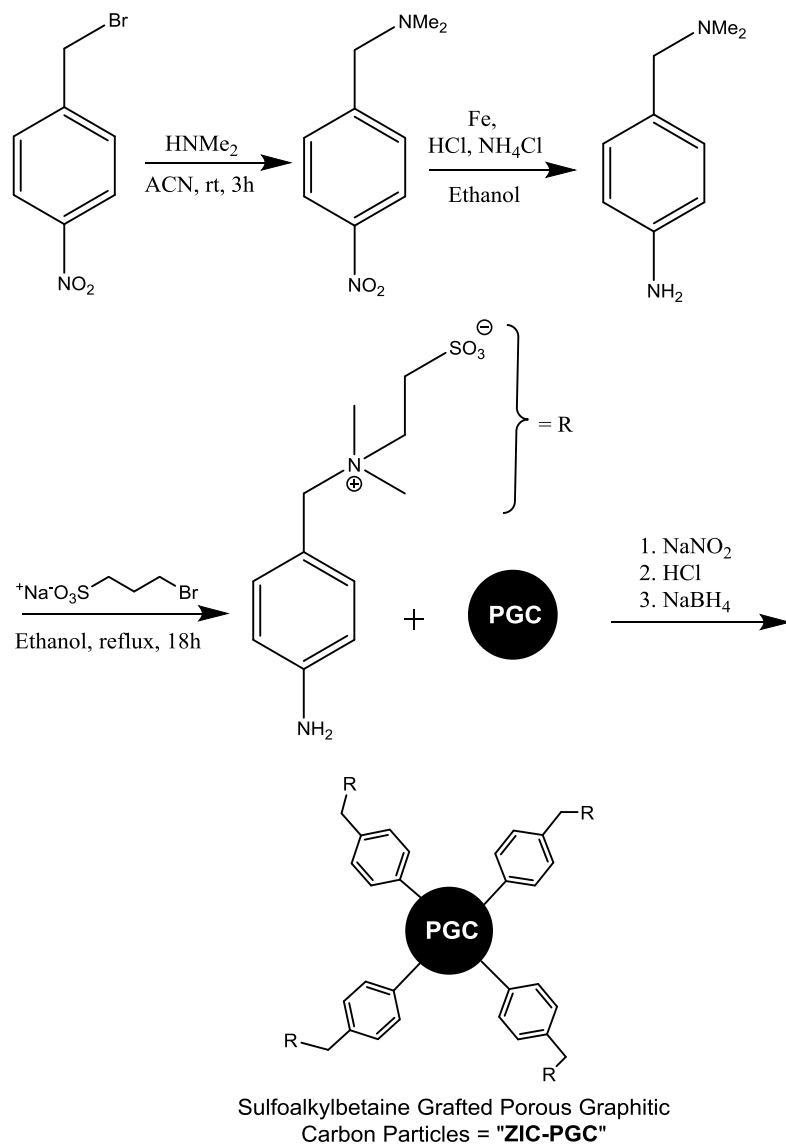


Figure 6.1. Scheme for the proposed synthesis of ZIC-PGC.

6.2.4 Improving the Performance of Carboxylate-PGC

As mentioned previously, the Carboxylate-PGC phase⁴ is arguably the most hydrophilic and one of the best performing diazonium-modified PGC phase reported to date. However it (similar to the phases reported in this thesis) generally suffered from low peak efficiencies and increased peak tailing. In a subsequent paper, the lower peak efficiency of Carboxylate-PGC was attributed to the slow mass transfer properties of the underlying PGC.¹⁶ While this may be partially true, it is likely that a significant contribution to the loss of peak efficiency and peak symmetry may be irregular gaps in surface coverage leading to inconsistent interactions between the analytes and the PGC surface. Although XPS data can provide insight as to overall average grafting efficiency, it cannot necessarily pinpoint the degree of grafting along different regions of individual particles. Indeed, it is thought that diazonium modification tends to occur more readily at the edge plane surfaces of PGC than at the basal plane surfaces.^{17,18}

To improve the surface coverage of carboxylate groups across the PGC surface I propose that an alternate route of functionalization be taken based on recent work by Belanger and co-workers.¹⁹ This method entails functionalization of polyacrylic acid onto the surface of PGC in a three-step process (**Figure 6.2**): 1) preparation and diazonium grafting of the polymerization initiator (*p*-(1-bromoethyl)aniline hydrobromide); 2) polymerization of the grafted initiators with *t*-butyl acrylate (*note: this step requires the handling of reagents under an inert atmosphere; seek expert guidance and/or consult Leonard et al*²⁰ *as appropriate before proceeding*); and 3) acid cleavage of the *t*-butyl groups to yield polyacrylic acid functionalized PGC (PAA-PGC).

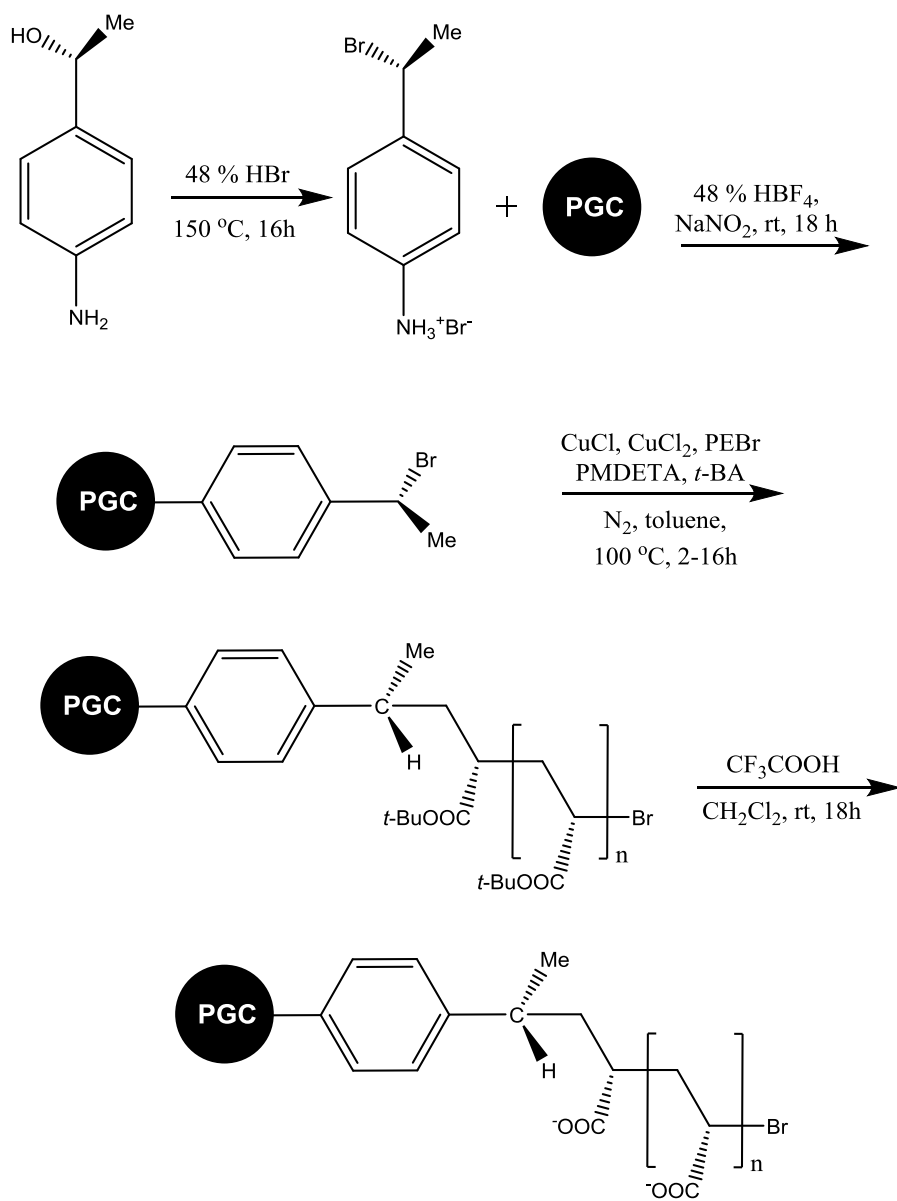


Figure 6.2. Scheme for the proposed synthesis of PAA-PGC. Legend: PEBr = 1-phenylethyl bromide; PMDETA = N,N,N',N',N''-pentamethyldiethylenetriamine; *t*-BA = *t*-butyl acrylate.

The chromatographic performance of this phase in the HILIC mode would then be compared to Carboxylate-PGC for a variety of polar analytes. It is anticipated that the higher coverage afforded by this polymer will yield narrower, more symmetrical peaks. Additionally, based on contact angle measurements of PAA-modified black pearls carbon¹⁹ it is likely that the PAA-PGC phase will display significantly greater hydrophilicity than Carboxylate-PGC.

6.3 References

- (1) Ibrahim, M. E. A.; Liu, Y.; Lucy, C. A. *J. Chromatogr. A* **2012**, *1260*, 126–131.
- (2) Iverson, C. D.; Zhang, Y.; Lucy, C. A. *J. Chromatogr. A* **2015**, *1422*, 186–193.
- (3) Iverson, C. D.; Lucy, C. A. *J. Chromatogr. A* **2014**, *1373*, 17–24.
- (4) Wahab, M. F.; Ibrahim, M. E. A.; Lucy, C. A. *Anal. Chem.* **2013**, *85*, 5684–5691.
- (5) Dinh, N. P.; Jonsson, T.; Irgum, K. *J. Chromatogr. A* **2011**, *1218*, 5880–5591.
- (6) Calculated from ACD labs software, V11.02, 2014.
- (7) Romanová, D.; Novotný, L. *J. Chromatogr. B Biomed. Sci. Appl.* **1996**, *675*, 9–15.
- (8) Guo, Y. *Analyst* **2015**, *140*, 6452–6466.
- (9) McCalley, D. V. *J. Chromatogr. A* **2015**, *1411*, 41–49.
- (10) Subirats, X.; Rosés, M.; Bosch, E. *Sep. Purif. Rev.* **2007**, *36*, 231–255.
- (11) Chirita, R.-I.; West, C.; Zubrzycki, S.; Finaru, A.-L.; Elfakir, C. *J. Chromatogr. A*

2011, *1218*, 5939–5963.

- (12) Greco, G.; Grosse, S.; Letzel, T. *J. Chromatogr. A* **2012**, *1235*, 60–67.
- (13) West, C.; Elfakir, C.; Lafosse, M. *J. Chromatogr. A* **2010**, *1217*, 3201–3216.
- (14) Liu, Y.; Lu, Y.; Prashad, M.; Repic, O.; Blacklock, T. J. *Adv. Synth. Catal.* **2005**, *347*, 217–219.
- (15) Ma, J.; Chen, D.; Lu, K.; Wang, L.; Han, X.; Zhao, Y.; Gong, P. *Eur. J. Med. Chem.* **2014**, *86*, 257–269.
- (16) Ibrahim, M. E. A.; Wahab, M. F.; Lucy, C. A. *Anal. Chim. Acta* **2014**, *820*, 187–194.
- (17) Ray, K.; McCreery, R. L. *Anal. Chem.* **1997**, *69*, 4680–4687.
- (18) McCreery, R. L. *Chem. Rev.* **2008**, *108*, 2646–2687.
- (19) Assresahegn, B. D.; Bélanger, D. *Adv. Funct. Mater.* **2015**, *25*, 6775–6785.
- (20) Leonard, J.; Lygo, B.; Procter, G.; Croup, F. *Advanced Practical Organic Chemistry Second edition*.

BIBLIOGRAPHY

- Acikara, O. B. (2013). Ion-exchange chromatography and its applications. In D. F Martin & B. B Martin (Eds.) *Column Chromatogr.* (pp. 31–58). Rijeka, Croatia: InTech.
- Adamczyk, B., Struwe, W. B., Ercan, A., Nigrovic, P. A., & Rudd, P. M. (2013). Characterization of fibrinogen glycosylation and its importance for serum/plasma N-glycome analysis. *Journal of Proteome Research*, *12*(1), 444–454.
- Alpert, A. J. (1990). Hydrophilic-interaction chromatography for the separation of peptides, nucleic acids and other polar compounds. *Journal of Chromatography A*, *499*, 177–196.
- Alpert, A. J. (2008). Electrostatic repulsion hydrophilic interaction chromatography for isocratic separation of charged solutes and selective isolation of phosphopeptides. *Analytical Chemistry*, *80*(1), 62–76.
- Assresahegn, B. D., & Bélanger, D. (2015). Multifunctional Carbon for Electrochemical Double-Layer Capacitors. *Advanced Functional Materials*, *25*(43), 6775–6785.
- Baergen, A. C., Chambers, S. D., & Lucy, C. A. (2008). Preparation of a carbon based aniline stationary phase for high performance liquid chromatography (Poster Presentation), presented at the 91st Canadian Chemistry Conference and Exhibition.

- Barrett, D. A., Pawula, M., Knaggs, R. D., & Shaw, P. N. (1998). Retention behavior of morphine and its metabolites on a porous graphitic carbon column. *Chromatographia*, 47(11-12), 667–672.
- Belanger, D. (2014). Modification of materials for energy storage applications (oral presentation), presented at the 97th Canadian Chemistry Conference and Exhibition.
- Bell, D. S., & Majors, R. E. (2015). Current state of superficially porous particle technology in liquid chromatography. *LCGC North America*, 33(6), 386–395.
- Benjamin, O. D., Weissmann, M., & Bélanger, D. (2014). Electrochemical modification of carbon electrode with benzylphosphonic groups. *Electrochimica Acta*, 122, 210–217.
- Bernal, J., Ares, A. M., Pol, J., & Wiedmer, S. K. (2011). Hydrophilic interaction liquid chromatography in food analysis. *Journal of Chromatography A*, 1218(42), 7438–7452.
- Billingham, B. E., Oladepo, S. A., & Loppnow, G. R. (2009). pH-Dependent UV resonance raman spectra of cytosine and uracil. *The Journal of Physical Chemistry B*, 113(20), 7392–7397.
- Boqué, R., & Heyden, Y. Vander. (2009). The limit of detection. *LC-GC Europe*, 22(2), 82–85.
- Borges, E. M., & Collins, C. H. (2012). Effects of pH and temperature on the chromatographic performance and stability of immobilized

poly(methyloctylsiloxane) stationary phases. *Journal of Chromatography A*, 1227, 174–180.

Borges, E. M., Rostagno, M. A., & Meireles, M. A. A. (2014). Sub-2 μm fully porous and partially porous (core-shell) stationary phases for reversed phase liquid chromatography. *RSC Advances*, 4(44), 22875–22887.

Brita Water Filtration Process. Retrieved November 21, 2015, from <https://brita.ca/water-filtration-process/>

Brons, C., & Olieman, C. (1983). Study of the high-performance liquid chromatographic separation of reducing sugars, applied to the determination of lactose in milk. *Analytica Chimica Acta*, 259(1), 79–86.

Buszewski, B., & Noga, S. (2012a). Hydrophilic interaction liquid chromatography (HILIC)-a powerful separation technique. *Analytical and Bioanalytical Chemistry*, 402(1), 231–247.

Calculated from ACD labs software, V11.02. (2014). Advanced Chemistry Development.

Caligur, V. Cyclodextrins. Retrieved November 14, 2015, from <http://www.sigmaaldrich.com/technical-documents/articles/biofiles/cyclodextrins.html>

Canals, I., Valkó, K., Bosch, E., Hill, a P., & Rosés, M. (2001). Retention of ionizable compounds on HPLC 8: influence of mobile-phase pH change on the

- chromatographic retention of acids and bases during gradient elution. *Analytical Chemistry*, 73(20), 4937–45.
- Carr, P., Snyder, L., Dolan, J. W., & Majors, R. E. (2010). New horizons in reversed-phase chromatography selectivity. *LCGC North America*, 28(6), 418–430.
- Chambers, S. D. (2014). Personal Communication.
- Chambers, S. D., McDermott, M. T., & Lucy, C. A. (2009). Covalently modified graphitic carbon-based stationary phases for anion chromatography. *The Analyst*, 134(11), 2273–2280.
- Chester, T. L. (2013). Recent developments in high-performance liquid chromatography stationary phases. *Analytical Chemistry*, 85(2), 579–89.
- Chirita, R.-I., West, C., Zubrzycki, S., Finaru, A.-L., & Elfakir, C. (2011). Investigations on the chromatographic behaviour of zwitterionic stationary phases used in hydrophilic interaction chromatography. *Journal of Chromatography. A*, 1218(35), 5939–5963.
- Claessens, H. A., & van Straten, M. A. (2004). Review on the chemical and thermal stability of stationary phases for reversed-phase liquid chromatography. *Journal of Chromatography. A*, 1060(1-2), 23–41.
- De Matteis, C. I., Simpson, D. A., Doughty, S. W., Euerby, M. R., Shaw, P. N., & Barrett, D. A. (2010). Chromatographic retention behaviour of n-alkylbenzenes and pentylbenzene structural isomers on porous graphitic carbon and octadecyl-bonded

- silica studied using molecular modelling and QSRR. *Journal of Chromatography. A*, 1217(44), 6987–93.
- De Matteis, C. I., Simpson, D. A., Euerby, M. R., Shaw, P. N., & Barrett, D. A. (2012). Chromatographic retention behaviour of monosubstituted benzene derivatives on porous graphitic carbon and octadecyl-bonded silica studied using molecular modelling and quantitative structure-retention relationships. *Journal of Chromatography. A*, 1229, 95–106
- Di Palma, S., Mohammed, S., & Heck, A. J. R. (2012). ZIC-cHILIC as a fractionation method for sensitive and powerful shotgun proteomics. *Nature Protocols*, 7(11), 2041–2055.
- Dinh, N. P., Jonsson, T., & Irgum, K. (2011). Probing the interaction mode in hydrophilic interaction chromatography. *Journal of Chromatography. A*, 1218(35), 5880–5591.
- Dinh, N. P., Jonsson, T., & Irgum, K. (2013). Water uptake on polar stationary phases under conditions for hydrophilic interaction chromatography and its relation to solute retention. *Journal of Chromatography A*, 1320, 33–47.
- Fekete, S., Veuthey, J.-L., & Guillarme, D. (2015). Comparison of the most recent chromatographic approaches applied for fast and high resolution separations: Theory and practice. *Journal of Chromatography. A*, 1408, 1–14.
- Forgács, E. (2002). Retention characteristics and practical applications of carbon sorbents. *Journal of Chromatography A*, 975(2), 229–243.

- Forgacs, E., & Cserhati, T. (1992). High-performance liquid chromatographic retention behavior of ring-substituted aniline derivatives on a porous graphitized carbon column. *Journal of Chromatography*, 600(1), 43–49
- Galalzidian, M. Principles of Chromatography. Retrieved September 8, 2015, from <http://www.slideshare.net/mahmoudgalalzidan/principles-in-chromatography>
- Gika, H. G., Theodoridis, G. A., Vrhovsek, U., & Mattivi, F. (2012). Quantitative profiling of polar primary metabolites using hydrophilic interaction ultrahigh performance liquid chromatography-tandem mass spectrometry. *Journal of Chromatography. A*, 1259, 121–127.
- González, B., Calvar, N., Gómez, E., & Domínguez, Á. (2007). Density, dynamic viscosity, and derived properties of binary mixtures of methanol or ethanol with water, ethyl acetate, and methyl acetate at T=(293.15, 298.15, and 303.15)K. *The Journal of Chemical Thermodynamics*, 39(12), 1578–1588.
- Greco, G., Grosse, S., & Letzel, T. (2012). Study of the retention behavior in zwitterionic hydrophilic interaction chromatography of isomeric hydroxy- and aminobenzoic acids. *Journal of Chromatography. A*, 1235, 60–67.
doi:10.1016/j.chroma.2012.02.031
- Gritti, F., & Guiochon, G. (2013). Perspectives on the evolution of the column efficiency in liquid chromatography. *Analytical Chemistry*, 85(6), 3017–35.

- Gritti, F., & Guiochon, G. (2013). The van Deemter equation: assumptions, limits, and adjustment to modern high performance liquid chromatography. *Journal of Chromatography. A*, 1302, 1–13.
- Gritti, F., Höltzel, A., Tallarek, U., & Guiochon, G. (2015). The relative importance of the adsorption and partitioning mechanisms in hydrophilic interaction liquid chromatography. *Journal of Chromatography. A*, 1376, 112–125.
- Guo, S., Duan, J., Qian, D., Tang, Y., Qian, Y., Wu, D., ... Shang, E. (2013). Rapid determination of amino acids in fruits of ziziphus jujuba by hydrophilic interaction ultra-high-performance liquid chromatography coupled with triple-quadrupole mass spectrometry. *Journal of Agricultural and Food Chemistry*, 61(11), 2709–2719.
- Guo, Y. (2011). Retention and selectivity of polar stationary phases for hydrophilic interaction chromatography. In P. G. Wang & W. He (Eds.), *Hydrophilic Interaction Liquid Chromatography (HILIC) and Advanced Applications* (pp. 401–426). Boca Raton, FL: CRC Press.
- Guo, Y. (2015). Recent progress in fundamental understanding of hydrophilic interaction chromatography (HILIC). *The Analyst*, 140, 6452–6466.
- Guo, Y., & Gaiki, S. (2005). Retention behavior of small polar compounds on polar stationary phases in hydrophilic interaction chromatography. *Journal of Chromatography A*, 1074(1-2), 71–80.

- Guo, Y., & Gaiki, S. (2011). Retention and selectivity of stationary phases for hydrophilic interaction chromatography. *Journal of Chromatography A*, 1218(35), 5920–5938.
- Gupta, P., & Mahajan, A. (2015). Green chemistry approaches as sustainable alternatives to conventional strategies in the pharmaceutical industry. *RSC Advances*, 5(34), 26686–26705.
- Harnisch, J. A., Gazda, D. B., Anderegg, J. W., & Porter, M. D. (2001). Chemical modification of carbonaceous stationary phases by the reduction of diazonium salts. *Analytical Chemistry*, 73(16), 3954–3959.
- Haun, J., Leonhardt, J., Portner, C., Hetzel, T., Tuerk, J., Teutenberg, T., & Schmidt, T. C. (2013). Online and splitless nanoLC × capillaryLC with quadrupole/time-of-flight mass spectrometric detection for comprehensive screening analysis of complex samples. *Analytical Chemistry*, 85(21), 10083–10091.
- Heaton, J. C., & McCalley, D. V. (2014). Comparison of the kinetic performance and retentivity of sub-2µm core-shell, hybrid and conventional bare silica phases in hydrophilic interaction chromatography. *Journal of Chromatography A*, 1371, 106–116.
- Heaton, J. C., Russell, J. J., Underwood, T., Boughtflower, R., & McCalley, D. V. (2014). Comparison of peak shape in hydrophilic interaction chromatography using acidic salt buffers and simple acid solutions. *Journal of Chromatography. A*, 1347, 39–48.

- Heaton, J., Gray, N., Cowan, D. A., Plumb, R. S., Legido-Quigley, C., & Smith, N. W. (2012). Comparison of reversed-phase and hydrophilic interaction liquid chromatography for the separation of ephedrines. *Journal of Chromatography. A*, 1228, 329–37.
- Hemström, P., & Irgum, K. (2006). Hydrophilic interaction chromatography. *Journal of Separation Science*, 29(12), 1784–1821.
- Hemström, P., Jonsson, T., Appelblad, P., & Jiang, W. (2011). HILIC after the hype: a separation technology here to stay. *Chromatography Today*, (June), 4–8.
- Hennion, M.-C., Coquart, V., Guenu, S., & Sella, C. (1995). Retention behavior of polar compounds using porous graphitic carbon with water-rich mobile phases. *Journal of Chromatography A*, 712(2), 287–301.
- Horie, K., Kamakura, T., Ikegami, T., Wakabayashi, M., Kato, T., Tanaka, N., & Ishihama, Y. (2014). Hydrophilic interaction chromatography using a meter-scale monolithic silica capillary column for proteomics LC-MS. *Analytical Chemistry*, 86(8), 3817–3824.
- Horvath, C. G., Preiss, B. A., & Lipsky, S. R. (1967). Fast liquid chromatography. Investigation of operating parameters and the separation of nucleotides on pellicular ion exchangers. *Analytical Chemistry*, 39(12), 1422–1428.
- Hutchinson, J. P., Remenyi, T., Nesterenko, P., Farrell, W., Groeber, E., Szucs, R., ... Haddad, P. R. (2012). Investigation of polar organic solvents compatible with Corona Charged Aerosol Detection and their use for the determination of sugars by

hydrophilic interaction liquid chromatography. *Analytica Chimica Acta*, 750, 199–206.

Ibrahim, M. E. A. (2014). *Development and Characterization of New Stationary Phases for Hydrophilic Interaction Liquid Chromatography. Ph.D Thesis*. University of Alberta.

Ibrahim, M. E. A., Liu, Y., & Lucy, C. A. (2012). A simple graphical representation of selectivity in hydrophilic interaction liquid chromatography. *Journal of Chromatography. A*, 1260, 126–131.

Ibrahim, M. E. A., & Lucy, C. A. (2013). Stationary phases for HILIC. In B. A. Olsen & B. W. Pack (Eds.), *Hydrophilic Interaction Chromatography: A Guide for Practitioners* (Vol. 177, pp. 43–85). Hoboken, NJ: John Wiley & Sons.

Ibrahim, M. E. A., Wahab, M. F., & Lucy, C. A. (2014). Hybrid carbon nanoparticles modified core-shell silica: a high efficiency carbon-based phase for hydrophilic interaction liquid chromatography. *Analytica Chimica Acta*, 820, 187–94.

Ikegami, T., Tomomatsu, K., Takubo, H., Horie, K., & Tanaka, N. (2008). Separation efficiencies in hydrophilic interaction chromatography. *Journal of Chromatography. A*, 1184(1-2), 474–503.

Iqbal, P., Critchley, K., Attwood, D., Tunnicliffe, D., Evans, S. D., & Preece, J. A. (2008). Chemical manipulation by X-rays of functionalized thiolate self-assembled monolayers on Au. *Langmuir : The ACS Journal of Surfaces and Colloids*, 24(24), 13969–76.

- Isokawa, M., Kanamori, T., Funatsu, T., & Tsunoda, M. (2014). Recent advances in hydrophilic interaction chromatography for quantitative analysis of endogenous and pharmaceutical compounds in plasma samples. *Bioanalysis*, 6(18), 2421–2439.
- Iverson, C. D., & Lucy, C. A. (2014). Aniline-modified porous graphitic carbon for hydrophilic interaction and attenuated reverse phase liquid chromatography. *Journal of Chromatography. A*, 1373, 17–24.
- Jandera, P. (2011). Stationary and mobile phases in hydrophilic interaction chromatography: a review. *Analytica Chimica Acta*, 692(1-2), 1–25.
- Jansen, R. J. J., & van Bekkum, H. (1995). XPS of nitrogen-containing functional groups on activated carbon. *Carbon*, 33(8), 1021–1027.
- Jensen, D. S., Gupta, V., Olsen, R. E., Miller, A. T., Davis, R. C., Ess, D. H., ... Linford, M. R. (2011). Functionalization/passivation of porous graphitic carbon with di-tert-amylperoxide. *Journal of Chromatography. A*, 1218(46), 8362–8369.
- Jiang, W., & Irgum, K. (1999). Covalently bonded polymeric zwitterionic stationary phase for simultaneous separation of inorganic cations and anions. *Analytical Chemistry*, 71(2), 333–344.
- Kahsay, G., Song, H., Van Schepdael, A., Cabooter, D., & Adams, E. (2014). Hydrophilic interaction chromatography (HILIC) in the analysis of antibiotics. *Journal of Pharmaceutical and Biomedical Analysis*, 87, 142–154.

- Kanya, Z., Cserhati, T., & Forgacs, E. (2003). Using principal component analysis for the study of the retention behaviour of phenol derivatives under reversed-phase conditions. *Chromatographia*, *57*(7/8), 451–456.
- Karatapanis, A. E., Fiamegos, Y. C., & Stalikas, C. D. (2009). HILIC separation and quantitation of water-soluble vitamins using diol column. *Journal of Separation Science*, *32*(7), 909–917.
- Katz, E., Ogan, K. L., & Scott, R. P. W. (1983). Peak dispersion and mobile phase velocity in liquid chromatography: the pertinent relationship for porous silica. *Journal of Chromatography A*, *270*, 51–75.
- Kawachi, Y., Ikegami, T., Takubo, H., Ikegami, Y., Miyamoto, M., & Tanaka, N. (2011). Chromatographic characterization of hydrophilic interaction liquid chromatography stationary phases: hydrophilicity, charge effects, structural selectivity, and separation efficiency. *Journal of Chromatography A*, *1218*(35), 5903–5919.
- Kirkland, J. J. (1996). Stability of silica-based, monofunctional C18 bonded-phase column packing for HPLC at high pH. *Journal of Chromatographic Science*, *34*(7), 309–313.
- Kirkland, J. J., van Straten, M. A., & Claessens, H. A. (1995). High pH mobile phase effects on silica-based reversed-phase high-performance liquid chromatographic columns. *Journal of Chromatography A*, *691*(1), 3–19.

- Knox, J. H., Kaur, B., & Millward, G. R. (1986). Structure and performance of porous graphitic carbon in liquid chromatography. *Journal of Chromatography A*, 352, 3–25.
- Knox, J. H., & Wan, Q.-H. (1996). Surface modification of porous graphite for ion exchange chromatography. *Chromatographia*, 42(1-2), 83–88.
- Koupparis, M. A., Megoulas, N. C., & Gremilogianni, A. M. (2013). HILIC for food, environmental, and other applications. *Chemical Analysis*, 177(Hydrophilic Interaction Chromatography), 239–264.
- Kumar, A., Heaton, J. C., & McCalley, D. V. (2013). Practical investigation of the factors that affect the selectivity in hydrophilic interaction chromatography. *Journal of Chromatography. A*, 1276, 33–46.
- Le Comte, A., Pognon, G., Brousse, T., & Belanger, D. (2013). Determination of the quinone-loading of a modified carbon powder-based electrode for electrochemical capacitor. *Electrochemistry*, 81(10), 863–866.
- Lebègue, E., Brousse, T., Gaubicher, J., & Cougnon, C. (2013a). Chemical functionalization of activated carbon through radical and diradical intermediates. *Electrochemistry Communications*, 34, 14–17.
- Lebègue, E., Brousse, T., Gaubicher, J., & Cougnon, C. (2013b). Spontaneous arylation of activated carbon from aminobenzene organic acids as source of diazonium ions in mild conditions. *Electrochimica Acta*, 88, 680–687.
- doi:10.1016/j.electacta.2012.10.132

- Leonard, J., Lygo, B., & Procter, G. (2013). *Advanced Practical Organic Chemistry* (3rd ed.). Boca Raton, FL: CRC Press.
- Li, X., Jiang, J., Zhao, X., Wang, J., Han, H., Zhao, Y., ... Qian, X. (2013). N-glycoproteome analysis of the secretome of human metastatic hepatocellular carcinoma cell lines combining hydrazide chemistry, HILIC enrichment and mass spectrometry. *PLoS One*, *8*(12), e81921/1–e81921/15.
- Liang, C., & Lucy, C. A. (2010). Characterization of ion chromatography columns based on hydrophobicity and hydroxide eluent strength. *Journal of Chromatography. A*, *1217*(52), 8154–60.
- Liu, K., Aggarwal, P., Lawson, J. S., Tolley, H. D., & Lee, M. L. (2013). Organic monoliths for high-performance reversed-phase liquid chromatography. *Journal of Separation Science*, *36*(17), 2767–81.
- Liu, Y., Lu, Y., Prashad, M., Repic, O., & Blacklock, T. J. (2005). A practical and chemoselective reduction of nitroarenes to anilines using activated iron. *Advanced Synthesis & Catalysis*, *347*(2-3), 217–219.
- Liu, Y.-C., & McCreery, R. L. (1995). Reactions of organic monolayers on carbon surfaces observed with unenhanced raman spectroscopy. *Journal of the American Chemical Society*, *117*(45), 11254–11259.
- Longworth, J., Noirel, J., Pandhal, J., Wright, P. C., & Vaidyanathan, S. (2012). HILIC- and SCX-based quantitative proteomics of *Chlamydomonas reinhardtii* during

- nitrogen starvation induced lipid and carbohydrate accumulation. *Journal of Proteome Research*, 11(12), 5959–5971.
- Lucy, C. A. (2015). Exploration and Understanding of Hydrophilic Interaction Liquid Chromatography (HILIC). Presented at Simon Fraser University.
- Ma, J., Chen, D., Lu, K., Wang, L., Han, X., Zhao, Y., & Gong, P. (2014). Design, synthesis, and structure-activity relationships of novel benzothiazole derivatives bearing the ortho-hydroxy N-carbamoylhydrazone moiety as potent antitumor agents. *European Journal of Medicinal Chemistry*, 86, 257–69.
- Madden, J. E., Avdalovic, N., Jackson, P. E., & Haddad, P. R. (1999). Critical comparison of retention models for optimisation of the separation of anions in ion chromatography. *Journal of Chromatography A*, 837(1-2), 65–74.
- Madden, J. E., & Haddad, P. R. (1998). Critical comparison of retention models for optimisation of the separation of anions in ion chromatography. *Journal of Chromatography A*, 829(1-2), 65–80.
- Madden, J. E., & Haddad, P. R. (1999). Critical comparison of retention models for the optimisation of the separation of anions in ion chromatography. *Journal of Chromatography A*, 850(1-2), 29–41.
- Majors, R. E. (2008). Column pressure considerations in analytical HPLC. *LC-GC Europe*, 21(5), 268–280.

- Majors, R. E. (2012). Current trends in HPLC column usage. *LC-GC North America*, 30(1), 20–34.
- Majors, R. E. (2014). HPLC column technology 2014: state of the art. *LCGC North America*, 32(s4), 8,10.
- Marrubini, G., Mendoza, B. E. C., & Massolini, G. (2010). Separation of purine and pyrimidine bases and nucleosides by hydrophilic interaction chromatography. *Journal of Separation Science*, 33(6-7), 803–816.
- Masheter, A. T., Wildgoose, G. G., Crossley, A., Jones, J. H., & Compton, R. G. (2007). A facile method of modifying graphite powder with aminophenyl groups in bulk quantities. *Journal of Materials Chemistry*, 17(29), 3008–3014.
- Mazzeo, J. R., D. Neue, U., Kele, M., & Plumb, R. S. (2005). Advancing LC Performance with Smaller Particles and Higher Pressure. *Analytical Chemistry*, 77(23), 460 A–467 A.
- McCalley, D. V. (2007). Is hydrophilic interaction chromatography with silica columns a viable alternative to reversed-phase liquid chromatography for the analysis of ionisable compounds? *Journal of Chromatography. A*, 1171(1-2), 46–55.
- McCalley, D. V. (2010). Study of the selectivity, retention mechanisms and performance of alternative silica-based stationary phases for separation of ionised solutes in hydrophilic interaction chromatography. *Journal of Chromatography. A*, 1217(20), 3408–3417.

- McCalley, D. V. (2015). Study of retention and peak shape in hydrophilic interaction chromatography over a wide pH range. *Journal of Chromatography. A*, *1411*, 41–49.
- McCreery, R. L. (2008). Advanced carbon electrode materials for molecular electrochemistry. *Chemical Reviews*, *108*(7), 2646–2687.
- Melmer, M., Stangler, T., Premstaller, A., & Lindner, W. (2011). Comparison of hydrophilic-interaction, reversed-phase and porous graphitic carbon chromatography for glycan analysis. *Journal of Chromatography A*, *1218*(1), 118–123.
- Mercier, T., Tissot, F., Gardiol, C., Corti, N., Wehrli, S., Guidi, M., ... Decosterd, L. A. (2014). High-throughput hydrophilic interaction chromatography coupled to tandem mass spectrometry for the optimized quantification of the anti-Gram-negatives antibiotic colistin A/B and its pro-drug colistimethate. *Journal of Chromatography A*, *1369*, 52–63.
- Michael, C., & Rizzi, A. M. (2015). Quantitative isomer-specific N-glycan fingerprinting using isotope coded labeling and high performance liquid chromatography-electrospray ionization-mass spectrometry with graphitic carbon stationary phase. *Journal of Chromatography A*, *1383*, 88–95. doi:10.1016/j.chroma.2015.01.028
- Michael, C., & Rizzi, A. M. (2015). Tandem mass spectrometry of isomeric aniline-labeled N-glycans separated on porous graphitic carbon: Revealing the attachment position of terminal sialic acids and structures of neutral glycans. *Rapid Communications in Mass Spectrometry*, *29*(13), 1268–1278.

- Michel, M., & Buszewski, B. (2009). Porous graphitic carbon sorbents in biomedical and environmental applications. *Adsorption*, *15*(2), 193–202.
- Moretton, C., Crétier, G., Nigay, H., & Rocca, J.-L. (2008). Heart-cutting two-dimensional liquid chromatography methods for quantification of 2-acetyl-4-(1,2,3,4-tetrahydroxybutyl)imidazole in Class III caramel colours. *Journal of Chromatography A*, *1198*, 73–79.
- Moulder, J. F., Chastain, J., & King, R. C. (1995). *Handbook of x-ray photoelectron spectroscopy : a reference book of standard spectra for identification and interpretation of XPS data*. Eden Prairie, MN.: Physical Electronics.
- Mythbusters. Top Shelf Vodka Myth. Originally aired April 29, 2006. USA: Discovery Media.
- Nawrocki, J. (1997). The silanol group and its role in liquid chromatography. *Journal of Chromatography A*, *779*(1-2), 29–71.
- Nemoto, T., Lee, X.-P., Kumazawa, T., Hasegawa, C., Fujishiro, M., Marumo, A., ... Sato, K. (2014). High-throughput determination of nonsteroidal anti-inflammatory drugs in human plasma by HILIC-MS/MS. *Journal of Pharmaceutical and Biomedical Analysis*, *88*, 71–80.
- Neue, U. D. (2007). Stationary phase characterization and method development. *Journal of Separation Science*, *30*(11), 1611–1627.

- Neue, U. D., VanTran, K., Iraneta, P. C., & Alden, B. A. (2003). Characterization of HPLC packings. *Journal of Separation Science*, 26(3/4), 174–186.
doi:10.1002/jssc.200390025
- Noga, S., Bocian, S., & Buszewski, B. (2013). Hydrophilic interaction liquid chromatography columns classification by effect of solvation and chemometric methods. *Journal of Chromatography. A*, 1278, 89–97.
- Nováková, L., Havlíková, L., & Vlčková, H. (2014). Hydrophilic interaction chromatography of polar and ionizable compounds by UHPLC. *TrAC Trends in Analytical Chemistry*, 63, 55–64.
- Nuebauer, M., & Franz, H. (2014). *Optimizing and Monitoring Solvent Quality for UV-Vis Absorption, Fluorescence and Charged Aerosol Detectors* (Thermo Scientific, Technical Note 140). Germering, Germany.
- Ortmayr, K., Hann, S., & Koellensperger, G. (2015). Complementing reversed-phase selectivity with porous graphitized carbon to increase the metabolome coverage in an on-line two-dimensional LC-MS setup for metabolomics. *Analyst*, 140(10), 3465–3473.
- Pabst, M., & Altmann, F. (2008). Influence of electrosorption, solvent, temperature, and ion polarity on the performance of LC-ESI-MS using graphitic carbon for acidic oligosaccharides. *Analytical Chemistry*, 80(19), 7534–7542.
- Pabst, M., Grass, J., Fischl, R., Léonard, R., Jin, C., Hinterkörner, G., ... Altmann, F. (2010). Nucleotide and nucleotide sugar analysis by liquid chromatography-

- electrospray ionization-mass spectrometry on surface-conditioned porous graphitic carbon. *Analytical Chemistry*, 82(23), 9782–9788.
- Peacock, K. S., Ruhaak, L. R., Tsui, M. K., Mills, D. A., & Lebrilla, C. B. (2013). Isomer-specific consumption of galactooligosaccharides by bifidobacterial species. *Journal of Agricultural and Food Chemistry*, 61(51), 12612–12619.
- Pena-Pereira, F., Kloskowski, A., & Namiesnik, J. (2015). Perspectives on the replacement of harmful organic solvents in analytical methodologies: a framework toward the implementation of a generation of eco-friendly alternatives. *Green Chemistry*, 17(7), 3687–3705.
- Pereira, L. (2008). Porous graphitic carbon as a stationary phase in HPLC: theory and applications. *Journal of Liquid Chromatography & Related Technologies*, 31(11 & 12), 1687–1731.
- Pereira, L. (2011). HILIC&MS sensitivity without silica. *LC-GC North America*, 29(3), 262–269.
- Pereira, L., Aspey, S., & Ritchie, H. (2007). High temperature to increase throughput in liquid chromatography and liquid chromatography–mass spectrometry with a porous graphitic carbon stationary phase. *Journal of Separation Science*, 30(8), 1115–1124.
- Periat, A., Debrus, B., Rudaz, S., & Guillarme, D. (2013). Screening of the most relevant parameters for method development in ultra-high performance hydrophilic interaction chromatography. *Journal of Chromatography. A*, 1282, 72–83.

- Periat, A., Kohler, I., Bugey, A., Bieri, S., Versace, F., Staub, C., & Guillarme, D. (2014). Hydrophilic interaction chromatography versus reversed phase liquid chromatography coupled to mass spectrometry: effect of electrospray ionization source geometry on sensitivity. *Journal of Chromatography A*, 1356, 211-220.
- Pietrogrande, M. C., Benvenuti, A., Previato, S., & Dondi, F. (2000). HPLC analysis of PCBs on porous graphitic carbon: retention behavior and gradient elution. *Chromatographia*, 52(7/8), 425-432.
- Pognon, G., Cougnon, C., Mayilukila, D., & Bélanger, D. (2012). Catechol-modified activated carbon prepared by the diazonium chemistry for application as active electrode material in electrochemical capacitor. *ACS Applied Materials & Interfaces*, 4(8), 3788-3796.
- Pohl, C. (2013). Recent developments in ion-exchange columns for ion chromatography. *LCGC North America*, (Suppl.), 16-22.
- Qiu, H., Loukotková, L., Sun, P., Tesařová, E., Bosáková, Z., & Armstrong, D. W. (2011). Cyclofructan 6 based stationary phases for hydrophilic interaction liquid chromatography. *Journal of Chromatography A*, 1218, 270-279.
- Ray, K., & McCreery, R. L. (1997). Spatially Resolved Raman Spectroscopy of Carbon Electrode Surfaces: Observations of Structural and Chemical Heterogeneity. *Analytical Chemistry*, 69(22), 4680-4687.

- Romanová, D., & Novotný, L. (1996). Chromatographic properties of cytosine, cytidine and their synthetic analogues. *Journal of Chromatography B: Biomedical Sciences and Applications*, 675(1), 9–15.
- Roodenko, K., Gensch, M., Rappich, J., Hinrichs, K., Esser, N., & Hunger, R. (2007). Time-resolved synchrotron XPS monitoring of irradiation-induced nitrobenzene reduction for chemical lithography. *The Journal of Physical Chemistry. B*, 111(26), 7541–9.
- Ross, P., & Knox, J. H. (1997). Carbon-based packing materials for liquid chromatography: applications. *Advances in Chromatography*, 37, 121–162.
- Sadikin, S., Zhang, D. D., Inloes, R., & Redkar, S. (2011). Ghost peak investigation in a reversed-phase gradient LC system. *LC-GC North America*, 29(5), 394–400.
- Sakhi, A. K., Russnes, K. M., Smeland, S., Blomhoff, R., & Gundersen, T. E. (2006). Simultaneous quantification of reduced and oxidized glutathione in plasma using a two-dimensional chromatographic system with parallel porous graphitized carbon columns coupled with fluorescence and coulometric electrochemical detection. *Journal of Chromatography A*, 1104(1), 179–189.
- Sandra, P., Sandra, K., Pereira, A., Vanhoenacker, G., & David, F. (2010). Green chromatography. Part 1: introduction and liquid chromatography. *LC-GC Europe*, 23(5), 242–259.

- Sanjay Kumar, D., & Harish Kumar, D. R. (2012). Importance of RP-HPLC in analytical method development: a review. *International Journal of Pharmaceutical Sciences and Research*, 3(12), 4626–4633.
- Schlichtherle-Cerny, H., Affolter, M., & Cerny, C. (2003). Hydrophilic interaction liquid chromatography coupled to electrospray mass spectrometry of small polar compounds in food analysis. *Analytical Chemistry*, 75(10), 2349–2354.
- Schuster, G., & Lindner, W. (2011). Chocolate HILIC phases: development and characterization of novel saccharide-based stationary phases by applying non-enzymatic browning (Maillard reaction) on amino-modified silica surfaces. *Analytical and Bioanalytical Chemistry*, 400(8), 2539–2554.
- Schuster, G., & Lindner, W. (2013). Additional investigations into the retention mechanism of hydrophilic interaction liquid chromatography by linear solvation energy relationships. *Journal of Chromatography. A*, 1301, 98–110.
- Schwer, C., & Kenndler, E. (1991). Electrophoresis in fused-silica capillaries: the influence of organic solvents on the electroosmotic velocity and the zeta potential. *Analytical Chemistry*, 63(17), 1801–1807.
- Shaaban, H., & Gorecki, T. (2015). Current trends in green liquid chromatography for the analysis of pharmaceutically active compounds in the environmental water compartments. *Talanta*, 132, 739–752.
- Shen, W., Li, Z., & Liu, Y. (2008). Surface chemical functional groups modification of porous carbon. *Recent Patents on Chemical Engineering*, 1(1), 27–40.

- Small, H., Stevens, T. S., & Bauman, W. C. (1975). Novel ion exchange chromatographic method using conductimetric detection. *Analytical Chemistry*, 47(11), 1801–1809.
- Smith, M. B. (2013). *March's Advanced Organic Chemistry: Reactions, Mechanisms, and Structure* (7th ed.). Hoboken, NJ: John Wiley & Sons.
- Snyder, L. R., Kirkland, J. J., & Dolan, J. W. (2011). *Introduction to Modern Liquid Chromatography* (3rd ed.). Hoboken, NJ: John Wiley & Sons.
- Snyder, L. R., & Poppe, H. (1980). Mechanism of solute retention in liquid—solid chromatography and the role of the mobile phase in affecting separation. *Journal of Chromatography A*, 184(4), 363–413.
- Soukup, J., & Jandera, P. (2014). Adsorption of water from aqueous acetonitrile on silica-based stationary phases in HILIC (aqueous normal-phase) liquid chromatography. *Journal of Chromatography A*, 1374, 102–111.
- Spackova, V., & Pazourek, J. (2013). Identification of carbohydrate isomers in flavonoid glycosides after hydrolysis by hydrophilic interaction chromatography. *Chemical Papers*, 67(4), 357–364.
- Subirats, X., Rosés, M., & Bosch, E. (2007). On the effect of organic solvent composition on the pH of buffered HPLC mobile phases and the pK_a of analytes—a review. *Separation & Purification Reviews*, 36(3), 231–255.

- Tang, D.-Q., Zou, L., Yin, X.-X., & Ong, C. N. (2014). HILIC-MS for metabolomics: An attractive and complementary approach to RPLC-MS. *Mass Spectrometry Reviews*. doi:10.1002/mas.21445
- Tao, S., Huang, Y., Boyes, B. E., & Orlando, R. (2014). Liquid chromatography-selected reaction monitoring (LC-SRM) approach for the separation and quantitation of sialylated N-glycans linkage isomers. *Analytical Chemistry*, *86*(21), 10584–10590.
- Teutenberg, T., Hollebekkers, K., Wiese, S., & Boergers, A. (2009). Temperature and pH-stability of commercial stationary phases. *Journal of Separation Science*, *32*(9), 1262–74.
- Teutenberg, T., Wiese, S., Wagner, P., & Gmehling, J. (2009). High-temperature liquid chromatography. Part II: Determination of the viscosities of binary solvent mixtures-Implications for liquid chromatographic separations. *Journal of Chromatography A*, *1216*(48), 8470–8479.
- Thiébaud, D., Vial, J., Michel, M., Hennion, M.-C., & Greibrokk, T. (2006). Evaluation of reversed phase columns designed for polar compounds and porous graphitic carbon in “trapping” and separating neurotransmitters. *Journal of Chromatography A*, *1122*(1), 97–104.
- Tornkvist, A., Markides, K. E., & Nyholm, L. (2003). Chromatographic behaviour of oxidised porous graphitic carbon columns. *The Analyst*, *128*(7), 844.

- Tswett, M. (1906). Adsorption analysis and chromatographic method. Application on the chemistry of the Chlorophylls. [machine translation]. *Berichte Der Deutschen Botanischen Gesellschaft*, 24, 384–393.
- Tyteca, E., Guillarme, D., & Desmet, G. (2014). Use of individual retention modeling for gradient optimization in hydrophilic interaction chromatography: Separation of nucleobases and nucleosides. *Journal of Chromatography A*, 1368, 125–131.
- UC Davis. 12B: General Theory of Column Chromatography. Retrieved September 8, 2015, from http://chemwiki.ucdavis.edu/Analytical_Chemistry/Analytical_Chemistry_2.0/12_Chromatographic_and_Electrophoretic_Methods/12B%3A_General_Theory_of_Column_Chromatography
- Unger, K. K., Ditz, R., Machtejevas, E., & Skudas, R. (2010). Liquid chromatography—its development and key role in life science applications. *Angewandte Chemie International Edition*, 49(13), 2300–2312.
- van Deemter, J. J., Zuiderweg, F. J., & Klinkenberg, A. (1956). Longitudinal diffusion and resistance to mass transfer as causes of nonideality in chromatography. *Chemical Engineering Science*, 5(6), 271–289.
- van Nuijs, A. L. N., Tarcomnicu, I., & Covaci, A. (2011). Application of hydrophilic interaction chromatography for the analysis of polar contaminants in food and environmental samples. *Journal of Chromatography A*, 1218(35), 5964–5974.

- Verspreet, J., Holmgaard Hansen, A., Dornez, E., Courtin, C. M., & Harrison, S. J. (2014). A new high-throughput LC-MS method for the analysis of complex fructan mixtures. *Analytical and Bioanalytical Chemistry*, *406*(19), 4785–4788.
- Wahab, M. F., Ibrahim, M. E. A., & Lucy, C. A. (2013). Carboxylate modified porous graphitic carbon: a new class of hydrophilic interaction liquid chromatography phases. *Analytical Chemistry*, *85*, 5684–5691.
- Wahab, M. F., Pohl, C. A., & Lucy, C. A. (2011). Ion chromatography on carbon clad zirconia modified by diazonium chemistry and functionalized latex particles. *The Analyst*, *136*(15), 3113–20.
- Wang, J., Guo, Z., Shen, A., Yu, L., Xiao, Y., Xue, X., ... Liang, X. (2015). Hydrophilic-subtraction model for the characterization and comparison of hydrophilic interaction liquid chromatography columns. *Journal of Chromatography A*, *1398*, 29–46.
- Wang, X., Lin, X., Xie, Z., & Giesy, J. P. (2009). Preparation and evaluation of a neutral methacrylate-based monolithic column for hydrophilic interaction stationary phase by pressurized capillary electrochromatography. *Journal of Chromatography. A*, *1216*(21), 4611–4617.
- Welch, C. J., Brkovic, T., Schafer, W., & Gong, X. (2009). Performance to burn? Re-evaluating the choice of acetonitrile as the platform solvent for analytical HPLC. *Green Chemistry*, *11*(8), 1232–1238.

- Welch, C. J., Nowak, T., Joyce, L. A., & Regalado, E. L. (2015). Cocktail chromatography: enabling the migration of HPLC to nonlaboratory environments. *ACS Sustainable Chemistry & Engineering*, 3(5), 1000–1009.
- Welch, C. J., Wu, N., Biba, M., Hartman, R., Brkovic, T., Gong, X., ... Zhou, L. (2010). Greening analytical chromatography. *TrAC, Trends in Analytical Chemistry*, 29(7), 667–680.
- West, C., Elfakir, C., & Lafosse, M. (2010). Porous graphitic carbon: a versatile stationary phase for liquid chromatography. *Journal of Chromatography. A*, 1217(19), 3201–16.
- World Anti-Doping Agency. (2015). <http://www.wada-ama.org>. Retrieved January 1, 2015, from <http://www.wada-ama.org>
- Wuts, P. G. M., & Greene, T. W. (2012). *Greene's Protective Groups in Organic Synthesis* (4th ed.). Hoboken, NJ: John Wiley & Sons.
- Xiong, Y., Zhao, Y.-Y., Goruk, S., Oilund, K., Field, C. J., Jacobs, R. L., & Curtis, J. M. (2012). Validation of an LC-MS/MS method for the quantification of choline-related compounds and phospholipids in foods and tissues. *Journal of Chromatography B*, 911, 170–179.
- Zhang, N., Wang, L., Liu, H., & Cai, Q.-K. (2008). Nitric acid oxidation on carbon dispersion and suspension stability. *Surface and Interface Analysis*, 40(8), 1190–1194.

- Zhang, R., Watson, D. G., Wang, L., Westrop, G. D., Coombs, G. H., & Zhang, T. (2014). Evaluation of mobile phase characteristics on three zwitterionic columns in hydrophilic interaction liquid chromatography mode for liquid chromatography-high resolution mass spectrometry based untargeted metabolite profiling of Leishmania parasites. *Journal of Chromatography. A*, *1362*, 168–179.
- Zhao, Y., Szeto, S. S. W., Kong, R. P. W., Law, C. H., Li, G., Quan, Q., ... Chu, I. K. (2014). Online two-dimensional porous graphitic carbon/reversed phase liquid chromatography platform applied to shotgun proteomics and glycoproteomics. *Analytical Chemistry*, *86*(24), 12172–12179.
- Zheng, W., Du, R., Cao, Y., Mohammad, M. A., Dew, S. A., McDermott, M. T., Evoy, S. (2015). Diazonium chemistry for the bio-functionalization of glassy nanostring resonator assays. *Sensors*, *15*(8), 18724-18741.
- Zhou, Z., Wu, X., Wei, Q., Liu, Y., Liu, P., Ma, A., & Zou, F. (2013). Development and validation of a hydrophilic interaction liquid chromatography-tandem mass spectrometry method for the simultaneous determination of five first-line antituberculosis drugs in plasma. *Analytical and Bioanalytical Chemistry*, *405*(19), 6323–6335.
- Zhu, R.-H., Li, H.-D., Cai, H.-L., Jiang, Z.-P., Xu, P., Dai, L.-B., & Peng, W.-X. (2014). Validated HILIC-MS/MS assay for determination of vandesine in human plasma: application to a population pharmacokinetic study. *Journal of Pharmaceutical and Biomedical Analysis*, *96*, 31–36.

APPENDIX 1: Conversion of Mol % to Volume %

By definition for a two component mixture, the mol % of component A is given by **Equation A-1**.

$$\text{mol \%}_A = \frac{\text{mol } A}{\text{mol } A + \text{mol } B} \times 100 \quad (\text{A-1})$$

Additionally, the moles of a liquid substance for a given volume is given by **Equation A-2**.

$$\text{mol } i = \frac{V_i \rho_i}{MW_i} \quad (\text{A-2})$$

where V = volume in mL, ρ = density in g/mL and MW = the molecular weight of the substance in grams.

Substituting **Equation A-2** into **Equation A-1** yields **Equation A-3**.

$$\text{mol \%}_A = \frac{\frac{V_A \rho_A}{MW_A}}{\frac{V_A \rho_A}{MW_A} + \frac{V_B \rho_B}{MW_B}} \times 100 \quad (\text{A-3})$$

Assuming that $V_A + V_B = 1$ and dividing **Equation A-3** by 100 yields **Equation A-4**:

$$X_A = \frac{\frac{V_A \rho_A}{MW_A}}{\frac{V_A \rho_A}{MW_A} + \frac{(1-V_A) \rho_B}{MW_B}} \quad (\text{A-4})$$

where X_A is the mole fraction of A

Rearranging and solving for V_A gives **Equation A-5**:

$$V_A = \frac{\frac{X_A \rho_A}{MW_B}}{\frac{\rho_A}{MW_A} + \frac{X_A \rho_B}{MW_B} - \frac{X_A \rho_A}{MW_A}} \quad (\text{A-5})$$

And:

$$\text{volume \% } A = V_A \times 100 \quad (\text{A-6})$$

APPENDIX 2: Log P and pK_a values for test analytes utilized in this thesis

Table A-2.1. Log P and pK_a values for test analytes utilized in this thesis. Data from Sci Finder.

Analyte	Log P	pK _a
(1 <i>R</i> ,2 <i>S</i>)-(-)- <i>N</i> -methylephedrine	1.62	13.88, 9.04
Acetaminophen	0.48	9.86, 1.72
Acetylsalicylic acid	1.40	3.48
Adenosine	-0.76	13.11, 3.82
Aniline	1.14	4.61
Benzoic acid	1.56	4.20
Benzyltrimethylammonium chloride (BTMA)	-1.87	n/a
Butylbenzene	4.25	n/a
Caffeine	-0.63	14.00
Cathine	0.36	12.07, 8.47
Cytidine	-1.81	13.48, 4.26
Cytosine	-1.96	9.00, 4.18
D-Galactose	-3.29	12.45
Diphenhydramine	2.99	8.76
D-Ribose	-2.81	12.46
D-Sucrose	-4.49	12.81
Ephedrine	1.00	13.96, 9.38
Ethylbenzene	3.23	n/a
Gentisic acid	1.40	3.01
Hexylbenzene	5.27	n/a
Hippuric acid	0.76	3.71
Naphthalene	3.36	n/a
norephedrine	0.36	12.07, 8.47
Nortryptiline	4.51	10.47
Pentylbenzene	4.76	n/a
Phenol	1.46	9.86
Phloroglucinol	0.01	9.06
Procainamide	1.32	9.09
Propylbenzene	3.74	n/a
Resorcinol	0.82	9.45
Salicylic acid	2.01	3.01
Thymidine	-0.84	9.55
Toluene	2.72	n/a
Uracil	-1.04	8.95
Uridine	-1.58	9.39
α -hydroxyhippuric acid	0.22	3.24